KFKI-74-11

G. GRÜNER

EXPERIMENTAL EVIDENCE FOR MANY-BODY EFFECTS IN DILUTE ALLOYS

Hungarian Academy of Sciences

CENTRAL
RESEARCH
INSTITUTE FOR
PHYSICS

BUDAPEST

KFKI-74-11

EXPERIMENTAL EVIDENCE FOR MANY-BODY EFFECTS IN DILUTE ALLOYS

G. Grüner

Imperial College, Department of Physics, London

and

Central Research Institute for Physics
Solid State Physics Department
Budapest

To be published in Advances in Physics

ABSTRACT

The macroscopic and local properties of 3d transition metal impurities in normal metals are reviewed and contrasted with the theoretical situation in this field.

The parameters of the Anderson and s-d exchange models are derived from direct and indirect experimental data using as a guide the HF approximation of the non-degenerate Anderson model. The basic observations about the magnetic-non-magnetic transition, and the behaviour of the magnetic, thermal and transport properties when going through the transition region are demonstrated for specific examples. A detailed comparison between the present status of theory and experiment is performed by inspecting the large body of experimental data of two typical alloys, which served as testing materials for the development of the existing theories. CuFe is often regarded as a typical "yes moment" system, and the experiments are therefore compared with the predictions based on the s-d exchange model; in case fo AlMn, the spin fluctuation concept was chosen as a theoretical basis. It is shown that various approaches of the models fail to describe the fine experimental details.Evidence is presented which calls for a unified theory with no distinction between magnetic /Kondo-type/ and non-magnetic /spin fluctuation/ alloys. It is suggested that the range of applicability of a model depends not only on the basic parameters of the dilute alloy, but on the temperature too, and the question of the relevance of the models to the actual state of affairs is to be answered by inspecting the temperature regions where the various approximations of the models are expected to work; the $T>>T_k$ properties are compared with the Kondo approach, the $T<<T_k$ properties with the spin fluctuation model, although in the latter case the analysis is based on the concept of a narrow resonance level, which is not a feature of the spin fluctuation concept only.

Finally, the basic experimental facts and indications are absorbed into a phenomenological model, which describes both the single particle resonances and the many body effects involved in resonance formation in classical dilute alloys.

ÖSSZEFOGLALÁS

A normál fémekben oldott 3db átmeneti fém szennyezések makroszkopikus és lokális tulajdonságait tekintjük át és hasonlitjuk össze az elméleti modellekkel. Az Anderson és s-d kicserélődési modell paramétereit határozzuk meg közvetlen és közvetett kisérleti adatokból, a nem-degenerált Anderson modell alapján. A mágneses- nemmágneses átmenet fő jellemzőit és az átmeneti tartományban a mágneses, termikus és transzport tulajdonságokat demonstráljuk egyes példákon. A kisérlet és elmélet közötti részletes összehasonlitást két olyan ötvözeten végezzük el, melyek az elméletek fejlődésében fő szerepet játszottak. A CuFe rendszert általában tipikus "jó momentum"-nak tekintik, ezért a kisérleteket az s-d kicserélődési modellel hasonlitjuk össze, az AlMn esetén a spin fluktuációs koncepciót választottuk elméleti bázisként. Megmutatjuk, hogy a modellek különböző közelitései nem irják le a finomabb kisérleti részleteket. Azon bizonyitékokat soroljuk fel ezután, melyek egy egyesitett elméletet kivánnak meg, nem téve különbséget mágneses /Kondo tipusu/ és nemmágneses /spin fluktuációs/ ötvözetek között. Megmutatjuk, hogy a modellek alkalmazhatósága nemcsak a modellparaméterektől, hanem a hőmérséklettől is függ; a modellek alkalmazhatóságára ugy adunk választ, hogy azokat a hőmérséklettartományokat vizsgáljuk meg, ahol a modellek közelitései megfelelőek; a $T>>T_k$ tulajdonságokat a Kondo közelitéssel, a $T<<T_k$ tulajdonságokat a spin fluktuációs modellel hasonlitjuk össze, bár az utóbbi esetben az analizis alapja egy keskeny rezonancianivó feltételezése, mely nemcsak a spin fluktuációs modell jellemzője.

Végül a fő kisérleti tényeket egy fenomenologikus modellbe foglaljuk össze, mely leirja mind az egyrészecske rezonanciákat, mind a többtest effektusokat, melyek megjelennek a klasszikus hig ötvözetek rezonanciáiban.

РЕЗЮМЕ

В работе рассматриваются и сравниваются с теоретическими моделями макроскопические и локальные свойства примесей 3d переходных металлов, растворенных в нормальных металлах. По непосредственным и посредственным экспериментальным данным, определены параметры модели Андерсона s-d обменной модели на основании модели Андерсона. На отдельных примерах демонстрируются основные характеристики перехода магнит-немагнит, магнитные и термические свойства, а также свойства переноса. Подробное сравнение экспериментальных данных и теории проводится на двух сплавах, которые сыграли главную роль в развитии теорий. Сплав CuFe обычно считается типичной системой, обладающей "хорошим моментом", поэтому эксперименты сравниваются с s-d обменной моделью, а в случае системы AlMn теоретической основой является концепция спиновой флуктуации. Показано, что различные подходы к модели не описывают более тонкие детали эксперимента. Перечислены доказательства, которые требуют обобщенной теории, в которой не делается различия между магнитными /типа Кондо/ и немагнитными /спиновой флуктуации/ сплавами. Показано, что применимость моделей зависит не только от параметров, но также и от температуры; на вопрос применимости моделей ответ дается таким образом, что исследуются те температурные диапазоны, в которых приближение дает удовлетворительные результаты; свойства при $T \gg T_K$ сравниваются в приближении Кондо, а свойства при $T \ll T_K$ - с моделью спиновой флуктуации, хотя в последнем случае основой анализа является предположение узкого резонансного уровня, который характеризует не только модель спиновой флуктуации. Экспериментальные результаты обобщаются в феноменологической модели, описывающей как одночастичные резонансы, так и многочастичные эффекты, появляющиеся в резонансах классических разбавленных сплавов.

ABSTRACT

CONTENTS

1. INTRODUCTION

2. BASIC PARAMETERS OF THE ANDERSON AND s-d EXCHANGE MODELS

3. THE HF APPROXIMATION: CLASSIFICATION OF THE DILUTE ALLOY SYSTEMS

3.1. Optical properties

3.2. Macroscopic properties

3.2.1. Transport phenomena

3.2.2. Specific heat

3.2.3. Magnetic susceptibility

3.2.4. Transport properties in magnetic field

3.3. Local properties

3.3.1. Magnetic hyperfine properties

3.3.2. Electric hyperfine properties

3.3.3. Electron spin resonance

3.4. The relevance of the HF approximation to the experiments

4. THE MAGNETIC-NONMAGNETIC TRANSITION: EVIDENCE OF MANY BODY EFFECTS

4.1. Anomalous temperature dependence of the magnetic, thermal and transport properties

4.2. Kondo temperatures

5. TWO TYPICAL EXAMPLES: CuFe AND AlMn

5.1. The CuFe alloy

5.1.1. High temperature properties

5.1.2. The transition to the nonmagnetic state

5.1.3. The temperature dependence of the susceptibility and the question of the spin polarized cloud

5.2. Another example: AlMn

5.2.1. Low temperature macroscopic paramteres

5.2.2. Charge perturbation around the Mn impurities in aluminium

5.2.3. High temperature state of AlMn

5.3. Common features of Kondo and spin fluctuation alloys

6. THE LOGARITHMIC AND SIMPLE POWER REGIMES: THE HIGH AND LOW ENERGY FLUCTUATIONS

6.1. The logarithmic regime: experiments at $T > T_k$

6.1.1. High temperature properties

6.1.2. Logarithmic temperature dependences at $T > T_k$

6.1.3. Kondo temperatures given by the s-d model

6.2. The simple power low regime: experiments at $T \quad T_k$

6.2.1. Resistivity at T = 0

6.2.2. Macroscopic paramters

6.2.3. Local properties

6.2.4. Transition temperatures given by the concept of the narrow resonance level

7. PHENOMENOLOGICAL DESCRIPTION OF RESONANCE FORMATION IN DILUTE ALLOYS

8. CONCLUSIONS

9. ACKNOWLEDGEMENTS

8. CONCLUSIONS

9. ACKNOWLEDGEMENTS

1. INTRODUCTION

A small concentration of 3d transition metal impurities can change the electric, thermal and magnetic properties of simple metals in a very distinct way, in contrast ot the effects caused by normal metal impurities. The drastic dependences of the various physical parameters on the temperature and on the magnetic field suggest that they are examples of Fermi surface phenomena and many-body effects. These anomalies were well known to experimentalist, but have not attracted wide theoretical interest until the last fifteen years.

The development of the theory stated with two seemingly not strongly connected questions: "Under what circumstances does a localised moment exist in a metal?", and "What are the consequences of the interaction between localised moment and the conduction electrons?"

A microscopic model was constructed by Anderson and Wolff - based on the ideas of Friedel - to answer the first question, and the Hartree-Fock approximation of this model served for a long time as a basis for classifying the alloys into nonmagnetic and magnetic ones. The second question has been attacked by using another model, the s-d model, which assumes, that the impurity is nothing but a well defined spin, interacting weakly with the conduction electrons; unden certain circumstances this model can be derived from the Anderson model. In spite of the weak interaction, perturbation theory does not work, and leads to divergences at low temperatures.

The success of this model to account for a number of low temperature anomalies observed led to a number of second generation approaches, which removed the divergence, and resulted in some kind of non-magnetic state below a certain temperature, with exotic properties rapidly disproved by another approximation or by the experiments. These disagreements generated a family of more sophisticated mathematical methods, which aim to solve the problem in principle, but not it detail.

Not questioning the clear intellectual interest of these simple and still not soluble models, their relevance to the actual situations has been questioned several times, (mainly be experimentalists). These doubts, together with efforts in bringing into close contact the theory and experiments generated a wide activity in this field.

This activity is reflected in a number of review papers, covering the whole aspect of the problem, ranging from purely experimental surveys (Van den Berg 1964, van Dam and Van den Berg 1970, Rizzuto 1974, Wolleben and Coles 1973), to theoretical ones, (Kondo 1969, Fisher 1970, 1971), together with attempts to analyze the experimental information in the light of the available theory, (Daybell and Steyert 1967, Heeger 1969).

The present Review falls into the latter category. It is an extended version of one part of a paper by Zawadowski and the author (1974), to apper in the Reports on Progress in Physics. While only the main experimental features of the dilute alloy problem are absorbed in the

latter Review, it is believed that a more elaborate discussion might be useful for experimentalits working in this field. This hope has initiated the present work, which attempts to bridge the gap between the present status of the theory and experiment. We address ourselves to the analysis of empirical trends and behaviours, which can, or cannot, be explained by the present theoretical "solutions" of the various models. We do not discuss the theoretical state of affairs in detail, which can be found in several lecture notes and reviews (see for example Anderson 1968, Kondo 1969, Fisher 1970, 1971), but try to point out the range of validity of the various approximations, and to make a clear distinction between the models and their approximative solutions. Although in the light of more sophisticated mathematical formalism, developed recently, the traditional "solutions" are now believed to have a rather limited range of validity, it is probably instructive to recall some examples and trials which aimed to bring into a close contact the theory and experiment.

This attempt sets a priori a limit to alloys systems which will be discussed in detail; we focus our attention on the behaviour of 3d transition metal impurities in simple metals (mainly noble metals and aluminium), where the original assumptions of the models - in particular the Anderson model (1961) - are best fulfilled. Furthermore, we do not discuss crystalline field effects, spin-orbit coupling, etc. These effects, while they might be im-

portant in particular situations, have not been treated in detail until now. The effects of impurities on superconducting properties, tunneling phenomena, impurity-impurity interactions, fall outside the scope of the present Review, too.

We start with the discussion of the basic parameters of the Anderson and s-d exchange models, and evaluate these parameters from various experiments. This effort leads to the understanding of the basic aspects of the formation of localised moments, and, furthermore, brings us to situations where the Hartree-Fock approximation is insufficient, and more elaborate discussion is necessary to describe higher order correlations and many-body effects. This part is followed by some general observations about the transition between the magnetic and non-magnetic states, discussed on specific examples. We then review the experimental results in the light of theory in more detail on two examples: on the CuFe and the AlMn systems. The former is regarded as a typical Kondo-alloy, the latter is believed to be a protoype of non-magnetic alloys, but near to the verge of the apperance of magnetism, with properties, described usually within the framework of the localised spin fluctuation theories. Chapter 6 is devoted to the discussion of the experiments, performed in two temperature regimes $T \gg T_k$ and $T \ll T_k$, where various physical parameters seem to be determined by similar dependences on the temperature, and we call them the logarithmic and simple

power law regimes. Finally, we try to find a general, and phenomenological picture of the resonance formation in dilute alloys, which is based on experimental information; the main features of this picture should be explained by a full solution of the theoretical models.

2. BASIC PARAMTERS OF THE ANDERSON AND s-d EXHANGE MODELS

The problem of localised moments in metals has been traditionally regarded as the sum of two more or less well separated parts: the formation of the localised moments, and their interaction with the conduction electrons; the connection between the two aspects was clarified only later.

The first aspect has been attacked by Friedel (1956, 1958), who used the concept of resonant scatterint, the model of Anderson (1961) and Wolff (1961) are essentially the mathematical formulations of these ideas.* The appearance of the magnetic moment on the impurity is the result of a balance between two processes: the correaltions between the impurity d-electrons, and the interaction of the impurity states with the conduction electrons.

The intra-atomic interactions favour the polarisation of the impurity states. Two energies play an important role in determining the strength of the polarisation. The intra-atomic exhange energy I, i.e. the difference between the energies of two d-electrons with parallel and anti-parallel spin. The configuration with parallel spins has the lower energy (Hund's rule). The second interaction, the Coulomb term is the electrostatic repulsion between

* Note: The extra orbital model of Anderson (1961) is more appropriate for describing 3d transition metal impurities in simple metals, then the Wolff (1961) model which is used to discuss the local moment formation in transition metal host, see Rivier and Zitkova (1970).

two electrons with antiparallel spins on the same orbital, or between electrons in different orbitals for both spin directions.

In the non-degenerate Anderson model only the Coulomb interaction appears, the corresponding term being $Un_{d\uparrow}n_{d\downarrow}$ where $n_{d\uparrow}$ and $n_{d\downarrow}$ are the number operators for the spin up and spin down electrons on the d-level of the impurity. In Anderson's model (1961) the impurity is a localised extra orbital embedded in a free electron see with energy E_{d6}. In the degenerate case the situation is more complicated, both I and U enter into the Hamiltonian. Intuitively it is clear that although bot I and U favour the polarisation of the impurity states, the concomitant effect of both can lead to a great variety of possible atomic levels and transition between these levels. However, theoretical indications suggest that one might simply replace U by $U + (2\ell + 1)I$ in the degenerate case, ($\ell = 2$ for d states), and then use the theoretical formulas obtained on the basis of the non-degenerate model. As the present status of theory for the degenerate Anderson model is anything but sufficient, we accept this suggestion, and hope for the best.

A considerable controversy exists in the literature about the values of I and U in a metallic state. Both of them are presumably reduced from their atomic values ($U \sim 20$ eV and $I \sim 2$ eV) due to the screening by the conduction electrons, although this screening should not be particularly strong as the impurity states are fairly lo-

calised. The effect of the d-d correlations in the metallic state has been calculated by Schrieffer and Mattis (1965) using the RPA approximation of the Anderson model, according to this calculation, the effective Coulomb interaction is largely reduced compaered to its bare value at $T=0$.

This renormalization, which predicts that the effective interaction energy $U_{eff} < U$ is analogous to the situation in strongly correlated electron gas, where it must be smaller than the bandwidth D. (Herring 1966). In both causes it follows from calculations going beyond the HF approximation, and it is the consequence of the fact, that correlation effects keep the electrons apart, thus reducing the interaction.

The interaction between the d-electrons and the conduction electrons is relatively simple. The conduction electrons penetrate into the d-shell, giving rise to a finite width Δ of the impurity states. These are the virtual bound states (vbs's) in Friedel's treatment. In the Anderson model this process is described by a V_{kd} intraction, and the Golden rule yields

$$\Delta = \pi |V_{kd}|^2 \rho_s(\varepsilon_F) \qquad /1/$$

where $\rho_s(\varepsilon_F)$ is the density of the conduction electron states at the Fermi-level for one spin direction. The virtual bound state has a Lorentzian form, if U and I is zero,

and

$$\rho_d(\omega) = \frac{1}{\pi} \frac{\Delta}{(\omega - E_d)^2 + \Delta^2} \qquad /2/$$

where $\rho_d(\omega)$ is the d-electron density, E_d the position of the d-level relative to E_F. In a metal the impurity potential is easily screened by the conduction electrons to preserve charge neutrality, therefore

$$\langle n_d \rangle = \int_0^{\varepsilon_F} \rho_d(\omega)\, d\omega \qquad /3/$$

is equal to the total number of d-electrons N introduced by the impurity; this self-consistent condition fixes the position of the virtual bound state. Various estimations predict the value of Δ near to one eV. Friedel using resonant scattering formalism arrives at $E_F/3$ for the cose of d-resonance ($\ell = 2$). Anderson and McMillan (1968) calculating the phase shift for a transition metal atom imbedded into muffin-tin potentials, (for situation appropriate for Fe in Cu), obtains a resonance which has a Lorentzian like shape, with $\Delta \sim 1$ eV.

Whether the impurity polarization survives the screening effect of the conduction electrons, or not, depends on the parameters U and Δ. For large U values compared to Δ the screening is not very effective, and the magnetic moment of the impurity persists in the metal, i.e.

$$\langle n_{d\sigma} \rangle \neq \langle n_{d-\sigma} \rangle \qquad /4/$$

while for very small U values the impurity polarization collapses. The transition between these two limits should

be smooth due to the local character of the problem.

The time period, over which the moment exists on the impurity site, is one of the fundamental parameters of the dilute alloy problem. As the d-states are not perfectly localised, and decay into the continuum of s-tates within the single particle lifetime $\hbar/\Delta$, the moment itself has a finite lifetime τ_m, although this time can be much longer than $\hbar/\Delta$. One expects increasing τ_m with increasing U/Δ. However, no satisfactory theory exists which relates τ_m to the above ratio in a self consistent way. While an infinite lifetime is physically inappropriate, it may be long enough for certain situations to cause measurable magnetic effects, like a Curie-Weiss susceptiblity.

The s-d exchange model is based on this supposition. It regards the impurity spin as a well defined quantity (with infinite lifetime), which interacts with the conduction electrons through a Heisenberg type interaction.

$$\mathcal{H}_{sd} = 2\,\mathcal{J}(r)\,S_{imp}\,s \qquad /5/$$

where S_{imp} is the impurity spin, s the spin of the conduction electrons. In contrast to the nuclear hyperfine interaction, an isotropic zero-range potential is a drastic oversimplification here. Beside the direct s-d interaction $\mathcal{J}_{ex}$, which is ferromagnetic, and of the order of 0.2 eV for 3d transition metal atoms (Heeger 1969), the main contribution to Eq /5/ arises from the covalent admixture of the d ans s-states (Anderson and Clogston

1961). This admixture tends to decrease the total polarization, this decrease which can be represented by a negative s-d coupling constant. This contribution to the s-d coupling is certainly a complicated function of r or its Fourier transform $J(k,k')$ to k and k'. Two effects are essential. First of all, the impurity states are not perfectly localised, and therefore Eq/5/ does not represent a zero range interaction. Moreover, such an exchange Hamiltonian describing the interaction between d-states and conduction electrons, sholud preserve the symmetry of the resonant scattering, therefore (Blandin 1968)

$$J(k,k') = J_{eff}\, P_l(\cos\Theta) \qquad /6/$$

where Θ the angle between k and k'; $P(\cos\Theta)$ the and different experiments measure different averages of over k and k'. Later on we use the notation $J_{eff} = (2l+1)J_{eff}$

Not surprisingly, the Anderson model can be transformed to have a form of Eq/5/, in the strongly magnetic limit, i.e. when U and $E_{d\sigma}$ are much larger than Δ. This transformation (Schrieffer and Wolff 1966) then couples the basic parameter of the s-d model to the parameters of the Anderson-model as*

$$J_{eff} = 2\,\frac{|V_{kd}|^2\, U}{E_d\,|E_d + U|} \qquad /7/$$

---

* Note: In the case of the degenerate Anderson model the transformation gives

$$J_{eff} = \frac{|V_{kd}|^2\, U}{E_d\,|E_d+U|\,S_{imp}} \qquad /7a/$$

where S_{imp} is the impurity spin, given by the Hund's rule (Schrieffer 1967)

While the Anderson-model reduces to the s-d exchange model for the strongly magnetic limit, and therefore the concept of describing the impurity as a well defined pre-existing quantity seems to be a reasonable starting point, this is not the case, when U is comparable with Δ and the lifetime of the moment is probably an important parameter. In the opposite limit, $U \ll \Delta$, the moment disppeares, and the impurity looks nonmagnetic. Since the relative magnitude of $U + 4I$ and Δ are fundamental, the determination of these parameters has an especial importance, and we next focus our attention on the evaluation of $U + 4I$, E_d and Δ when using the Anderson model, and J_{eff} and S_{imp} when comparing the experiments with the s-d exchange model.

3. THE H - F APPROXIMATION: CLASSIFICATION OF THE DILUTE ALLOY SYSTEMS

The complete solution of the Anderson model, in spite of its apparent simplicity, it still missing. The problem derives from the many-body interaction between the d-electrons, described by $U n_{d\uparrow} n_{d\downarrow}$ in the nondegenerate case. With the conventional Hartree-Fock (HF) approximation, replacing the effect of the opposite spin electrons by their time average, the model reduces to a one-electron problem, and can be solved easily. The solution defines a sharp boundary at $U\rho_d(\varepsilon_F) = 1$. In the so called nonmagnetic limit ($U\rho_d(\varepsilon_F) < 1$) the vbs in spin degenerate, and has the form of Eq/2/; the different physical parameters are determined by this spin degenerate state. In the magnetic limit ($U\rho_d(\varepsilon_F) > 1$) the vbs is split into two Lorentzian states, one with spin up, the other with spin down, with the energy difference between the two levels

$$\delta E_d = E_{d\sigma} - E_{d-\sigma} = U(\langle n_{d\sigma}\rangle - \langle n_{d-\sigma}\rangle) \qquad /8/$$

The charge neutrality requires $N = \langle n_\sigma \rangle + \langle n_{-\sigma} \rangle$ in this case.

The HF solution can be linked to the phase shift analysis used by Friedel by having

$$\eta_\sigma^{res}(\omega) = \cot^{-1} \frac{\bar{E}_{d\sigma} - \omega}{\Delta} \qquad /9/$$

for the phase shift of the scattered conduction electrons. With this formalism, the charge neutrality is expressed

by the Friedel sum rule (Friedel 1956)

$$N = \pi^{-1} \sum_{\sigma} \sum_{l} (2l+1) \eta_l(\varepsilon_F) \qquad /10/$$

including normal potential scattering with phase shifts η_0 and η_1 too.

Although it has been realized that the HF approximation breaks down progressively going towards larger $U\rho_d(\varepsilon_F)$ values, and overestimates the tendency towards the appearence of magnetic moment by neglecting correlations between electrons with opposite spin, it was believed for a long time to provide a firm theoretical background for the classification of alloys to "yes moment" and "no moment" system. This drastic distinction has been reinforced by experimentalists due to the limited temperature range of the early measurements (performed mainly between liquid helium and room temperature), and only later has it been realized that, by extending the temperature range of the experiments, alloys with magnetic behaviour at conventional temperatures can become non-magnetic by lowering the temperature, and that magnetic behaviour can appear at higher temperatures for alloys, where non-magnetic behaviour has been observed around room temperature.

However, the Friedel-Anderson picture, in the HF approximation serves as a theoretical basis for the single particle resonance formation, and many physical parameters are understandable by considering only this approximation. It is instructive therefore to review those experiments,

which support this scheme, and compare the experimental results with HF predictions.

3.1. Optical Properties

Optical and photoemission studies provide us with the most direct information on the vbs characteristics and on the parameters of the Anderson model. The excitation energies involved in these experiments are large, comparable to $U+4I$ and Δ, and electronic states far from the Fermi level can be studied: a distinct advantage compared with other methods. There are, however, several limitations: the class of alloy systems which can be investigated is rather limited, as the optical properties depend sensitively on the host properties, such as the host d-band absorption. In addition, relatively large impurity concentrations (usually above 1 at.%), are necessary to give significant changes in the optical and photoemission spectrum. In spite of these restrictions, these methods have proved to be powerful in this field, and the experimental reults can be adequately described within the framework of the HF theory.

The optical absorption measures the imaginary part of the dielectric constant, which is proportional to

$$\int \rho_f(\varepsilon)\,\rho_i(\varepsilon - h\nu)\,d\varepsilon \qquad /11/$$

at photon energy $h\nu$, where $\rho_f(\varepsilon)$ and $\rho_i(\varepsilon - h\nu)$ are the optical densities of the final and initial states. From

the various components of the absorption, the intraband transition from the d-level of the impurity to the continuum of the s-states (of the reverse process) can be separated. A simple energy balance consideration gives absorption peaks at $E_{d\sigma}$ and $E_{d-\sigma}$. The width of the observed absorption is larger than the pure d-level width Δ, but one can evaluate Δ and $E_{d\sigma}$ using theoretical expressions (Caroli 1963, Kjöllerström 1969). As the optical absorption is a rather fast process, the parameters determined by this method are probably the "bare" values of the model, i.e. are not influenced by low lying electron correlations. Photoemission, in principle, gives more detailed information about the electronic structure of dilute alloys than optical absorption, as the energies of the emitted electrons can be measured. The number of electrons, photoemitted at energy $\mathcal{E}$ for photon energy is proportional to the product

$$\rho_f(\mathcal{E})\,\rho_i(\mathcal{E}-h\nu) \qquad /12/$$

of the optical density of the final and initial states.

Figure 1 shows the differential absorptivity of CuNi (the difference between the absorptivity of the alloy and pure copper) for different Ni concentrations. A pronounced absorption appears near 1 eV, with a position which is independent of the concentration showing that the effect is due to single nickel impurities. Evaluation of the vbs parameters using Kjöllerström's (1969)

expression gives $E_d = -0.75$ eV and $\Delta = 0.27$ eV (Drew and Doezema 1972). The single absorption peak suggest that the vbs is spin degenerate. Intergrating the Lorentzian density of states characterized by the above parameters, $n_d = 8.9 \pm 0.1$ is obtained. As a Ni atom has 9 d-electrons this value of n_d confirms the charge neutrality hypothesis. Photoemission studies on the same alloy (but with higher Ni concentration) confirm the above vbs parameters (Seib and Spicer 1970). The interband optical absorption observed in AgMn alloys is shown in Figure 2. Two weak absorption peaks are observable at energies around 2 and 3 eV which can be attributed to the added manganese. These peaks indicate a double peaked vbs, in the HF approximation this corresponds to a spin splitting, characteristic to the magnetic limit. According to the analysis of Myers et al (1968) one d-level is 1.6 eV above, the other 3.2 eV below the Fermi surface. With these parameters $E_{d\sigma} - E_{d-\sigma} = 4.8$ eV. Photoemission experiments (Norris and Wallden 1969) indicate a d-level at an energy of 2.8 eV in agreement with the optical data. Moreover, Δ was found to be approximately 0.5 eV. As the splitting is much larger than the vbs width, one vbs is nearly completely filled, the other nearly empty, therefore $E_{d\sigma} - E_{d-\sigma}$ is close to $U+4I$. Therefore $U+4I$ is of about 5 eV, and $(U+4I)/\pi\Delta \sim 3$ placing AgMn in the magnetic limit, which is consistent with the observation of a double peaked vbs.

Recent optical (Steel and Therene 1972) and photoemission (Norin and Wallden 1969) experiments also suggest the same situation in AuMn and CuMn alloys, with a splitting energy of about 5 eV, showing that U + 4I as an intra-atomic property is not influenced strongly by the particular host.

While the experimental situation is not so clear for other alloys, recent experimental results on AuV, AuCr (Steel 1972) and AuFe (Beaglehole and Hendrickson 1969) alloys may be absorbed in a unified picture of the d-resonances. First of all, we can assume that for all of these cases U + 4I ~ 5 eV and $\Delta \sim 0.5$ eV, and so the vbs is split (except probably for Ti and Ni where $\rho_d(E_F)$ is small due to the nearly empty or nearly filled vbs). Then by going from V to Fe, the number of d-electrons increases, and due to the charge neutrality this results, in a progressive filling of the virtual bound state. For V impurities (N = 2 or 3) one virtual bound state is nearly half filled, as evidenced by a slight extra absorption, visible at low energies ($\omega < 0.5$ eV) in AuV (Steel 1972), while the other is well above ε_F and is not observable. In AuCr (N = 4) one virtual bound state is more than half filled, resulting in an interband transition at 1.2 eV (Steel 1972), the other still at high energies. AuMn (N = 5) is in agreement with this picture, as discussed before, and the structure of the optical absorption around 4 eV in AuFe (Beaglehole and

Hendrickson 1969) should correspond to a more than half filled (N = ( ) d-level. The situation is shown in Figure 3, where the position of the Fermi level relative to the d-levels corresponds to the measured absorption peaks. The vbs for nickel, however, is nearly full (N = 9) and so $\rho_d(\ _F)$ is small. Therefore, $(U + 4I)\rho_d(\varepsilon_F) < 1$ and AuNi is in the non-magnetic limit; indeed only one resonance was found which is probably spin-degenerate. (Drew and Doezema 1973)* The situation is far from being clear in Al based alloys. Recently Beaglehole and Will (1972) measured the optical reflectivity of AlMn and AlCu alloys. While an interband absorption at 5 eV below ε_F was observed in AlCu arising from the copper d-states, no pronounced structure, similar to the situation in noble metals, was found in the case of added magnanese impurities. However, a broad interband absorption is evident at energies above 0.5 eV with intensity corresponding to about 5 d-electrons. These observations seem to be contradictory from the HF point of view. As no direct splitting is observed it would be natural to assume that Mn impurities are non-magnetic in aluminium, and the virtual bound state has a single Lorentzian form. In that case, however,

---

* Note: Figure 3 may in some sense be misleading. The energy seapration between the two vbs-s is not U + 4I, but is given by Eq/8/, and therefore is not constant. δE_d is largest in the middle of the series, for Mn, but decreasing for larger and smaller N values.

most of the d-density of states should locate near to ε_f (corresponding to N = 5 and $E_d \sim 0$), and not observable in the experiment, unless Δ is unreasonably large. The dilemma could be resolved by assuming, that the vbs is neither a single Lorentzian, nor completely split: it reflects an intermediate situation between the magnetic and non-magnetic HF description. As the virtual bound state width in aluminium host is expected to be about twice that found in noble metals, i.e. $\Delta \sim 1$ eV (and experiments to be discussed later confirm this estimation), while U + 4I should be the same as in AgMn or AuMn $(U + 4I)\, \rho_d(\varepsilon_F)$ is near to one for manganese in aluminium, the conclusion is not unreasonable.

The Andrson-parameters of the various dilute alloys, investigated up to this time by optical and photoemission methods are given in Table 1. They serve as a firm experimental basis of the Friedel-Anderson scheme. According to the measured parameters U + 4I and Δ , which seem to be reasonably constant (within a factor of two) in the case of noble metals hosts, one would place the HF instability point near to V at the beginning, and near to Co at the end of the series. In the middle of the series $(U + 4I)\, \rho_d(\varepsilon_F) > 1$, and impurities are "magnetic", and at least Mn impurities are well beyond the magnetic-non-magnetic boundary, while at the beginning and at the end (probably only is the case of Ti and Ni), impurities are "non-magnetic". In constrast to this situation, manganese in aluminium seems to be near to the threshold of

of magnetism, $(U + 4I)\, \rho_d(\varepsilon_F) \sim 1$, while other impurities lie further towards the non-magnetic limit, but more detailed experiments are needed to arrive at a firm conclusion.

3.2. Macroscopic properties

Although optical and photoemission experiments give a rather complete picture of the resonance formation in dilute alloys, and confirm the virtual bound state characteristics, predicted by the Friedel-Anderson picture, they are not sensitive to Fermi-surface phenomena. Moreover, as the characteristic time for ejecting an electron from the d-shell is extremely short, they are probably insensitive to low lying fluctuations with a long lifetime. Macroscopic properties, however are sensitive probes of such processes, and unlike the optical data, are determined by effects occurring within an energy range kT around ε_F at temperature T. They should be therefore strongly influenced by dinamical correlations. As the HF approximation of the Anderson model excludes dynamical effects, one has to be carful when comparing the experimental results with theoretically derived formulas which are based on the HF treatment. However, this approximation can serve as a guide for the analysis of experiments, as it will indicate the situations where this approximation is appropriate and the cases where it is insufficient and more elaborate approximation of the models are necessary.

3.1.2. Transport phenomena

The impurity contribution to the transport properties: resistivity R , thermoelectric power S and Lorentz number L^{*} are given by the transport relaxation time $\tau(\omega)$ as

$$\sigma = e^2 K_0 \qquad \text{conductivity} \qquad /13/$$

$$S = \frac{1}{eT}\frac{K_1}{K_0} \qquad \text{thermoelectric power} \qquad /14/$$

$$L = \frac{1}{e^2T}\left(\frac{K_2}{K_0} - \frac{K_1^2}{K_0^2}\right) \qquad \text{Lorentz number} \qquad /15/$$

where $$K_n = G\int_{-\infty}^{\infty} \tau^{-1}(\omega)\,\omega^n \frac{df}{d\omega}\,d\omega$$

and f (ω) the Fermi function, G is a constant. The transport relaxation time can be expressed by the scattering amplitude of the conduction electrons in the case of isotrope scattering and when the optical theorem holds as $\tau^{-1}(\omega) = 2\,c\,\mathrm{Jm}\,t(\omega)$ where c the impurity concentration. In the Anderson model Jm t $(\omega) = |V_{kd}|^2 \rho_d(\omega)$ therefore the transport properties are determined by the density of the d-states near ε_F.

At T = 0 the impurity resistivity has a non-zero value, and is determined by the Fermi surface value of the scattering amplitude:

$$R_{imp}(T=0) = \frac{4\pi\hbar c}{e^2 k_F}\,\mathrm{Jm}\,t(\varepsilon_F) \qquad /16/$$

where $\frac{4\pi\hbar}{e^2 k_F} = R_0$ is the unitarity limit resistivity; with

---

* Note: $L = \lambda/\sigma T$ where λ the thermal conductivity.

the expression of the scattering amplitude, the resistivity at T = 0 is proportional to the density of d-states at ε_F. The thermoelectric power vanishes at T = 0, and the Lorentz number has the Sommerfeld value $L_0 = \pi^2/3\ (k_B/e)^2$ and is not influenced by the impurities.

The temperature dependences of the transport properties are determined by the temperature and by the energy dependence of the scattering amplitude. At low temperatures, making use the Sommerfeld expansion

$$\sigma_4 = \frac{ne^2}{m}\left[\tau^T(\varepsilon_F) + \frac{\pi^2 k^2 T^2}{6}\frac{\partial^2 \tau(\omega)}{\partial \omega^2}\Big|_{\omega=\varepsilon_F}\right] \quad /17/$$

and so $R(T)$ depends on the temperature dependence of the scattering amplitude, as well as on the even derivatives of it. The thermoelectric power depends on the odd derivatives

$$S_{imp} = \frac{k_B}{e}\frac{2\pi^2}{3}T\frac{\partial \tau(\omega)}{\partial \omega^2} \quad /18/$$

and vanishes for a symmetrical scattering amplitude, while L (T) is given by R (T) and S (T) as

$$L_{imp} = L_0\left[1 - \frac{32}{\pi^2}\frac{T^2}{R(T=0)}\frac{\partial R(T)}{\partial T^2} - S^2\right] \quad /19/$$

up to the second order of the Sommerfeld expansion.

The scattering amplitude can be expressed in terms of the phase shifts η_ℓ of the conduction electrons also, and

$$R_{imp}(T=0) = R_0 c \sum_\ell (2\ell+1)\sin^2(\eta_\ell(\varepsilon_F) - \eta_{\ell-1}(\varepsilon_F)) \quad /20/$$

where $\eta(E_f)$ is the phase shift of the corresponding partial wave at the Fermi level. For transition metal impurities the $\ell = 2$ phase shift dominates, η_0 and η_1 can be neglected. Similar type at expressions hold for the TEP and Lorentz number. In the non-magnetic limit of the Anderson model $\eta_\ell(E_f)$ is the same of both spin directions, and with the requirement of the charge neutrality (see Eq/10/)

$$R_{imp}(T=0) = R_0 c\, 5 \sin^2 \frac{N\pi}{10} \qquad /21/$$

The zero temperature resistivity is therefore determined only by the total number of d-electrons, and is not influenced by electron-electron interactions. Eq/21/ suggests increasing impurity resistivity going from Ti to the middle of the series which then dec reases by filling the d-shell. This behaviour has been observed in Al-based alloys /Fig. 4/, where the impurity resistivity has a maximum between Cr and Mn. The non-symmetric behaviour of $R_{imp}(T=0)$ versus N is due to the non-resonant phase shifts, η_0 and η_1 .

In the magnetic limit, the resistivity is given as a sum of the scattering from two independent channels according to the spin-split virtual bound states, and

$$R_{imp}(T=0) = R_0 c\, \frac{5}{2} \left[\sin^2 \eta_\sigma(\varepsilon_F) + \sin^2 \eta_{-\sigma}(\varepsilon_F)\right] \qquad /22/$$

(neglecting the non-resonant phase shifts). The phase shifts are related to the occupation numbers of the virtual bound states by the Friedel sum rule, $\eta_\sigma(\varepsilon_F) = \frac{N_\sigma \pi}{5}$.

The impurity resistivity is then double peaked if the vbs is spl t, hawing a minimum in the middle of the series, when $N_\sigma \sim 5$ and $N_{-\sigma} \sim 0$ (the situation for Mn impurities in noble metals). Fig. 5 shows the room temperature impurity resistivities in Cu and Au based alloys. The close relation between the impurity resistivities and the structure of the virtual bound state is more clearly seen in Fig. 6, where the positions of the virtual bound states with respect the Fermi level for a particular impurity are derived from the occupation numbers N increasing from Ti to Ni as shown in the Figure; the parameters U + 4I and Δ are taken from the optical data /see Fig. 3 /. The impurity resistivities follow well the structure of the virtual bound state, however, the measured values for Mn and Cr impurities are definitely larger than expected on this basis. This deviation can be ascribed to the feature HF approximation which neglects the important consequence of the magnetic impurities: the possibility of the spin-flip scattering. This scattering is important, when the impurity has a well defined spin (and we shall see, this is the case for Mn impuritieis in noble metals). Furthermore, in these cases the s-d model is appropriate, and then the resistivity in first Born approximations reads:

$$R_{s-d} = R_0 c J_{eff}^2 S(S+1) \qquad /23/$$

which is the so called Yoshida limit (Yoshida 1957). One

third of the resistivity comes from non spin flip, and 2/3 from the spin flip scattering. Making use the Schrieffer-Wolff transformation Eq/7/, one can immediately see that Eq/23/ gives three times the resistivity, than that given by the HF expression, Eq/22/. This disagreement is understood, as the HF approximation considers the two (spin up and spin down) scattering channels independently, therefore no spin-flip is allowed in this approximation (Stewart and Grüner 1973). For a numerical example we take the high temperature resistivities of CuMn and AuMn. From expression 22 , and using the optical data for $E_{d\sigma}$ and Δ one arrives at 0.95 $\mu\Omega$ cm/at %, roughly one third of the experimental value. Using Eq/23/ with S = 5/2 the experimental resistivites give j_{eff} = 0.5 eV this value is in accordance with other experimentally determined values of j_{eff}. Therefore, while Eq/22/ serves as a conceptual basis for describing the resistivity behaviour of Fig 6, for a complete understanding both the potential and spin flip scattering has to be taken into account; the importance of spin-flip scattering will become evident later.

De Haas van Alphen experiments which are closely related to the impurity resistivity, also provide us with direct evidence, that the scattering on transition metal impurities has a d-like symmetry. The anysotropy of the conduction electron lifetime due to the particular symmetry of the scattered conduction electrons is different for normal metal and transition metal impurities, and in

the latter case the experiments are in agreement with the assumption of pure d-symmetry for Cu-based alloys (Coleridge and Templeton 1971). The conduction electron lifetimes derived from the de Haas van Alphen experiments were found to be proportional to the transport relaxation times and show the some double peaked behaviour versus the impurity atomic number in copper host as shown in Fig. 5. In case of AlMn (Paton 1971) de Haas van Alphen experiments support the resistivity data, that the scattering is close to the unitarity limit corresponding to N = 5.

While the impurity resistivity and de Haas van Alphen effect parameters are related to the value of the scattering amplitude at the Fermi level*, the thermoelectric power reflects the energy derivative of $t(\omega)$, and so samples the energy dependence of the scattering process. In the non-magnetic limit S is given by

$$S_{imp} = \frac{\pi}{3} \frac{k_B^2}{e} \frac{T}{\Delta} \sin 2\eta_2(\varepsilon_F) \qquad /25/$$

neglecting again the non-resonant phase shifts. The vitual bound state width Δ comes from the energy derivative of $f_d(\omega)$ in Eq/18/, which in the HF approximation has a Lorentzian form. It is basic to observe however, that S reflects the value of $\frac{\partial \tau(\omega)}{\partial \omega}$ at ε_F, which can be different from Δ^{-1} when the virtual bound state has a form different from a simple Lorentzian one. Alterna-

---

* Note: This holds only at T=0. Due to the rather large width of the virtual bound state, the term, proportional to the energy derviative in Eq/17/ is neglected in the HF analysis.

tively, any temperature dependence of $\rho_d(\omega)$ is reflected in /25/ as well.

The thermoelectric power measurements of Boato and Vig (1969) and Cooper et al (1974) in Al-3d transition metal alloys show the same trend as given by Eq/25/, confirming that the virtual bound state is spin degenerate. Neglecting η_o and η_1 and taking $\eta_2(\varepsilon_F)$ from the resistivity data the measured S_{imp} values give $\Delta \sim 1$ eV for Ti and V impurities, while for Fe $\Delta \cong 0.5$ eV and for Mn $\Delta \simeq 0.27$ eV. The non-resonant phase shifts however are important in the latter case, as $\eta_2(\varepsilon_F)$ is near to $\pi/2$ (N = 5), and taking reasonable η_o and η_1 values $\Delta = 0.15$ eV was obtained (Cooper et al 1974). As such a change of factor four or six is not expected in Δ, as it depends mainly on the host properties, the small Δ value found for Mn (and possibly in case of Fe too) indicates a breakdown of the HF approximation going towards the magnetic - non-magnetic boundary, and shows that the scattering amplitude has either a sharper top at ε_F than expected for a simple Lorentzian resonance, and/or the scattering amplitude is strongly temperature dependent.

For copper and gold based alloys the thermoelectric power shows a rather complicated dependence on the impurity atomic number, due to the double peaked virtual bound states in the middle of the servies. (Christienson 1963, Brewing et al 1969). In CuNi the HF analysis gives

Δ = 0.25 eV (Klein and Heeger 1966), which is in good agreement with the optical data, as expected, since CuNi is far from the HF instability of the spin-split vitural bound state (Brewing et al 1969), and reasonable Anderson parameters were found for Cr and Mn impurities, but the objection raised against the HF expression in connection with the resistivity suggests, that any such kind of analysis should be revised.

3.2.2. Specific heat

In the absence of electron-electron interactions the concentration dependence of the electron specific heat coefficient γ_{imp} is proportional to the impurity density of states at the Fermi level. Within the non--magnetic limit of the Anderson model, the HF expression

$$\gamma_{imp} = \frac{3\pi^2}{2} k_B^2 \rho_d(\varepsilon_F) \qquad /26/$$

and knowing the position of the virtual bound state with respect of the Fermi level, Δ can be evaluated from γ imp. As the specific heat may be influenced by low lying fluctuations of the system due to dynamical correlations these fluctuations may lead to an enhanced specific heat. Therefore the deviation of the virtual bound state width, evaluated using Eq/26/ from values inferred from the optical data gives an additive information about the importance of electron-electron interactions.

The impurity contribution to the specific heat of CuNi gives a virtual bound state width $\Delta = 0.4$ eV (Klein and Heeger 1966), a reasonable value, see Table 1, this shows the absence of strong specific heat enhancement. The specific heat values of CuCo and AuV however, are much larger than expected, and evaluating the experimental values with Eq/16/ gives $\Delta = 0.2$ eV and 0.12 eV respectively. Clearly, the HF expression is insufficient to account for the specific heats of these alloys. The situation is similar for Al-based alloys: the specific heat of V, Cr and Mn impurities increases more rapidly than expected from the change of $\rho_d(E_f)$, consequently giving unreasonable small values using Eq/26/ (Aoki and Ohtsuka 1969). For example, $\Delta = 0.16$ eV for AlMn, which, together with our previous estimate $U + 4I \sim 5$ eV would imply that this alloy is far beyond the HF instability point in the magnetic region.

As the specific heat expreiments are restricted to low temperatures, du to the phonon contribution proportional to T^3, no specific heat data relevant to the HF analysis are available for "magnetic" alloys, because the experiments are influenced by interactions between impurity moments, or by the Kondo effect to be discussed later. The magnetic properties are usually connected with specific heat anomalies, mainly arising from ordering effects (du Chatelier and de Nobel 1962).

3.2.3. Magnetic susceptibility

The main features of the Friedel-Anderson picture are well reproduced by the optical, transport and thermal properties, although in some cases the HF approximation of d e model seems to be insufficient. All these parameters are related to the impurity scattering potential, which, in the HF approximation is spin degenerate in the non-magnetic and spin-split in the magnetic limit. This distinction is clearly reflected by the magnetic properties, which have a particular importance. In fact, the notation "magnetic" and "non-magnetic" impurities came from the magnetic measurements, and the magnetic (Curie-Weiss dependence) and non-magnetic (temperature independent Pauli paramagnetism) behaviour was only later related to the properties of the virtual bound state. The connection between the magnetic properties and virtual bound state parameters in clear (at least within the HF approximation). In the case of the spin degenerate virtual bound state the impurity states with opposite spin are equally occupied resulting in no net moment and so in Pauli paramagnetism. The spin split virtual bound state, on the other hand gives a finite z-component of the magnetization $m_z = \mu_B (\langle n_\sigma \rangle - \langle n_{-\sigma} \rangle)$ with infinite lifetime, and therefore leads to a paramagnetic, strongly temperature dependent susceptibility. In the non-magnetic limit the spin and orbital suscep-

tibility is given by (Dworin and Narath 1970)*

$$\chi_{spin} = 2\,\mu_B^2\,\rho_d(\varepsilon_F)\,\eta_{spin} \qquad 27a$$

$$\chi_{orb} = 2^{\,2}\,\rho_d(\varepsilon_F)\,\eta_{orb} \qquad 27b$$

where in the HF approximation the so called enhancement factors

$$\eta_{spin}^{-1} = \left[1 - (U + 4I)\right]\rho_d(\varepsilon_F)/5 \qquad 28a$$

$$\eta_{orb}^{-1} = \left[1 - (U - 1)\right]\rho_d(\varepsilon_F)/5 \qquad 28b$$

the total impurity susceptibility $\chi_{imp} = \chi_{spin} + \chi_{orb}$. The spin enhancement diverges at $(U + 4I)\,\rho_d(\varepsilon_F) = 1$, while the enhancement of the orbital contribution is determined by U - I; the condition for the occurence of spin magnetism is therefore more favourable than that of orbital magnetism. When the impurity is far from the magnetic limit, and the enhancements are small, the orbital susceptibility dominates, but is overwhelmed by the spin component going towards the magnetic limit.

When $(U + 4I)\,\rho_d(\varepsilon_F) > 1$ a net magnetic moment develops and in the phase-shift formulation

$$S_{imp} = \frac{1}{\pi}\left[\eta_{2\sigma}(\varepsilon_F) - \eta_{2-\sigma}(\varepsilon_F)\right] \qquad /29/$$

The susceptibility shows a Curie behaviour

$$\chi_{imp}(T) = \frac{\mu_{eff}^2}{3k_B T} \qquad /30/$$

characteristic to isolated, well defined spins.

---

* Note: Eq.27 and 28 are derived on the basis of the degenerate Anderson model; the nondegenerate model gives $\chi_{orb} = 0$.

The experiments support this classification of the HF approximation, and generally, temperature independent susceptibility was observed in cases, where the transport and thermal properties indicate spin degenerate virtual bound state, while strong and temperature dependent susceptibility was found in cases, when the virtual bound state is spin split.

The fairly small, and temperature independent susceptibility of AuNi and CuNi alloys indicates a small enhancement (Klein and Heeger 1966) η spin ~ 4 for CuNi if one includes X_{orb} (which is probably unenhanced) in the analysis. The small enhancement found in this case is the consequence of the small d-density of states at $\mathcal{E}_F$. For CuCo, AuCo χ is temperature independent (Rizzuto 1974) at low temperatures, but enhanced, this enhancement correlates with the small effective width's derived from the specific heat. Moreover, at high temperatures χ is slightly temperature dependent, and can be fitted with a Curie-Weiss law, the Curie-constant θ being of the order of room temperature.

In this respect, these borderline alloys, where $(U + 4I)\ \rho_d\ (\mathcal{E}_F) \sim 1$, look "magnetic" at high, and "non-magnetic" at low temperatures, a behaviour which cannot be explained by the HF approximation.

The evaluation of the impurity susceptibility in Al-based alloys is influenced by the paramagnetic behaviour of pure aluminium (Aoki and Ohtsuka 1969). X_{imp} however, is nearly temperature independent. The enhancement

increases rapidly going towards the middle of the series, showing that an increase of $\rho_d(\varepsilon_F)$ gives increasing enhancement factors, in accordance with Eq/28/, but an analysis of η_{spin}, using the HF expression, gives incompatible parameters U + 4I and Δ, suggesting the breakdown of the HF approximation for impurities where $(U + 4I)/\pi\Delta \sim 1$.

Cr, Mn and Fe in noble metals on the other hand show a Curie-Weiss susceptibility in a broad temperature range (Hurd 1967, 1969) and can be fitted by

$$\chi_{imp}(T) = \frac{\mu_{eff}^2}{3k_B(T+\Theta)} + \chi_\infty \,. \qquad /31/$$

The detailed concentration dependence of the susceptibility confirms that the finite Curie temperatures do not arise from impurity-impurity interactions, and are an inherent properties of the single impurities. Θ is the smallest in the middle of the series (for Mn impurities it is practically zero), and increases going away from the symmetrical case. This behaviour, which correaltes with the increase of the density of d-states at the Fermi level, or in the s-d model with J_{eff} suggest, that Θ reflects the strength of the interaction of the localised moment with the conduction electrons. The magnetic moments evaluated from $\chi_{imp}(T)$ have a well defined trend: μ_{eff} is the largest in the middle of the series, and decreases with increasing or decreasing N. This behaviour - similar to that found in nonmetallic compounds of iron group metals - shows the spin and orbital moments

are decoupled, and the orbital moment is quenched. The reason for this however is different in the two cases: for the compounds this quenching is brought about by the crystalline field, for the impurity case crystalline field splitting is presumably small, and the quenching is due to the fact that $(U - I)\,\rho_d(\varepsilon_F) < 1$ which does not allow the orbital moment to develop. Furthermore, the paramagnetic moments are close, but definitely smaller than $\mu_{eff} = g\ S(S+1)$ with g=2 and S corresponding to the Hund's rule. This reduction is understood within the Anderson model, and is due to the overlap of the two virtual bound states. In fact the observed μ_{eff} values together with the transport properties can be analyzed using the HF scheme with two phase shifts corresponding to the spin up and spin down electrons (Daniel 1962). In the s-d model the antiferromagnetic polarization caused by the impurity in the conduction electron gas is responsible for this reduction, and then

$$\mu_{off} = \mu_{imp}\left[1 - (2l+1)\, j_{eff}\, \rho_s(\varepsilon_F)\right]$$

where the factor $(2\ell + 1)$ is due to the consequence of Eq/6/. In CuMn for example the measured spin S=2, 13 (Hurd 1969), and with the bare spin S=5/2, Eq/32/ gives $J_{eff} = -0.3$ eV. The larger reduction of S suggest increasing J_{eff} for Cr and Fe impurities, a tendency compatible with the Schrieffer-Wolff transformation Eq/7/. Altrough the doserved μ_{eff} values are explained within the framework of both models, and by virtue of the

Schrieffer-Wolff transformation one arrives at the same result, there is a fundamental difference between the two descriptions: in the Anderson model the reduction of μ_{eff} occurs at the impurity site, in the s-d model it is due to the polarization of the conduction electron gas.

3.2.4. Transport properties in magnetic field

Among the magnetic field dependence of the various transport properties the giant negative magnetoresistance, was one of the first effects described by the s-d exchance model. It arises from the freezing in of the spin flip scattering by the application of an external magnetic field. The magnetic field induces a finite energy difference between the initial and final state, this difference is equal to $-2\mu_B H_0$ (for a spin up final state) in case of spin flip scattering. As only electrons within an energy region kT around $\mathcal{E}_F$ are allowed to take part in the scattering, this spin flip process is frozen in, when $\mu_B H_0 / kT > 2$, leaving only the non spin-flip process operating at high magnetic fields. Using the perturbation theory (with zero potential scattering)* in second order (Beal-Monod and Weiner 1968)

$$\frac{R_{imp}(H_0)}{R_{imp}(H=0)} = 1 - \frac{4g^2\mu_B^2 H_0^2}{27(k_B T)^2} \qquad /133/$$

---

* Note: For the effect of potential scattering as well as for the third order calculation of the magnetoresistance see Beal-Monod and Weiner, (1968).

at low external magnetic fields. As no spin flip scattering process is considered, it is not surprising, that the HF approximation in the magnetic limit does not give the above effect, and results only in a change of the potential scattering, through the slightly magnetic field dependent phase shifts. In actual situations both effects (the freezing in of spin flip scattering and the change of the potential scattering) has to be taken into account, but whenever a well defined moment appears, the former is dominating.

In CuMn and CuFe alloys (Monod 1967), the magnetoresistance is proportional to H^2, as in Eq/33/, and J_{eff} = -0.30 eV for CuMn and -0.9 eV for CuFe. Similar values were found for manganese and iron impurities in gold (Rohrer 1968).

It should be mentioned, that impurity-impurity interactions give similar effects than the external magnetic field, and this behaviour is understood as the freezing in the spin flip scattering by internal fields produced by the impurities (see for example Beal-Monod and Matho, 1972).

3.3. Local properties

Local methods provide us with very important information on the microscopic properties of dilute alloys, and have especial importance due to the local character of the problem. The various local properties, in fact, have a rather close relation to the parameters, measured by macroscopic methods, and a concomitant analysis of both macroscopic and local informations often results in a rather complete picture, if often contradictory at first sight. Up to this time Mössbauer effect (ME), nuclear magnetic resonance (NMR), nuclear orientation (NO) and electron spin resonance (ESR) have been wiledy applied to study the dilute alloy properties. Other techniques like neutron scattering, while potentially very useful, are only recently being used to study this subject. We confine ourselves therefore only to those methods, which have contributed essentially to our understanding of this field.

The advantage of nuclear methods lies in the fact, that the interaction energy between the nuclei and the electrons is small compared with the electron energies, characteristic of the dilute alloys, and so the nuclear system is a passive observer of the electronic properties. This situation does not hold for ESR where the perturbation of the electronic system supplies the information, and therefore makes the interpretation of the experiments more difficult.

The time scale of the various methods compared with the characteristic electron lifetime is critical. In the case of nuclear methods it is determined by the inverse Larmor frequency ω_0^{-1} which depends on the nuclear gyromagnetic factor and on the hyperfine interaction. When ω_0^{-1} is larger than the lifetime of the electron excitations, time averages, when ω_0^{-1} is smaller, instantaneous electronic properties are measured. As ω_0 is of about $10^7 \ldots 10^9$ sec^{-1}, while the characteristic electron lifetimes are usually of about 10^{-12} (depending however sensitively on the particular alloy), these methods measure time-average properties, except of few case of NO, a method which works at very low temperatures. In the case of NMR the time evolution of the electronic processes can also be studied by measuring the nuclear relaxation times. The resolution of the various methods are determined either by the inhomogneous broadening, always present even in pure metals, or by the lifetime of the excited nuclear states, resulting in a lifetime broadening in the particular measurement. Using these methods one can investigate the impurity hyperfine properties, which are related to the susceptibility localised on the impurity site. Such kinds of experiments are sensitive probes of effects like impurity-impurity interactions, which are difficult to separate from the single impurity effects by macroscopic methods. Measurement of the host properties (mainly by the NMR method) gives

information on the spin and charge perturbation around the impurities.

Various nuclear methods measure the energy difference and the transition rates between the nuclear Zeeman levels. In an external magnetic field H_0 the nuclear energy is given by

$$\mathcal{H} = -\gamma_N \hbar J H_0 \qquad /34/$$

where γ_N is the nuclear gyromagnetic factor and J the nuclear spin. Magnetic interactions between the nuclear magnetic moment and the local magnetic fields, and electric interactions between the nuclear electric quadrupole moment and electric field gradients act as a perturbation of the nuclear Zeeman levels. The magnetic interation can be represented by a hyperfine field H_{hf}, and similarly to Eq/34/

$$H_m = -\gamma_N \hbar J H_{hf} \qquad /35/$$

where H_{hf} has three components: the Fermi contact H^f, the dipolar H^d and the orbital H^o term. The effect of the electric interaction on the nuclear Zeeman levels is more complicated due to the tensor character of the field gradient. Assuming however, that the asymmetry paramter is zero, the quadrupole Hamiltonian has a simple form

$$H_Q = \frac{3e^2m}{4J(2J-1)} qQ \qquad /36/$$

where Q the nuclear quadrupole moment, q the main component of the field gradient tensor, and m are the eigenvalues of J^Z (Cohen and Reif, 1965).

Both the magnetic and electric interactions induce a change in the static and dinamic properties of the nuclear system. In one respect they result in a change of the position and shape of the NMR signal measured by steady state methods or that of the Mössbauer line. On the other hand they influence the transition probabilities between the different energy levels and lead to relaxation effects measured by transient NMR techniques. As the static and dynamic properties are influenced by the same interaction mechanism, one expects a close relation between them. In the following we discuss briefly the basic parameters measured by nuclear methods and their relation to the local properties, as well as experiments in the light of the Anderson model.

3.1.3.1 Local magnetic properties

The local magnetic properties of dilute alloys have been recently discussed by Narath in several excellent Review Papers (1972b, 1974) and so we will only briefly recount the basic features.

In simple metals, where the d-band character is negligible, the dominant magnetic term is the Fermi-contact interaction between the nuclei and the electrons

$$H = \frac{8\pi}{3}\gamma_N\gamma_e\hbar J\sum_i S_i\,\delta(r_i) = AJ\sum_i S_i\,\delta(r_i) \qquad /137/$$

where γ_e is the electron gyromagnetic factor, S_i the electron spin and r_i the position of the i^{th} the electron

in the metal. The summation is over the conduction electrons. The static component of the interaction /37/ gives rise to a shift of the resonance line, proportional to the Z-component of the electron polarization the magnitude of this shift can be described by an effective field

$$\Delta H = -\frac{A}{\gamma_N \hbar} \langle \sigma_z \rangle = H_{hf} \langle \sigma_z \rangle \qquad /38/$$

The transverse fluctuations of the electronic system at the Larmor frequency $\omega_0 = \gamma_n H_0$ lead to a relaxation of the nuclear system towards thermal equilibrium. (This relaxation process, expressed by the spin lattice relaxation time T_1 is determined by the imaginary part of the dynamical susceptibility, $\chi''(\omega_0, q=0)$.) With

$$\langle \sigma_z \rangle = H_0 (\gamma_e \hbar)^{-1} \chi(0,0)$$

the resonance shift relative to the external magnetic field is given by

$$K = \frac{\Delta H}{H_0} = \frac{2 H_{hf}}{\gamma_e \hbar} \chi(0,0) \qquad /39/$$

The relaxation time can be evaluated similarly, and the relation between K and T_1 is given by the well known Korringa relation

$$K^2 T_1 T = S' \qquad S' = \left(\frac{\gamma_e}{\gamma_N}\right)^2 \frac{\hbar}{4\pi k_B} \qquad /40/$$

for a free electron gas. The electron-electron interaction influences both K and T_1, leading to a modified S' value.

The impurity electron states are d-like and so the d-spin susceptibility induces a hyperfine field at the impurity nuclear site through the core-polarisation effect. Furthermore, the orbital susceptibility, given by Eq/27b/ contributes to the hyperfine field, while the s-contact hyperfine field can be neglected. The impurity Knight shift has therefore two components

$$K_{imp} = K_d + K_{orb} \qquad /41/$$

where

$$K_d = H^d \chi \quad \text{and} \quad K_{orb} = H^{orb} \chi_{orb} \qquad /42/$$

χ_d and χ_{orb} are given by Eq/27/. The hyperfine coupling constant is negative for the spin and positive for the orbital contribution and H^{orb} is about an order of magnitude larger than H^d. The expressions of the relaxation rates and the Korringa products for the spin and orbital contribution have a simple form as the enhancement factors appearing in the susceptibility are independent of the wave number. While the zero frequency susceptibilities are enhanced by η, $\mathrm{Im}\,\chi(\omega_0, q)$ is enhanced by η^2, and so η drops out from the Korringa relation

$$(K^2 \; T_1 \; T)_d = 5 \; S' \qquad (K^2 \; T_1 \; T)_{orb} = 10 \; S' \qquad /43/$$

where the factors 5 and 10 come from the $(2\ell + 1)$ fold degeneracy of the d-states. Although the relation /43/ has been derived within the framework of the HF approximation, it should have a more general validity, as it is

independent of the enhancement factor. By measuring K_{imp} and $T_{1\ imp}$ and using equation /41/, /42/ and /43/ the two contributions of the local susceptibility can be separated, whereas in the macroscopic susceptibility X_{spin} and X_{orb} is inseparable mixed together.

While the line shift is the most drastic effect observed by continuous wave NMR, a pronounced impurity signal broadening is also observed due to the interaction between the impurities.

Table 2 shows the impurity Knight shifts and relaxation times of non-magnetic alloys, taken from Narath (1972b), and for CuCo from Wade and Asayama (1971). The decomposition of the shifts and relaxation times into the spin and orbital parts using Eqs/42/ and /43/ gives the K_d and K_{orb} values shown in the columns 4 and 5. In CuNi the orbital part dominates (this alloy being far from the HF instability point) resulting in a positive impurity shift. This is the situation in CuCo as well, but the spin contribution is increased as this alloy is closer to the magnetic limit. The increase of the spin susceptibility going towards larger $(U + 4I)\ \rho_d(\varepsilon_F)$ values is evident in the case of the 3d impurities in aluminium. While the orbital part changes by only a factor of two going from V to Mn, the spin contribution shows a large increase, similar to the macroscopic susceptibility. Last column of Table 2 shows the d-hyperfine coupling constans derived by comparing K_d with X_d, using Eq/30/. For the Al-based

alloys H^d is close to the core polarisation coupling constant - 120 kG/μ_B, indicating that the susceptibility is localised to the impurity site, while in the case of noble metal hosts H^d is reduced compared with the Al-alloys. The main new result of the impurity hyperfine studies is the demonstration of the existence of the orbital susceptibility, which underlines the importance of the orbital degeneracy in the case of 3d-transition metal impurities.

When the impurities are "magnetic", a greatly increased local hyperfine field is expected due to the large spin susceptibility, which, moreover is temperature dependent, the orbital susceptibility in this case gives a small temperature background. Among the magnetic alloys the impurity hyperfine properties of CuFe have been widely investigated by ME in a broad temperature range. The hyperfine field splitting of the Mössbauer line can be related directly to the impurity spin, derived from the susceptibility by $S_z = \chi_{imp} H/g\mu_B$. Fig. 7 shows the ^{57}Fe hyperfine fields versus the susceptibility, the latter is given by a Curie-Weiss law in the whole temperature range; this analysis in due to Golibersuch and Heeger (1968). The proportionality of H_{hf} to the macroscopic susceptibility indicates no change in the local parameters, such as the localisation of the impurity states as a function of temperature (such a temperature dependent localization would result in a T-dependent H_{hf}). The straight line drawn through the experimental points gives H^d = -47 K Oe/μ_B

a hyperfine field coupling constant, considerably smaller than those found for impurities in aluminium. This anomalous low value is still the subject of considerable speculation. It has been suggested to arise from the positive s-plarisation (Campbell 1970) or due to the orbital contribution to the hyperfine field (Hirst 1971). The reduction of H^d however, seems to be correlated with the matrix properties rather than with the impurities itself. While it is near to the core polarisation constant in Al-based alloys, values near to that observed in CuFe were found for other impurities in noble metal hosts, and the reduction is even larger in the case of 3d-hosts (Narath 1972). This correlation with the matrix properties suggest, that H^d may reflect the extension of the virtual bound state due to the momentum and energy dependence of the s-d interaction.

The host hyperfine field properties are determined by the conduction electron polarisation contribution in simple hosts (where the d-band contibutes negligibly to the hyperfine field) and reflect the distribution of the magnetization around the impurities. This magnetization has been first derived within the s-d exchange model, and is given by the familiar Rudermann-Kittel - Kasuya - Yosida (RKKY) spin perturbation (Kittel 1963).

$$\langle \sigma(r) \rangle = \frac{9\pi}{2} \frac{(2l+1)\, j_{eff}}{\hbar^2 \varepsilon_F} \frac{r\cos 2k_F r - \sin 2k_F r}{(k_F r)^4} \langle S_z^{imp} \rangle \qquad /44/$$

The oscillatory behaviour is the consequence of the Fermi-gas character, the amplitude is proportional to the Z-component of the impurity spin, and to the exhange

constant.

As $\langle S_z^{imp} \rangle = \frac{\chi_{imp} H}{g\mu_B}$ the amplitude of the oscillation is proportional to the impurity susceptibility. Integration over r leads to a finite polarization, to the so called Zeener term, proportional to $J_{eff} \rho_s(\epsilon_F)$.

This spin perturbation can also be derived from the Anderson model, where in the magnetic case the two virtual bound states result in change perturbations which are different for the opposite spin electrons. The difference between the two charge perturbations is determined by the Anderson parameters $E_{d\sigma}$ and U + 4I. When one virtual bound state is nearly full, and the other nearly empty, the resulting perturbation has a spatial dependence similar to the RKKY perturbation. Comparing the oscillation amplitude, derived in this way with Eq/44/ one gets back the Schrieffer-Wolff result (Blandin 1967). This one-to-one correspondence, in contrast to the resistivity, derives from the fact that both in the HF approximation, and in the derivation of the RKKY oscillation, Eq/32/, the impurity moment is fixed, and no spin dynamics is involved. This correspondence can be used to define an effective s-d coupling constant J_{eff} for small $(U + 4I)/\Delta$ values, well outside the Schrieffer-Wolff limit. By comparing the resulting spin perturbations, obtained from both models,

$$J_{eff} = \frac{2(2l+1)}{3} \frac{\epsilon_F g\mu_B}{m\pi Z} |\sin\delta| \qquad /45/$$

where δ is the difference of the spin up and spin down phase shift

$$\delta = \frac{\pi m}{\mu_B (2l+1)}$$

with $m = g\mu_B \langle S_z \rangle$.

This value of J_{eff} should probably also hold for borderline cases, where U + 4I and E_d are comparable with Δ.* It should be mentioned, however, that while the form of the spin perturbation of Eq/44/ holds rather well for small distances in the Schrieffer-Wolff limit, preasymptotic effects (Klein 1969), have an increasing importance, when the energy dependence of the scattering is large at the Fermi level, i.e. for cases when E_d is comparable to Δ. As Eq/44/ has been derived by assuming $J(k, k') = \text{Const.}$, these preasymptotic effects may probably be incorporated into the s-d model, by taking into account the wave-number dependence of the s-d exhange constant. By all means, the appearance of preasymptotics suggest a progressive breakdown of the well defined character of the impurity moment for smaller $(U + 4I)/\Delta$ values.

The distribution of the z-component of the magnetization causes a hyperfine field distribution according to Eq/38/, this is measurable only by NMR which has an energy resolution about two orders of magnitude larger than that of the Mössbauer-effect. When the hyperfine field shift at a

---

* Note: The two perturbations, derived from the Anderson and s-d models have the same form only in the symmetrical case, when $E_d = U/2$, otherwise the phases of the two oscillations are different, making the comparison somewhat ambiguous.

particular neighbour shell is larger than the original line width, a satellite apperars near to the central line othervise it contributes to the broadening of the main line. This broadening is expressed as

$$\langle \Delta H \rangle = j_{eff} \frac{g(2\ell+1)\pi}{\gamma\hbar\, \varepsilon_F} \left\langle \frac{\cos 2k_F r}{r^3} \right\rangle \langle S_z^{imp} \rangle \qquad /46/$$

where the bracket means an average over the lattice sites. $\langle \Delta H \rangle$ is the line width of the distribution of the local magnetization, this distribution is usually assumed to have a Lorentzian form. $\langle \Delta H \rangle$ therefore is proportional to the z-component of the impurity magnetization, and so reflects X_{imp}. The amplitude of the oscillation can be determined from a computer analysis of the NMR line. Such an analysis has been performed in a number of cases and the relation between $\langle \Delta H \rangle$ and X_{imp} is well established. A nearly temperature independent line boradening was found in AlMn (Alloul et al 1971), the line width was proportional to the external magnetic field, giving evidence that the line boradening has a magnetic origin. The oscillation amplitude is in general in agreement with the value of $\mathcal{J}_{eff}$ given by Eq/45/ with m inferred from the macroscopic susceptibility. Moreover, the field dependence of the resonance signal is about twice as strong in AlMn than in AlCr (Grüner et al 1971), and scales with the ratio of the macroscopic susceptibilities. Following the classicial investigation of Owen et al (1966) on CuMn, systematic measurements of Sugawara (1961) on Cu-based alloys showed, that the line boradening reflects the scheme emerging from the susceptibility:

while strong and temperature dependent line broadening was found for Cr, Mn and Fe impurities, $\langle \Delta H \rangle$ was temperature independent and much smaller in case of Co and Ni. The detailed line-shape analysis of Chapman and Seymour (1958), Mizumo (1971) and Golibersuch (1970) resulted in J_{eff} = 0.5 eV for manganese impurities in copper, and the effective s-d exchange constants increase rapidly going towards the beginning and towards the end of the 3d-series, in accordance with Eq/45/ and /46/. No shift of the resonance signal was found, however, in these case, indicating the absence of a Ze ner-like polarization.

While the relaxation process due to the magnetic interaction given by Eq/37/ is well understood in simple metals and in the case of impurity hyperfine properties in dilute alloys, the situation becomes complicated when looking at the relaxation of the host nuclear system, as different processes of the concomitant spin flip of the electronic and nuclear spins must be taken in to account. At low external magnetic fields the direct relaxation process, the real excitation of the impurity through a mutual electron-nuclear spin flip is important (Benoit et al 1963) while in high magnetic fields this process is forbidden in lowest order, and the virtual excitation of the impurity spin, which is then de-excited by the interaction with the conduction electrons is dominant (Giovannini and Heeger 1969 , Sólyom 1971). While it was claimed that experiment could be described by

either of these processes, giving some information on the dynamics of the impurity spin embedded in a simple host, recent experiments of Alloul and Bernier (1972) revealed that the relaxation process determined by the dipole-dipole interaction between the impurity and nuclear spins is dominant. Due to the complexitiy of the problem, however, the situation is not completely clear even in cases where the existence of the impurity spin is not in question as in CuMn, and while large contribution to the hos spin-lattice relaxation time were observed in a number of alloys like AlMn (Alloul et al 1971) and CuFe (Alloul and Bernier 1972; Potts and Welsh 1971), attempts to account for the observed relaxation effects have been unsuccessfull. For details of relaxation processes and their separation see the Review Paper of Alloul and Bernier /1974/.

3.1.3.2 Local electric properties

The electric field gradient q determining the strength of the electric interaction (called quadrupole effect in the following) arises as a result of the distribution of conduction electrons which screen the impurity. This charge perturbation is determined by the features of the impurity scattering potential, and so has a rather close relation to the transport properties. In the asymptotic range ($r \to \infty$), it has its well known Friedel form

(Friedel 1958).

$$\Delta\rho(r) = \frac{-\alpha}{2\pi^2 r^3}\cos(2k_F r + \varphi) \qquad /47/$$

where the oscillation amplitude α and phase factor φ can be expressed either by the scattering amplitude $t(\ .\ )$ or by phase shifts $\eta_\ell(\varepsilon_F)$.

The expression for α and φ, analogous to the expression of the resistivity, Eq/20/

$$\begin{aligned} \alpha\cos\varphi &= \tfrac{1}{2}\sum_\ell (-1)^\ell (2\ell+1)\sin 2\eta_\ell(\varepsilon_F) \\ \alpha\sin\varphi &= \sum_\ell (-1)^\ell (2\ell+1)\sin^2\eta_\ell(\varepsilon_F). \end{aligned} \qquad /48/$$

Neglecting again the non-resonant phase shifts, in the non-magnetic limit the oscillation amplitude is the same for both spin directions, and using Friedel sum rule $\alpha = 5$ in $N\mathcal{T}/10$. Thus α goes as the square root of the resistivity, see Eq/21/. In the magnetic limit the charge perturbation can be expressed as the sum of perturbations by the two virtual bound states, and one arrives to a formula for a similar to the expression for the resistivity Eq/22/. Broadly speaking the behaviour of the resistivity and oscillation amplitude versus the impurity atomic numbers should have a close similarity, both in the magnetic and non-magnetic limits. An important difference between α and $\mathcal{R}_{imp}$, that while the temperature dependence of the resistivity (and the other transport and thermal properties as well) is determined by both the temperature and energy dependence of the scattering amplitude, and they enter in $\mathcal{R}_{imp}(T)$ in a symmetrical way,

the oscillation amplitude in the asymptotic limit reflects only the temperature dependence of the Fermi level value of $t(\varepsilon_F)$, (Grüner and Hargitai 1971) i.e.

$$\alpha(T) = Re\left[t(\omega)\exp(ikr)\right] \qquad /49/$$

The energy dependence of the scattering amplitude is reflected by the behaviour of the charge perturbation near to the impurities. Inside a coherence length, defined by

$$\xi_\Gamma = \frac{v_F}{2\Gamma} \qquad /50/$$

for a scattering amplitude having a Lorentzian form with a width Γ serious deviations are found from the asymptotic expression, Eq/47/. The main effect is a strongly reduced oscillation amplitude for distances $r < \xi_\Gamma$, the effect depends also on the position of the resonance, and is largest if $E_d=0$ (Mezei and Grüner 1972). It is important to realize, that Γ defined in Eq/50/ is not the same width of the resonance than that one infers from the macroscopic properties. It is determined by the average energy dependence of the scattering, simply because the charge perturbation is not a Fermi surface effect, and not only by the behaviour of $t(\omega)$ within a region kT around ε_F. This difference can be very pronounced, if the virtual bound state has a form, different from a simple Lorentzian resonance.

The distribution of the screening charge around the impurities gives rise to a field gradient, expressed as

$$\Delta q(r) = \frac{8\pi}{3} \beta \Delta\varrho(r) \qquad /51/$$

where β is the so called anti shielding factor, resembling the host atom properties. The quadrupole interaction Eq/36/ between Q and Δq has an energy which is usually much smaller than the energy difference between the nuclear Zeeman energies, and can be treated as a perturbation. In first order only parts of the transitions between the Zeeman levels are perturbed, giving the so called first order quadrupole effect, while in second order the central $(-\frac{1}{2} \rightarrow \frac{1}{2})$ transition is also influenced by the quadrupole interaction (second order quadrupole effect). The expression for the modified Zeeman energies will not be reproduced here (Das and Hahn 1958), we only mention, that for a single field gradient Δq the shift of the Zeeman levels depend on the angle between the external magnetic field and the orientation of Δq resulting in a particular distribution in policrystalline samples. In simple metals with qubic symmetry $q = 0$ and no quadrupole effect occurs, the situation is the same for the impurity site in dilute alloys at low concentrations, where the impurity is surrounded with qubic symmetry. The distribution of the field gradient in the host matrix due to the charge perturbation around the impurities results however, in a change of the host resonance signal parameters. Due to the particular angular dependence of the quadrupole perturbation the effect on the main resonance signal is an amplitude reduction and usually only

a slight boradening is observed. The amplitude reduction can be characterised by the so called first and second order wipe out numbers n_1 and n_2, and the signal intensity, due to some statistical consideration is given by Rowland 1960)

$$D = D_S(1-c)^{n_1} + D_C(1-c)^{n_2} \qquad /52/$$

at impurity concentration c where D_S and D_C are the satellite and central components of the resonance signal. The measured wipe out numbers correspond to the number of nuclei within a sphere with radius r_1 and r_2, which feel a field gradient larger than a critical value q_{r_1} and q_2 corresponding to the first and second order quadrupole effect. The radius of the spheres is given by $r_{1,2}/a_0 = \left(\frac{3n_{1,2}}{4\pi N'}\right)$ where N' the number of atoms in the unit cell, thus giving a characteristic range of the perturbation. Though this a highly oversimplified picture, it works well for practical purposes probably becaues of the drastic distance dependence of the charge perturbation. The measured wipe out numbers can be related to the amplitude α of the charge perturbation, assuming the assymptotic from Eq/49/ with this assumption α is proportional to n. When large preasymptotic effects are expected a more elaborate line shape analysis is necessary.

The magnetic and electric perturbations can be separated by measuring the parameters of the resonance signal at various external magnetic fields: while the effect of the spin perturbation is proportional to the

external magnetic field, the first order quadrupole effect is independent of H, and the second order effect is proportional to H^{-1}.

A rather powerful technique, worked out in the last years, detects pure quadrupole transitions between enegy levels, split by the quadrupole interaction. By this method, the charge perturbation at different neighbours of the impurities can be detected separately, allowing the radial dependence of the perturbation to be determined (Minier 1969, Berthier and Minier 1972).

The quadrupole effect investigation on copper or aluminium based alloys clearly show the increased scattering of conduction electrons in case of transition metal impurities. Large quadrupole effect (about 3-10 times larger than for normal metal impurities) was observed by Rowland and Shiotani (1965) and by Tompa (1972) in CuNi, CuPt and CuPd alloys, the oscillation amplitudes scale roughly with the impurity resistivities and are adequately described by resonant phase shifts $\eta_2(\varepsilon_f)$. Such kind of analysis gives $_d$ = 9,6 for CuNi in reasonable agreement with the optical data. A strongly increased quadrupole effect was observed in Al-3d transition metal alloys (Brettel and Heeger 1967, Grüner 1972) where the first order wipe out numbers extrapolated to T=0 show the same single peaked behaviour like the impurity resistivity shown in Fig.3., and the oscillation amplitude can be described by $\alpha = 5 \sin \frac{N\pi}{10}$, the temperature dependence of this perturbation will be

discussed later. Among the magnetic impurities, the change perturbation around Mn in copper has been measured (Lumpkin 1967, Tompa 1971), and the results are in agreement with the HF picture resulting in a small $\mathcal{L}$, similarly to the small impurity resistivity. Here again a phase shift analysis using different $\eta_2(\epsilon_F)$ values for different spin directions works with more or less sucess, however, spin flip scattering is probably as important as for the resistivity.

3.3.3. Electron spin resonance

Electron spin resonance in dilute alloys has been observed only in few situations, aminly in cases of Mn and Cr impurities. The narrow resonance lines found indicate long living impurity spins, which are weakly coupled to the sorrounding. Here the s-d model gives an appropriate description, and many features of ESR have a close relation to NMR. The basic difference between the coupling of the conduction electrons to impurity spins and nuclear spins (i.e. large coupling and same resonance frequencies of the coupled systems in the former case) however, have a strong influence to the dynamics, leading to bottleneck effects etc. The main aspects of ESR in alloys were discussed by Wolleben and Coles (1973) and with a more detailed comparison between the theoretical and experimental status by Heeger (1969).

Instead of recapitulating these ideas - which are based mainly on arguments using the s-d exchange model - we will discuss another aspect of ESR, which can be linked to the parameters of the Anderson model: the measurement of the spin-flip scattering cross section σ_{sf}. In the HF model the basic mechanism of the spin flip of the conduction electrons when on the impurity sites (note that in HF no spin flip occurs between the d-levels) is the spin-orbit interaction, which splits the d-level into sub-levels $j = \ell \pm \frac{1}{2}$. The spin flip scattering cross section σ_{sf} can be expressed by the phase shift of the conduction electrons η_j as

$$\sigma_{sf} = \frac{4}{3} \frac{4\pi}{k_F^2} \sum_{\ell} \frac{\ell(\ell+1)}{2\ell+1} \sin^2\left[\eta_{\ell-\frac{1}{2}}(\varepsilon_F) - \eta_{\ell+\frac{1}{2}}(\varepsilon_F)\right] \quad /53/$$

(Ferrel and Prange 1966). The difference between the phase shifts for the two virtual bound states split by the spin-orbit interaction is proportional to $\rho_d(\varepsilon_F)$ in case of small splitting when the difference between the two density of states at the Fermi level can be neglected. The spin-orbit splitting is the subject to an enhancement in a similar way to the orbital part of the impurity susceptibility, and so the spin flip scattering cross section is given by

$$\sigma_{sf} = \frac{4\pi^3}{k_F^2} \frac{\lambda^2 \rho_d^2(\varepsilon_F)}{\left[1 - (U - I)\rho_d(\varepsilon_F)\right]^2} \quad /54/$$

for the $\ell = 2$ scattering in the HF approximation of the Anderson model, where λ is the spin-orbit coupling parameter. The importance of Eq/54/ lies in the fact

that σ_{sf} is proportional to the squared density of d-states in contrast to the impurity resistivity which is determined only by the total number of d-electrons and so gives no direct information on Δ.

The spin-flip scattering cross section can be measured directly by transmission electron spin resonance technique as it is inversely proportional to the spin-lattice relaxation time of the conduction electrons (Monod and Schultz 1969, Monod 1968), or can be determined from the local moment electron spin resonance parameters in the bottleneck regime (Gossard et al 1967). In both cases one measures the linewidth of the resonance signal as a function of the impurity concentration and evaluates σ_{sf} from the concentration dependence. The method has been applied for normal metal impurities in Li and Na (Asik et al 1966) and in Cu (Monod 1968). In both cases σ_{sf} could be described by p-scattering and the width of the resonance was found to be about 3-4 eV. In the case of transition metal impurities in copper (Gossard et al 1967, Monod and Schultz 1969, Monod 1968) the phases shift analysis gives a proper description for both the non-magnetic (Ti and Ni) and magnetic (Cr, Mn and Fe) impurities and the behaviour of σ_{sf} versus the impurity atomic number - showing a close resemblance to the impurity resistivity - can be described with the width $\Delta = 0.5$ eV. This derivation of the virtual bound state width is probably more accurate than that derived from the transport properties and specific heats as the enhancement of the

spin-orbit coupling which enters in the expression of σ_{sf} is much smaller than the spin enhancement entering in the macroscopic properties.

Recent transmission electron spin resonance experiments in aluminium based alloys (Huisjen et al 1971) show the same pattern as the impurity resistivity shown in Fig. 3, and the evaluation of σ_{sf} based on the HF expression Eq/54/ gives $\Delta \sim 1.0$ eV for V, Cr, Mn and Ti impurities. Though the determination of Δ is the subject of uanmbiguity through the spin-orbit enhancement, the internal consistency of the virtual bound state widths derived for the different impurities gives a confidence of the method of evaluation.

3.4. The relevance of the HF approximation to the experiments

In Table 3 we summarised the results of the previous analysis of the macroscopic and local parameters of various alloys; we included in the Table the available data for Zn based alloys, which have not discussed here (but see Bell 1973 and Rizzuto (1974)). The symbols M and NM refer to cases, where the HF approximation (together with spin flip scattering in the magnetic cases) was proved to be an appropriate basis for the analysis, giving consistent values for the basic parameters $U + 4I$, E_d and Δ. The meaning and interpretation of Table 3 - which is essentially an up to date version of that analysed first by Friedel (1956) is clear: $U + 4I$ as an intra-atomic property must be more or less constant, so that the condition for the appearance of magnetic moment is determined mainly by the density of states at the Fermi level $\rho_d(\mathcal{E}_F) = \frac{1}{\pi}\left((E_d - \mathcal{E}_F)^2 + \Delta^2\right)^{-1}$. The change from the magnetic to non-magnetic behaviour for the same host is brought about by the variation of the position of the virtual bound state, E_d. In Au or Cu, the vbs is nearly full for Ni, nearly empty for Ti, $\rho_d(E_F)$ is small for both cases, therefore these impurities are non-magnetic behaviour; V and Co being borderline cases. In fact, in order to get this separation properly $(U + 4I)/\Delta \sim 10$ is required, this ratio is well confirmed by the optical experiments. For the same impurity in

different hosts E_d/Δ is constant due to charge neutrality (the slightly different screening by s and p electrons can safely be neglected), and the change of the vbs width Δ is essential. As Δ is proportional to $\rho_s(\varepsilon_F)$, increasing vbs width is expected in the Au, Cu, Zn and Al series, explaining the reduced number of magnetic impurities. A somewhat more qualitatively, an increase of Δ by a factor two or three explains the borderline situation for AlMn in contrast to the strongly magnetic CuMn. This increase is reasonable, as $\rho_s(\varepsilon_F)$ changes by roughly the same factor, and is in accordance with the experimental values $\Delta \sim 1.0$ eV and $\Delta \sim 0.5$ eV respectively.

Question marks in Table 1 indicate the situations, where a HF analysis breaks down, and result in inconsistent Anderson parameters. In fact the breakdown of the HF approximation is a continuous one approaching either from the magnetic of non-magnetic side (see the progressive increase of the specific heat of Al-based alloys for example) and so the distinciton is somewhat arbitrary. This gradual changeover from the non-magnetic to the magnetic limit is more clearly seen in experiments performed in ternary alloys like $Cu_{1-x}\ Zn_x\ Fe$ (Caplin 1967, Caplin et al 1968, Waszink and Coles 1967). By changing the realtive concentration of the copper and zinc constituents a gradual disappearance of the magnetic moment is observed, which is explained, at least within the framework of the rigid band approximation, by the change of the host density of states. Though local configuration effects may be important,

the gradual change from the non-magnetic to the magnetic limit is convincingly demonstrated.

However, aside these borderline cases, the HF approximation of the Anderson model describes properly the resonance formation in dilute alloys both for non--magnetic and magnetic cases far from the instability point. This is in contrast to what is expected as this approximation neglects the correlation effects, and therefore overestimates the tendency towards the appearance of magnetic moment, similarily to the case of band magnetism. What is then the significance of a HF description, in particular of a representation like Fig. 2 and 3, and why does it work even for strong correaltions? Clearly a single particle representation of the correlation effect has the same meaning in the present case, as the pseudoparticle band structure for the Hubbard model (for a review see Zinamon and Mott 1970). In the Anderson model the impurity having one electron has energy E_d, and if another electron is placed at the impurity, it's energy is raised by U, due to the Coulomb correlations. This correlation effect can be described also in terms of electron hopping between the impurity and conduction electrons, in a similar fashion then the polar fluctuations on 3d metals, the impurity has zero, one and two electrons for a certain period of time, and $\frac{\Delta}{E_d + U}$ for example gives the proportion of time when the impurity is double occupied. This correlation effect is absorbed into a single particle

picture, where the correlation energy is replaced by a potential energy and the weight of the appropriate state is then given by an integration up to the fermi level. For large correlation energies the weight of double occupancy is strongly reduced, the impurity spends more and more time having one electron, and then the interaction between this localised electron and the continuum states can be well represented by an s-d exchange. Rapid on and off hopping modifies this interaction similarly to the effect of itinerancy to the ordinary exchange in 3d metals. The lifetime of this state however is important in the present case, as aldough being finite, can be much longer than the lifetime of the particular experiments. The HF approximation predicts a moment with infinite lifetime, but the effect of any finite lifetime τ_m is not observable by the experiment as long as $\hbar/kT < \tau_m$. The HF approximation therefore, will be approximately correct)as regards its success of describing the experiments as long as $kT > \hbar/\tau_m$, but serious deviations are expected at lower temperatures. In the Anderson model, τ_m depends on the parameters $U + 4I$ and Δ , and one expects increasing τ_m with increasing $(U + 4I)/\Delta$ ratio. For the s-d model the relevant parameter is $J_{eff}\rho_S(\varepsilon_F)$, and for small coupling τ_m is presumably long, and decreases with increasing coupling constant. One may push this argument further,

by saying, that at temperatures below $\hbar/kT_m$ the impurity should look nonmagnetic, as the lifetime of the polarization is then smaller, then the time required to align the spin by the external magnetic field. Therefore, as τ_m is finite for any isolated impurity in a metallic host, the impurity is non-magnetic at T=0.

The question of having a magnetic-nonmagnetic transition for the "magnetic" alloys, as well as the relation of the nonmagnetic state to that in HF sense is the subject of the following chapters.

4. THE MAGNETIC-NONMAGNETIC TRANSITION: EVIDENCE OF MANY BODY EFFECTS

In the previous chapter we summarised the results of the various experiments on the basis of the Anderson and s-d models and determined the basic parameters characterising to the impurity within the framework of both models. According to this analysis some alloys show non-magnetic behaviour accompained with a spin degenerate virtual bound state. Other impurities behave as classical "yes moment" systems, characterised by strongly temperature dependent Curie-Weiss susceptibilites and double peaked virtual bound states. In the latter cases the experimental findings (including magnetic and electric properties) can be interpreted within the framework of both models. We have some indication, like the temperature dependence of the susceptibility in AuV and CuCo alloys, that at least some impurities in some host behave non-magnetically at low and magnetically at high temperatures, and there is a smooth transition between the two regions. The question immediately arises whether similar situations occur in other cases when extending the temperature range of the experiments; the arguments presented in the end of the last chapter suggest, that the answer is yes.

In fact, historically, the idea of the non-magnetic--magnetic transition came from a different side and was initiated by the theoretical investigation of the so

called reistance minimum well known for the experimentalists for about 30 years. The minimum in the resistance (for a review of the early experiments see G. J. Van den Berg 1964), as a function of temperature, accompained with the magnetic behaviour of the impurities (Sarachik et al, 1964, Caplin et al, 1967) appears as the consequence of the increase of the impurity resistivity with decreasing temperature. As the latter is proportional to the impurity concentration and the phonon contribution to the resistivity goes as T^5 this gives a temperature where the minimum occurs $T_{min} \tilde{} c^{1/5}$ as observed experimentally.

A typical example is shown in Fig. 7, where a minimum of the resistivity occurs progressively at higher temperatures for higher impurity concentrations.*

As the minimum is found in the case of magnetic impurities, the problem has been attacked using the s-d model. Although the coupling constant $J_{eff}\, \rho_S(\varepsilon_F) \ll 1$, and therefore, perturbation expansion is expected to give reasonable results, a second order calculation of the resistivity leads to

$$R_{imp}(T) = c R_{s\text{-}d}\left(1 + \rho_s(\varepsilon_F) J_{eff} \frac{kT}{D}\right) \qquad /55/$$

Note:* Beside the resistance minimum, a pronounced maximum is observable in the sample with highest Mn concentration. This maximum arises from the impurity--impurity interactions, which leads to magnetic ordering and to depression of spin flip scattering at low temperatures (Yoshida 1957, Silverstein 1966). By increasing the manganese concentration the maximum moves towards higher temperatures, and coincides with the minimum, resulting in a peculiar temperature dependence of R .

where D the width of the free electron band, R_{s-d} being defined in Eq/23/. The resistivity - taking into account all the leading logarithmic terms - diverges at

$$T_K = T_F \exp\left(-\frac{1}{J_{eff}\,\rho_s(\varepsilon_F)}\right) \qquad 56$$

for $J_{eff} < 0$.

The logarithmic increase of the resistivity is called the Kondo-effect, the characteristic temperature T_k the Kondo-temperature. The divergence is the result of the internal degree of freedom of the impurity, which in the mathematical formalism appears as $[S^+ \; S^-] \neq 0$. This noncommutativity together with the sharp Fermi surface leads to the breakdown of perturbation theory, and to a many body effect: the impurity provides a coupling between the electrons scattered subsequently on it- unlike a normal scattering potential which has no internal degree of freedom .

Clearly a diverging scattering amplitude is not a true physical solution, as the cross section cannot exceed the unitarity limit. Subsequent theoretical efforts have been concentrated on the removal of the divergence, using either Green's function decoupling and diagrammatic methods or scattering theory these methods have been shown later to be equivalent (see for example Kondo 1969). The main features of the solutions can be summarized as having a singlet ground state at T=0, a many body resonance in the scattering amplitude pinned at ε_F with a width of the order of kT_k. The transition from the high to the low temperature state is smooth and is

broadened by fluctuations, as expected for a zero dimensional system. As the spin being a pre-existing quantity in the s-d model cannot disappear, the physical picture prepared on the basis of this model was some kind of many-body spin correlation built up in the surrounding electron gas. As this correlation has an energy of the order of kT_K, a characteristic length $\xi_K = v_F/2k_BT_K$ can be anticipated (Heeger 1969).

The characteristic temperature is drastically dependent on $J_{eff}\rho_s(\varepsilon_F)$, and this parameter varies from alloys to alloys, therefore one might expect that this so called "Kondo effect" is not restricted to low temperatures, and certain alloys with non-magnetic behaviour at ordinary temperatures could also been Kondo-alloys. The weak resistance minimum found in AlMn and AlCr (Caplin and Rizzuto, 1968) however, initiated a new approach to the problem. As the macroscopic parameters α and γ indicated a borderline situation for these alloys, a natural starting point is the nonmagnetic Anderson model, the nearly magnetic behaviour $(U + 4I)/\pi\Delta \sim 1$ then results in an enhanced response against thermal fluctuations. Lifetime arguments, similar to those presented in the end of the last chapter, lead to the prediction of a high temperature magnetic state, and a magnetic-nonmagnetic transition around a characteristic temperature $kT_K = \hbar / \tau_{sf}$. The RPA expression gives a definite relation between τ_{sf} and the parameters of the non-degenerate Anderson model (Rivier 1968),

(Zuckermann Rivier and 1968)

$$\tau_{sf} = \left(1 - U/\pi\Delta\right)^{-1}. \qquad 57$$

However, τ_{sf} diverges at the HF instability point, and attempts to remove this divergence were only partially succesful. As in this model the impurity is a'priory non-magnetic no spin correlations are expected in this case.

The main features, predicted by both models are similar: disappearing effective moment at low temperatures, specific heat anomaly and anomalous transport properties when going through the transition. These predictions are in broad agreement with the experiments for a wide range of alloys. The temperature dependeces of the various phyisical parameters have been displayed in Review Papers (Daybell and Steyert 1968, van Dam and Van den Berg 1970) and will not be reproduced here, instead we recall some specific examples. Although the characteristic temperature, where the magnetic-nonmagnetic transition occurs is variably called as the Kondo and spin fluctuation temperature (depending on the model chosen by the experimentalists to compare with their results) we use the notation Kondo temperature, unless stated otherwise.

4.2. Anomalous temperature dependences of the magnetic, thermal and transport properties

Among the various macroscopic and local properties influenced by the afore mentioned transition, the temperature dependence of the macroscopic susceptibility gives the most clear evidence, that this transition is connected with the gradual disappearance of the effective moment with lowering of the temperature. The Curie-Weiss behaviour, observed in a number of alloys can be represented as a Curie-law of non-interacting well defined spins, but with a temperature dependent effective moment as

$$\chi(T) = \frac{\mu_{eff}^2(T)}{3k_B T} \qquad 58$$

As the susceptibility approaches a finite value at $T=0^{\circ}K$, the effective moment, which is a well defined finite value at high temperatures, idappears at zero temperature. Fig. 9 shows the temperature dependence of the effective moment in AuV alloys (Van Dam et al 1972). While the detailed curve depends heavily on impurity-impurity interactions, the gradual disappearance of μ_{eff} is evident for all concentrations. The temperature dependence of the total susceptibility measured by macroscopic methods is the consequence of the disappearance of the impurity magnetisation. Recently Narath (1972a) measured the temperature dependence of the im-

purity Knight shift in AuV alloys in a wide temperature range. The temperature dependence of K_{imp} is attributed to the temperature dependent local spin susceptibility, which was shown to be the same as that determined by the macroscopic susceptibility. It has to be noted, that the susceptibility, in fact, measures the z-component of the magnetization, therefore the finite susceptibility at T=0 meas only that $\langle S_Z \rangle = 0$; from the impurity hyperfine field studes it follows, that $\langle S_Z^{imp} \rangle = 0$ at T=0 too.

The temperature dependence of the impurity specific heat gives a further evidence that we are faced with a magnetic-nonmagnetic transition and that the high temperature well defined impurity spin disappears at low temperatures. The transition is connected with a borad specific heat anomaly. If the high temperature impurity spin is completely removed from the system at T=0, then a total entropy change

$$\Delta S = \int_0^\infty \frac{C_v(T)}{T} dT = R \ln (2S+1) \qquad 59$$

is expected. The specific heat experiments are restricted to low temperatures as the phonon term (proportional to T^3) becomes important at large T and therefore only alloys with low Kondo temperatures can only be measured to obtain the anomaly. Sepcific heat measurements of Frank et al (1961) on CuFe alloys indicated anomalous $C_v(T)$ with a peak of around 7^oK, but the total entropy change could not be evaluated as the transition extends

up to rather high temperatures. Recent careful specific heat experiments of(Triplett and Phillips 1971) on CuCr alloys, where the Kondo temperature is low enough to extend the temperature range well above T_k , shown in Fig. 10 are free from impurity-impurity interactions and the total entropy change due to the single impurities can be evaluated. The area under the anomaly is given by $\Delta S = R \ln 4$, corresponding to the high temperature impurity spin 3/2, and shows the complete removal of the spin degeneracy at high temperatures, or in other words, the complete disappearance of the high temperature impurity spin; the total spin (impurity + conduction electrons) is zero at T=0.

The magnetic-nonmagnetic transition is connected with anomalies in the transport properties. Fig. 11 shows the thermoelectric power measured in various alloys. There is a broad anomaly with a well defined peak in each case but occuring at rather different temperatures, ranging from $1^{o}K$ to about $300^{o}K$. The sign of the thermoelectric power depends on the potential scattering contribution and is negative when the d-level of the impurity has more than five electrons and positive when the virtual bound state is less than half filled. According to the HF solution and to the analysis of the previous chapter, the alloy AuFe is well beyond the instability point and it is a classical "yes moment" alloy while AuCo and AlMn are near to the magnetic-nonmagnetic boundary. In spite of this difference the tem-

perature dependence of the thermoelectric power looks remarkably similar for the different alloys and the difference shows up only in the temperature where the peak of the thermoelectric power occurs. On the basis of this similarity one would tend to say that the distintion between strongly magnetic and nearly magnetic magnetic impurities is artificial and the only difference is in the Kondo temperature $k_B T_k$ which, however, is rather different for different situations.

Fig. 12 shows the temperature dependence of the impurity resistivity in CuFe alloys, measured by Daybell and Steyert (1968). Though there is some ambiguity due to the substaction of the phonon term and that of the deviations from Matthiessen's rule R_{imp} rises monotonously with decreasing temperature and reaches a constant value at T=0. The transition from the high temperature limit (which however, is not reached even at the highest temperatures) to the T=0 value is smooth and extends over more than one decade. Recent measurements, using very low concentration alloys (Star 1971, Star et al 1973) have proved that the detailed temperature dependence, shown in Fig. 12 is influenced by impurity-impurity interactions especially at low temperatures; however, it does not alter the main conclusions.

Looking at the expressions of the transport properties Eqs/17/ and /18/ the above behaviour of R_{imp} and S_{imp} indicates a strongly energy and/or temperature dependent scattering amplitude near the Fermi energy, this temperature or energy dependence is characterized by kT_k.

4.2. Kondo temperatures

The gradual changeover of the high temperature magnetic behaviour to the low temperature non-magnetic one connected with the anomalies discussed before has been observed in a number of dilute alloys, and by now a systematic dependence on the impurity atomic number and on the host properties has emerged. Looking at the temperature dependence of S_{imp} of the various alloys shown in Fig. 11 it is immediately seen that the characteristic temperatures of different impurities in the same host cover a rather broad temperature range, and that T_k depends sensitively on the particular host. Fig. 13 shows the characteristic temperatures of 3d-transition metal impurities in copper and gold, determined from the temperature dependence of the transport, thermal and magnetic properties*. In the case of Mn impurities the transition is not accessible by macroscopic methods

---

* Note: Different authors use different definitions of the Kondo temperature, when determined on experimental grounds. In case of the susceptibility, the Curie temperature is usually taken as a measure of T_k, in the case of resistivity, the temperature, where R_{imp} reaches half of the T=0 value, while the temperature where the peak occurs in C_v or S gives another estimate of T_k. Although various theoretical expressions give definite relations between T_k and the above experimentally determined temperatures, at this point it is essential to emphasise only, that they result in broadly the same values.

and one can estimate the Kondo temperatures by NO experiments (Williams et al 1969, Campbell et al 1967, Floquet 1971) where the deviation of the impurity magnetisation from the free spin behaviour indicates the finite Kondo temperature.

First of all, the symmetrical behaviour of T_k with respect to N = 5 should be noted, it shows a close correlation with the symmetrical HF picture. Alloys, which were compatible with the HF nonmagnetic limit, fit into the overall behaviour with T_k much higher than the conventional temperature region, for the "borderline" cases T_k is of the order of room temperature.

As mentioned earlier, both Kondo and spin fluctuation theories account for the anomalous temperature dependences, they can in principle explain the characteristic temperatures too. The s-d coupling constant is inversely proportional to S, therefore Eq/56/ together with the Hund's rule immediately leads to a V-shaped behaviour in logarithmic representation. Although the spin fluctuation concept cannot make a firm prediction, and Eq/57/ is certainly not correct, in principle it also predicts a drastic increase of T_k with decreasing $\rho_d(\varepsilon_F)$, as observed. One should be careful, however, to accpet these straightforward explanations, as the models are expected to be appropriate only in limited ranges of parameters. The s-d model is valid only when $(U + 4I)/\Delta \gg 1$, and it is not clear how to deal with borderline situations; the LSF on the other hand is supposed to be appropriate

when $(U + 4I)/\Delta \ll 1$, i.e. strictly speaking only in the nonmagnetic regime.

Arguments about the validity of the models for particular stituations can be formulated in the following way: The two models represent two characteristic fluctuation times. In the spin fluctuation picture it is the time τ_{sf} determined by the d-d correlations at the impurity site, in the s-d model it is the time of s-d correlations τ_k. If these characteristic times are independent then an alloy with $\tau_{sf} > \tau_K$ should behave differently than with $\tau_K > \tau_{sf}$, and so distinct differences are expected between different alloys, for the former situation the Kondo, for the latter the LSF theories should apply. Alternatively τ_{sf} and T_k may be strongly correlated or perhaps idential, although they are formulated by a different language, and then the nautre of the transition and the low temperature nonmagnetic state is similar for all cases.* The similar overall behaviour of the thermoelectric power, Fig. 11 suggest, that the latter situation is more appropriate, but the answer of this question neads a closer inspection of the experimental results, and a more thoroughful comparison with the prediction of the two models is necessary.

---

* Note: This argument is based on the features of the non-degenerate model, where only fluctuations between magnetic and nonmagnetic states are considered. Fluctuations between degenerate orbitals, both of them magnetic, however result in a finite spin even for rapid fluctuations, and then the s-d model still applies, this might be the situation for Mn where fluctuations between S=5/2 N=5 and S=2 N=6 or 4 can occur in a minimum polarity fashion.

5. TWO TYPICAL EXAMPLES: CuFe and AlMn

In the last few years two alloy systems have been attracted wide interest, and by now the large body of experimental data (including both macroscopic and local properties) on these alloys allows to make a rather complete analysis, and a detailed comparison between theory and experiment.

Due to the pronounced Curie-Weiss suceptibility CuFe has been regarded for a long time as a typical "yes moment" system, and indeed Kondo compared his theoretical result with experiments performed on this alloy. Later on it was the first alloy which was suggested to have a spin-compensated state at accessible temperatures (Daybell and Steyert 1967) and the nautre of the non-magnetic state has been investigated in detail by macroscopic as well as by local methods (Heeger et al 1967, Golibersuch and Heeger 1969). Finally in the last two years, very careful measurements have cleared up a number of spurious effects arising mainly from impurity--impurity interactions, and have led to a rather complete experimental situation regarding the low temperature properties. Manganese is aluminium, however, has been thought to be nonmagnetic in Anderson sense ($U/\pi\Delta < 1$) and the observation of a weak resistance minimum on this alloy by Caplin and Rizzuto (1968) initiated the idea of localised spin fluctuations. The low temperature properties were found to be different from CuFe at that

time, leading to the conclusion that these two systems represent the two possible kinds of impurities, predicted by the theory.

It is tempting therefore to choose these alloys to test the available theoretical approaches and their relevance to the experimental situation in detail.

5.1. The CuFe alloy

In order to follow the time development of the ideas about the alloy CuFe,we will start with the analysis of the high temperature properties, where all the different experiments indicate the existence of a well defined impurity moment. As a second step we analyse experiments perfromed around and below T_k, and compare them with theoretical expressions based on the s-d model to get an insight into the nature of the transiton and that of the zero temperature ground state. In particular, the temperature dependence of the various parts of the susceptibility has been measured several times, and widely diverging ideas emerged to explain the experimental findings; therefore we inspect the experimental data related to this question in detail.

5.1.1. High temperature properties: experiments at $T \gg T_k$

The high temperature impurity resistivity and susceptibility measurements on Cu-3d transition metal alloys - discussed briefly in Chapter 3.2 - indicate a double peaked virtual bound state and a finite impurity moment, in the middle of the series. The HF approximation of the Anderson model offers a natural explanation of these experiments and gives a consistent description for both the transport and magnetic properties, at high temperatures.

At room temperature the impurity resistivity $R_{imp} = 8 \mu\Omega$ cm/at % (Star 1971), while the susceptibility has a Curie-Weiss form in the 6...300°K range, with $\mu_{eff} = 3,7 \mu_B$ corresponding to S = 3/2 and $\Theta = 32°K$. Together with the Friedel sum rule these parameters can be described with two phase shifts, different for the spin up and spin down wlectrons according to the spin splitted virtual bound state. Such analysis gives $\eta_{2\sigma}(\varepsilon_F) = \pi$ and $\eta_{2\sigma}(\varepsilon_F) = \frac{2\pi}{5}$ in the case of CuFe (Hurd 1969). According to this analysis, which is supported by thermoelectric power measurements one virtual bound state is below the Fermi level and is completely filled, while the other crosses it, due to the Friedel charge neutrality condition.

The study of the local spin perturbation around the Fe impurities by NMR method gives an information on the exchange coupling between the impurity spin and conduction electrons. This perturbation has an amplitude proportional to $(2\ell + 1) j_{eff} \rho_S(\mathcal{E}_F)$. ^{63}Cu NMR measurements result in j_{eff} = 1 eV (Golibersuch 1969, Mizuno 1971) a somewhat larger value than that found in CuMn j_{eff} = 0,5 eV, as expected. More sophisticated methods like nuclear spin-lattice relaxation time measurements and ESR experiments indicate again well defined impurity moment at high temperatures and give an insight into the dynamics of the impurity spin. These experiments further support the conclusion that at high temperatures iron impurities in copper are magnetic in the sense that a well defined impurity spin appears with life-time long enough to result in a paramagnetic susceptibility as well as observable spin dynamics.

5.1.2. The transition to the non-magnetic state

All the anomalies connected with the magnetic-nonmagnetic transition and discussed in the Chapter 4 have been observed and widely studied in CuFe. Among the transport properties the impurity resistivity has been investigated in most detail. As the transition extends over several decades, the precise measurement of the impurity contribution to R is difficult: at high temperatures the phonon scattering has increasing im-

portance, and the substaction of the pure metal resistivity from that of the dilute alloy to obtain the impurity resistivity can be misleading as deviations from Matthiessen's rule are observed also in the case of non-magnetic impurities. On the other hand at low temperatures impurity-impurity interactions are becoming more and more important and very low concentrations have to be used, requiring high measuring accuracy to resolve the temperature dependence. The impurity resistivity shows an increase from the high temperature limit $8\,\mu\Omega$ cm/at % with decreasing the temperature (see Fig. 12). At low temperatures this increase flattens off and saturates at T = 0°K at $R_{imp} = 14{,}8\,\mu\Omega$ cm/at %. This value can be interpreted within the framework of the Kondo model. In the so called "atomic limit", when $E_{d\sigma} \gg \Delta$, potential scattering can be neglected, the zero temperature resistivity is determined by the unitarity limit of the spin scattering, which in the degenerate case for five independent scattering channels reads (Schrieffer 1967)

$$R_{imp} = R_0\, 2S\ \mu\Omega\,\text{cm/at\%} \qquad 60$$

For spin 3/2, and with $R_0 = 3{,}8\,\mu\Omega$ cm/at % for Cu host, Eq/60/ gives 11,4 $\mu\Omega$ cm/at % good in agreement with the observations.

Assuming however, that the spin-flip scattering is frozen in at T = 0 (simply because the total spin

disappears well below T_k), and that the charge neutrality is important, than a spherical symmetric ground state requires $\eta_\sigma(\epsilon_F) = \eta_{-\sigma}(\epsilon_F)$ and therefore

$$R_{imp} = R_o 5 \sin^2 \frac{N\pi}{10} \qquad /61/$$

which accounts for the T = 0 resistivity with N = 6 or 7.

While both predictions are in agreement with the experimental value for this particular case, comparison of R_{imp} in CuFe and CuCr clearly favours the second description. R_{imp} = 20 $\mu\Omega$ cm/at % for CuCr, and the difference between the zero temperature resistivities is not understandable on the basis of Eq/60/ as both impurities have the same high temperature spin. However, the charge neutrality limit gives a natural explanation of this difference, as N $\sim$ 5 for Cr (see Figures 3 and 4). Therefore, spin-flip scattering seems to be frozen in at T = 0, and the non spin flip scattering amplitude saturates at the charge neutrality limit.

Although the main features of R_{imp} versus T as shown in Figure 12 are essentially correct, the fine details of the temperature dependence have been cleared up only recently. According to Knook (quoted by Star 1971) and Loram et al (1970b) the resistivity may be varying logarithmically up to room temperature, in agreement with the prediction of the s-d model, although comparison with Eq/55/ is not possible due to the considerable uncertainty of the high temperature data. The statement however, is reinforced by the measurement of

the impurity resistivity in a range of $Cu_xAu_{1-x}Fe$ alloys (Loram et al 1970). In spite of that the characteristic temperature varies more than one decade for the various compositions, the temperature dependence of the impurity resistivities of the various alloys could be matched together to an univeral curve depending only on T_K for the different compositions. Fig. 14 shows the spin resistivity, after substracting the high temperature potential scattering background, for several $Cu_xAu_{1-x}Fe$ alloys. The upturn at about $5T_K$ for the CuFe alloy is due to the phonon term, and after a reasonable correction for this effect the resistivity seems to be the same at high temperatures for all the alloys. A closer inspection of Figure 14 shows that the resistivity can be fitted with an $\ln T$ law over some rather restricted temperature intervals and the slope changes appreciable even well above T_K.

The temperature dependence has been fitted to one of the most ambitious theoretical expressions based on the s-d model, to the Hamman (1965) curve of the resistivity

$$R_{imp}(T) = \frac{R_o}{2}\left\{1 \pm \left[1 \pm S(S+1)\pi^2/(\ln T/T_K)\right]\right\} \qquad /62/$$

The two free parameters S and T_K were chosen to be correct at least at temperatures around T_K gives $S = 0.77$, clear in contrast to the measured value of the high temperature spin $S = 3/2$. As Eq/62/ was obtained on the basis of a Green's function decoupling-

-scheme, it's correctness cannot be estimated, however can be definitely disproved on experimental grounds.

Below about 0,1 T_K the experimental points show a deviation even from the functional form of the Hamman expression (Loram et al 1970). This region has been investigated by Star (1971) in detail who used very low concentration alloys (below 100 ppm Fe) to avoid impurity-impurity interactions. Though concentration dependent effects have been observed even in this concentration range, below about 2,5°K, the resistivity could be fitted rather well with

$$R_{imp}(T) = R_{imp}(T=0)\left[1-\left(\frac{T}{\Theta}\right)^2\right] \qquad /63/$$

with $\Theta = 22^{\circ}K$. Figure 15 shows the low temperature part of the impurity resistivity on a T^2 scale for two different impurity concentrations. While at high concentrations the experimental points are in good agreement with the expression

$$R_{imp}(T) = R_0\left[\cos^2\delta_v - \frac{16}{3}\cos 2\delta_v\left(\frac{T}{T_k}\right)\ln\left(\frac{T}{T_k}\right)\right]^2 \qquad /64/$$

where δ_v is the phase shift of the potential scattering, which has been obtained by the Appelbaum - Kondo ground state theory (1968), the simple power low observed at low concentrations is in clear disagreement with it. As any ground state theory should word in the vicinity of $T = 0^{\circ}K$, the disagreement immediately rules out the validity of this theoretical approach. This situation holds for all the various ground state theories, which failed to produce simple power law behaviours until now, (see for example Kondo 1969).

The thermoelectric power shows a broad bump around 30°K, and omparing the experimentally found behaviour with the predictions of the s-d model, one arrives essentially to the same conclusion as from the inspection of the resistivity. The TEP calculated with the same approximation as the resistivity, progressively deviates from the measured curve going towards low temperatures, and the theory cannot produce a thermoelectric power, which is proportional to T near T = 0 as observed.

The determination of the impurity specific heat is even more complicated than that of the transport properties due to the phonon term which becomes dominant at high temperatures. On the other hand in the low temperature region one is faced with the problem of impurity-impurity interactions again. Due to these limitations the whole temperature range has not been measured in CuFe, and even the low temperature behaviour has only been cleared up recently. Specific heat measurements of Triplett and Phillips (1971) on CuCr and CuFe alloys, showed that the behaviour of the impurity specific heat is remarkably similar in the two alloys, and the difference shows up only in the temperature. Accepting this similarity the two systems can be viewed together, and so the measured temperature range extends from 0,01 T_K to about 5 T_K. In the high temperature region around and above T_K C_v can be fitted adequately with the Bloomfield-Hamman (1969) expression, (full line of Figure 15) derived on the basis of the Kondo

model, this agreement is similar to that of the resistivity with the Hamman curve. As both expressions are derived from the same model under the same approximations, the same conclusions based on $\mathcal{R}_{imp}(T)$ and $C_v(T)$ are not surprising. The similar type of deviation from the theoretical curve as found in the case of resistivity is observed here too, and the impurity specific heat tends to be a linear function of T going towards $T = 0^{o}K$. Fig. 16 shows the low temperature specific heat results of Frank et al (1961), Brock et al (1970) and Triplett and Phillips (1971). The concentration dependence is evident and can be accounted for by interactions (Star 1971). In the zero concentration limit the specific heat is given by

$$C_v = 8\ mJ/mole\ k^2 T.$$

The linear temperature dependence in again clear in contrast with the Appelbaum - Kondo (1968) expression, (full line in Figure 16) and the good fit claimed earlier can be attributed to Fe pairs.

It appears therefore, that all the classical approaches of the s-d model Nagaoka-Hamman-Bloomfield--Müller-Harmann-Zittartz theory and gorund state theories fail to describe all the fine details of the transport and thermal properties of the experiments. This deviation between theory and experiment is most pronounced at temperatrues $T \ll T_K$ where simple power laws govern the temperature dependences, clear in contrast with the theoretical predictions.

5.1.3. The temperature dependence of the susceptibility and the question of the spin polarized cloud

As the Kondo effect is basically a spin correlation problem, the behaviour of the magnetic properties when going through the transition has a primarily importance. The two theoretical concepts were claimed to give fundamentally different description of the non-magnetic behaviour at low temperatures. From the point of view of the s-d exchange model, the non-magnetic state is the result of the compensation of the well defined high temperature impurity spin by the surrounding electron gas and that of a build up of a non-perturbative long range spin polarization around the impurity, the characteristic distance of the polarization is determined by the coherence length $\xi_{T_K} = \frac{V_F}{k_B T_K}$. The detailed distance dependence of this coherence effect depends on the properties of the ground state and on the low lying excitations. While different approximations of the S-d exchange model predict different distance dependence of the spin polarization, and they result even in different coherence length, they agree in the fact that the compensation takes place outside the impurity cell in the surrounding electron gas. This must be clearly so within the framework of the s-d exchange model as it excludes the possibility of a spin compensation at the impurity site by assuming an infinite lifetime of the localized moment. On the other

hand the localized spin fluctiation concept regards the impurities as non-magnetic at T = 0 with S = 0, and therefore no extra spin correlations are expected in the surrounding electron gas. The question, whether the spin correlation appears in the time average z-component of the magnetization measured by ME and NMR methods or not has attracted wide interest, and resulted in a large activity including both experimental and theoretical aspects.

A number of different types of experiments have been performed in the last few years resulting in a rather complete experimental picture about the distribution of the magnetization in the local moment + conduction electron system. The bulk susceptibility measurements give information on the total polarization including both the s- and d-type electrons. The hyperfine field at the impurity site measured by ME method is proportional to the polarization localized to the impurity site, while host NMR samples the polarization outside the impurity cell. All of these measurements are available in CuFe permitting a detailed analysis of this spin correlation problem.

The bulk susceptibility has a Curie-Weiss form down to about $6^{o}K$ (Hurd 1969). Though this behaviour has been accepted as the manifestation of the local impurity moment without any theoretical justification, the observed temperature can be analyzed on the basis of the high temperature behaviour of the susceptibility

predicted by the Kondo and Anderson models. Perturbation treatment of the s-d exchange model for the total susceptibility gives up to logarithmic accuracy

$$\chi(T) = \frac{g^2\mu_B^2 S(S+1)}{3k_BT}\left[1 + \frac{j_{eff}\rho_s(\varepsilon_F)}{1 - j_{eff}\rho_s(\varepsilon_F)\ln\frac{kT}{D}}\right] \qquad /65/$$

which in the $7 < T/T_K < 100$ region can be approximated by a Curie-Weiss dependence

$$\chi(T) = \frac{g^2\mu_B^2 S(S+1)/1.22}{3k_B(T + 4.5T_K)} \qquad /66/$$

For CuFe $\theta = 32^oK$, and so $T_K = 7^oK$. Based on the Anderson model in the strongly magnetic limit Scalapino (1967) also derived a Curie type behaviour, which by virtue of the Schrieffer-Wolff transformation gives identical result to Eq/65/.

Daybell and Steyert (1968) extended the temperature range of the measurements down to 40mK. Below T_K the susceptibility could be fitted by

$$\chi(T) = \frac{2{,}52\,\mu_B^2}{T + 14} + \frac{0.168\,\mu_B^2}{T + 0.045} \qquad /67/$$

implying two contributions to the susceptibility below the Kondo temperature. Chaikin and Jensen (1970) observed the same behaviour and a small θ value $+14^oK$ in contrast to the high temperature Curie constant, this was interpreted as the evidence of the build up of an extra contribution to the susceptibility. Recently Tholence and Tournier (1970) performed very detailed magnetization measurements using low concentration alloys. The analysis of the concentration

and field dependence of the magnetization in the 1,3...33°K region demonstrated the importance of the impurity-impurity interactions even at concentrations below 100 ppm (similarly to the case of transport properties) and for single impurities

$$\chi(T) = \frac{\mu_{eff}^2}{3k_B(T+\Theta)} \qquad /68/$$

with $\mu_{eff} = 3{,}4\,\mu_B$ and $\Theta = +29°K$. Comparing this behaviour with the high temperature data of Hurd (1969) the Curie-Weiss law seems to hold even at temperatures well below T_K. The deviation from this law found by others was shown to arise from the impurity-impurity interactions, which change the Kondo temperature for impurity pairs, this conclusion was reached also by Hirschkoff et al (1971).

Although macroscopic susceptibility measurements are influenced by the contribution of the nuclear susceptibility below 1°K, specific heat measurements (Triplett and Phillips 1971) performed at various external magnetic fields indicate a simple power law for the susceptibility, given by

$$\chi(T) = \chi(T=0)\left[1 - \left(\frac{T}{\Theta_\chi}\right)^2\right] \qquad /69/$$

in the 0,01...1°K region, in accordance with the third law of thermodynamics, which requires $\partial\chi/\partial T \to 0$ as $T \to 0$.

That component of the susceptibility which is localised on the impurity is reflected by the hyperfine

field at the impurity site which can be measured by investigate the splitting of the Mössbauer line of the ^{57}Fe nucleus. Due to the large enhancement of the spin component, the orbital part of the hyperfine field can be neglected, and the splitting is proportional to $H_o + H_{hf}$ where $H_{hf} = H^d \langle S_z \rangle$. The experimental data can be analyzed in two different ways, either by fitting the field dependence of the hyperfine splitting with a Brillouin function assuming free spin behaviour (Frankel et al 1967), (Kitchens et al 1965) or by relating $\langle S_z \rangle$ directly to the susceptibility using the relation $\langle S_z \rangle = \frac{\chi H_o}{g \mu_B}$ and assuming g=2. The former method has the drawback of neglecting the non-free behaviour of the impurity spin (Scalapino 1966, Yoshida and Okiji 1965) while the latter neglects the saturation of the localized moment as well as assumes that g=2 and is independent of the temperature. By all means, analyzing the experimental data in the whole temperature range by one of the methods should give a consistent picture about the temperature dependence of the susceptibility localized on the impurity site. In the high temperature region $\langle S_z \rangle$ is proportional to the bulk susceptibility as the matrix polarization term can be neglected. Plotting H_{hf}/H_o as a function of the total susceptibility in the $T \gg T_K$ temperature range (Figure 7) the value of the hyperfine field per spin is given by

$$H^d = -94 \text{ kOe}$$

(Golibersuch and Heeger 1969). Including also the low temperature Mossbauer data H_{hf} can still be described by

$$H_{hf} \sim (T + \Theta)^{-1}$$

with $\Theta = +32$ in the whole temperature region both below and above T_K. As the same Curie-Weiss behaviour has been observed for the bulk susceptibility, this temperature dependence of the hyperfine field shows that the susceptibility is localized on the impurity site both above and below T_K. This can be shown more directly by comparing the $T \ll T_K$ hyperfine field data with the zero temperature susceptibility $\chi = \frac{\mu_{eff}^2}{3k_B\Theta}$ with the parameters given by Tholence and Tournier (1970), and using the high temperature coupling constant. Figure 17 shows the ^{57}Fe hyperfine field as a function of external magnetic field for $T \ll T_K$ the dashed line is computed with the above assumptions. While there is a slight departure from linearity in the high field region due to the saturation of the impurity spin, the excellent agreement at low external magnetic field supports the conclusion what we have drawn from the comparison of the temperature dependence of the hyperfine field and bulk susceptibility: the susceptibility is localized on the impurity site even in the nonmagnetic region $T \ll T_K$ and if there is an extended spin perturbation below T_K it should be an oscillatory one similarly to the familiar RKKY os-

cillation, with however negligible net average.

Host nuclear magnetic resonance is a sensitive probe of this distribution of the magnetization, and the properties of the ^{63}Cu NMR line are related directly to the behaviour of the spin perturbation around the impurities. A long range negative definite polarization would result in a net shift of the resonance line towards lower frequencies, while oscillatory distribution of the spin perturbation results only in a boradening of the signal similarly to the effect of the RKKY oscillation. In an attempt to find the long range spin polarization around the iron impurities in the nonmagnetic region Heeger et al (1968) performed a very detailed analyzis of the ^{63}NMR properties measured in a borad temperature range. In the first publication Heeger et al(1968) it has been claimed that the linewidth scales with the bulk susceptibility both below and above T_K. Later on Golibersuch and Heeger (1969) compared the line broadening with the local susceptibility measured by ME, and with this representation an excess line broadening appears at low temperatures, called "quasispin", with the following characteristics: it has no long range negative definite part as no line shift has been observed (Sugawara 1960). Moreover, the distance dependence is the same as the RKKY oscillation, as confirmed by measuring the effect of the electronic mean free path in CuAlFe alloys (Golibersuch

1970). Experiments on alloys with a wide range of impurity concentrations (Potts and Welsh 1972) suggest, that the effects are due to single impurities, even in the concentration region where the susceptibility is heavily influenced by impurity-impurity interactions. The argument is simply, that the contribution to the NMR signal from nuclei sensing large perturbations are wiped out, and only distant neighbours are reflected in the boradening. However, these arguments have met considerable scepticism, and the effect is regarded still as due to impurity interactions (Narath 1972). Recent very careful experiments of Alloul (private communication) using low impurity concentrations where impurity interaction effects are small for the susceptiblity indicate however, that the excess NMR line broadening is in fact a single impurity effect, which together with the information obtained from experiments on ternary alloys (Golibesuch 1970) can be interpreted as a temperature dependent s-d coupling $\mathcal{J}_{eff} \times \rho_S(\varepsilon_F)$: at temperatures $T \quad T_k$, this coupling is given by the Schricffer-Wolff transformation, and here $\mathcal{J}_{eff}\rho_S(\varepsilon_F) < 1$ (Weak coupling limit) at temperatures below T_k it increases and approaches to a limit $\mathcal{J}_{eff}\ \rho_S(\varepsilon_F) = 1$ at $T = 0$, which follows from Eq/45/ when $\langle S_z \rangle = 0$. Although this interpretation is certainly an over-simplifiaction of the actual state of affairs, it seems to be more appropriate from experimental point of view that the traditional spin compensation picture.

5.2. Another example: AlMn

When 3d-transition metal impurities are introduced into aluminium no evidence is found for the existence of localized magnetic moments, therefore, the impurities are usually regarded as nonmagnetic in the sense, that $(U + 4I)/\pi\Delta < 1$ for theses cases. The basic observation supporting this conclusion is the single peaked behaviour of the impurity resistivity versus the impurity atomic number N, as shown in Figure 4. This behaviour can adequately fitted to

$$R_{imp} = 5R_0 \sin^2 \frac{N\pi}{10} \qquad /69/$$

derived from the HF approximation of the Anderson model in the nonmagnetic limit. Eq/69/ however, holds for any spherical symmetric ground state, when $\eta_{2\sigma}(\varepsilon_F) = \eta_{2\sigma}(\varepsilon_F)$ and expresses only the charge neutrality condition; we have found, that Eq/69/ describes properly the T=0 resistivity of CuFe and CuCr. Therefore, a single peaked resistivity, compatible to Eq/69/ should hold at T=0 irrespectible to the parameters U + 4I and Δ. In fact, the estimation of the basic parameters fo the Anderson model leads to $\Delta \sim 1{,}0$ eV for impurities in aluminium, which, together with U + 4I = 5 leads to $(U + 4I)/\pi\Delta \sim 1{,}5$ and places AlMn in the magnetic limit. This conclusion has also been reached by Heeger (1969). This latter point, however, has not

been realized, and the interpretation of the low temperature anomalous properties has been approached from the nonmagnetic limit, and AlMn was the first example suggested to have localized spin fluctuation properties.

We begin with the discussion of the low temperature macroscopic properties: susceptibility, specific heat and transport phenomena. Although recent spin fluctuation theories seem to be able to describe even quantitatively these experiments, we keep only thel physical idea of localized spin fluctuations put forward by Caplin and Rizzuto (1968). After this, we turn to the discussion of a local parameter, the charge perturbation around the impurities, which is related closely to the transport properties, and finally we discuss the nature of the high temperature behaviour of this alloy.

5.2.1. Low temperature macroscopic parameters

The first and most evident indication of the nearly magnetic behaviour of the 3d-transition metal impurities is the sharp rise of the susceptibility in the middle of the series. This fact can be accounted for by claiming that it is due to the enhanced response of the impurity against a static external field, and

$$\chi_{spin} = \eta \chi_{Pauli} = \frac{10 N \mu_B^2}{T} \frac{\eta}{\Delta} \qquad /70/$$

where η the enhancement factor, which in the HF approximation is given by Eq/28/. η/Δ can be interpreted as an effective width of the virtual bound state, and Caplin and Rizzuto (1968) suggest, that this effective width is also appropriate to describe the thermal smearing of the scattering cross section. Therefore Eq/7/ neglecting the temperature dependence of t ε_F itself gives

$$R_{imp}(T) = R_{imp}(T=0)\left[1 - \frac{\pi^2}{3}\left(\frac{\hbar}{\Delta}\right)^2 k_B^2 T^2\right] \qquad /71/$$

The impurity resistivity follows indeed an initial T^2 dependence at low temperatures, (Caplin and Rizzuto 1968), Babic et al 1972b, Kovács-Cseténi et al (1972) with θ = 5 30°K and changes gradually to linear T dependence around 130°K. The two independent estimates of η/Δ , based on Eq/70/ and /71/ and shown in the first two columns of Table 4, provides a strong evidence for the connection of the two parameters involved.

This suggestion can be extended to account for other physical properties as well. The thermoelectric power is linear at low temperatures, S = -0.07 + 0.005 T eV/°K (Cooper et al 1974) which, when including non-resonant phase shifts gives a further estimation of η/Δ. The enhancement of the impurity specific heat

(Aoki and Ohtsuka 1969) can be written as

$$\gamma_{imp} = \frac{(2l+1)2\pi}{3} k_B^2 (\eta/\Delta)^{-1} \qquad /72/$$

with the same arguments as before, and η/Δ can be evaluated. These parameters, together with those obtained by inspecting the enhancement of the depression of superconducting transition temperatures (Babic et al 1972), and the enhancement of the effective mass m^* measured by de Haas van Alphen effect (Paton 1971) are included in Table 4.

The internal consistency of the effective widths supports the reality of such kind of analysis of the experimental data. It is important to emphasise, however, tha main aspects and the real meaning of this analysis. The simple power laws for the temperature dependences of the transport, thermal and magnetic properties is the consequence of a "normal" scattering amplitude (the derivatives of $t(\omega)$ are finite at the Fermi level). Moreover, the enhanced response of the system against static and dynamic perturbations driven by the external magnetic field nad by the thermal fluctuations seems to be similar. The meaning of the effective width η/Δ is not clear. It is basic to observe that macroscopic properties sample the scattering amplitude in the energy region kT around E_F but give no information of the characteristics of t at larger energies, and moreover, the temperature dependence of the scattering amplitude itself cannot be ruled out.

5.2.2. Charge perturbation around Mn impurities in Al

The low temperature macroscopic parameters provide us with important information on the low energy fluctuations, and can be interpreted by assuming that manganese in aluminium is non-magnetic, $(U + 4I)/\pi\Delta \quad 1$, but near to the HF boundary, resulting in an effective width γ/Δ . Then the temperature dependences can be thought to arise due to the thermal smearing of this narrow resonance, which behaves as an ordinary scattering centre, and only the width γ/Δ is determined by many-body effects (d-d correlations).

The properties of the charge perturbation around 3d-transitional metal impurities can give some more insight into the many-body effects involved. As mentioned in Chapter 2 the scattering amplitude $t(E_F)$ is reflected by the oscillation amplitude in the asymptotic range, therefore, the temperature dependence of the narrow resonance itself can be measured by this way. Assuming simple thermal smearing, the energy dependence dominates in the transport properties (see Equation 17) therefore $t(E_F,T)$ should indicate, whether this assumption is correct or not. Moreover, the energy dependence of the scattering amplitude is reflected by the spatial behaviour of the charge perturbation, therefore one can search for coherence effects by measuring this radial distribution. A further advantage of the method is, that while the macroscopic experiments were restricted

to the $kT \ll \eta/\Delta$ temperature region as the change of the matrix parameters (such as the phonon term in the case of resistivity or specific heat) hampers the precise determination of the temperature dependences in broad temperature interval, and so no information was gained on the high temperature behaviour of the manganeses impurity in aluminium, 6harge perturbation can be measured in a borad temperature range, as no corrections due to the matrix are necessary.

The way of measurement of this perturbation by investigating the quadrupole effect on the NMR signal were discussed in Chapter 3.3.2. The temperature dependence of the oscillation amplitude around 3d-transition metal impurities in aluminium was determined recently (Grüner and Hargitai 1971, Grüner 1972), by measuring the first order wipe out numbers n_1. As the wipe out numbers are of the order of 1500, the characteristic distance of the measurement is around 20 Å. Figure 18 shows the amplitude of the charge perturbation at T = 0 and T = 420°K, while the temperature dependence of the oscillation amplitude and impurity resitivity normalised to the T = 0 values are shown in Figure 18.

The dependence of α (which is proportional to n_1 and can be evaluated by a computer procedure) on the atomic number N shows a single peaked distribution, similar to the impurity resistivity at T = 0. In case

of one resonant phase shift the oscillation amplitude is given by

$$\alpha = 5 \sin \eta_2(\varepsilon_F) \qquad /73/$$

with $\eta_2(\varepsilon_F) = \frac{N\pi}{10}$. The full line of Figure 18 is calculated by Eq/73/ using the impurity atomic numbers shown in the figure. The good agreement between the calculated and measured dependence on N has the same meaning as in the case of the impurity resistivity: both parameters can be interpreted based on a spin degenerate virtual bound state at T = 0. At high temperatures, this dependence, however, becomes double peaked due to the strong temperature dependence of the charge perturbation around Mn and Cr impurities, and resembles the situation occurring in noble metal hosts. This behaviour was regarded as the basic evidence of a spin-split virtual bound state in the HF approximation of the Anderson model, when the impurities are "magnetic". The high temperature behaviour found here indicates a similar behaviour and the onset of the development of a double virtual bound state in AlMn.

The difference of the temperature dependence of the oscillation amplitude and impurity resistivity has a particular importance as the two parameters are determined by the scattering amplitude in a different way. While the temperature dependence of α is determined only by the temperature dependence of the

scattering amplitude at the Fermi level /Equation 49/, the resistivity reflects both the temperature and energy dependence of $t(\omega,T)$, see Equation 17. Both parameters are given by a T^2 dependence at low temperatures, but with different characteristic temperatures The characteristic temperature determining the temperature dependence of the oscillation amplitude $\Theta_\alpha = 860 \pm 100^\circ K$ while the resistivity gives $\Theta_R = 530 \pm 30^\circ K$. Comparing Equations 49 and 17, the two characteristic temperatures suggest that the temperature and energy dependence enters symetrically into the expression of the conductivity, and so $\Theta_\alpha = \sqrt{2}\,\Theta_R$ (Rivier and Zlatic, 1972) as observed. Therefore, the scattering amplitude has a strong energy dependence at ε_F, which in case of a Lorentzian resonance can be represented by a width $\eta/\Delta = 0.12$ eV.

While a good overall agreement is obtained at T = 0 between the calculated and measured oscillation amplitudes, a closer inspection shows, that α is somewhat smaller than the calculated values for AlMn and AlCr. This reduction might be due to the strong energy dependence of the scattering, which results in preasymptotic effects. As discussed in Chapter 3.3.2 these preasymptotic effects are important when r is smaller than the coherence length ξ_{Γ_α}. Comparing the measured oscillation amplitudes with the theory of preasymptotic behaviour (Mezei and Grüner 1972)

a rough estimation gives $\left\{ \begin{matrix} \\ \Gamma_{av} \end{matrix} \right.$ ~ 10 Å and Γ_{av} ~ 0.5 eV. The behaviour of the charge perturbation near to the impurities, i.e. on the first few neighbour shells, should be influenced more heavily by this preasymptotic behaviour. Recent pure quadrupole resonance experiments of Berthier and Minier (1973 a,b) indeed show the depression of the charge perturbation for AlMn and AlCr. The contrasting behaviour obtained in this case to that of an impurity Sc, where no such effects are expected is shown in Figure 20. The points on the figure are the measured values of the quadrupole coupling constants, the full line is the asymptotic expression, neglecting the oscillation, i.e. $\Delta q \sim \alpha / r^3$, with α taken from Eq/73/ with N = 5,5 and 4,5 for Mn and Cr, and 2,5 for Sc. While a good agreement is obtained for AlSc, and no presymptotic effects are present, the strong depression in AlMn and AlCr shows a clear evidence of the effect. Although the perturbation is oscillating - as evidenced by the nonmonotonous decrease of Δq -, the experimental values are in good agreement with $\Gamma \sim$ 0.5 eV when analysed on the basis of the theory. This experimental value has an especial importance, when contrasted with the "bare" width Δ of the resonance and with the effective width η/Δ, determined from the temperature dependence of the resistivity and charge oscillation amplitude. $\Delta \sim$ 1.0 eV is the unrenormalized (single particle) density of states,

while η/Δ is the measure of the energy derivative of the density of states at ε_F. The small η/Δ value indicates a sharp top of $\rho_d(\varepsilon_F)$, which, moreover, is temperature dependent, as evidenced by $\alpha(T)$. Γ_{av} obtained from the NMR experiments (presymptotics) is an average width of the density of states, and $\Gamma_{av} \sim 0.5$ eV implies that a large part of $\rho_d(\varepsilon_F)$ is distributed over large energy regions in order to compensate the effect of the sharp to at ε_F. Therefore, these experiments call for a complicated density of states, in contrast to the HF prediction which gives a Lorentzian resonance, for which η/Δ, Γ_{av} and Δ should be the same. The above analysis is one of the basic supports of the phenomenological model to be discussed in Chapter 6.

3.3.2.3. High temperature state of AlMn

The low temperature macroscopic properties of AlMn have a close similarity to those found in CuFe, in spite of the fact that the two systems were traditionally regarded as belonging to different class of alloys. In both systems simple power laws of temperature appear at temperatures below about 0.1 T_K showing that the low temperature behaviour of the impurities are controlled by the same physical processes. Due to the high Kondo temperature of AlMn early macroscopic measurements were restricted to

the low temperature region, allowing no direct insight into the high temperature properties, around T_K. The behaviour of the charge perturbation around the impurities (which parameter is free from complicated correction procedures), however, indicates the onset of development of a double peaked virtual bound state at high temperatures, and so magnetic behaviour in the Friedel-Anderson sense.

Recent measurements of the macroscopic properties in particular the impurity resistivity reinforce this conclusion, moreover, allow to make direct comparison with experiments performed in CuFe alloys. The high temperature behaviour of the impurity resistivity (after corrections for the deviations from the Matthiessen's rule) show a linear temperature dependence followed by a flattning of around room temperature (Babic et al 1971, K-Cseténi et al 1972, Babic et al 1972b, Kedves et al 1972). This temperature dependence has a close similarity to the universal curve shown in Figure 13, and to the temperature dependence of the impurity resistivity of AuV (Ford private communication). These main features were reproduced recently by Rivier and Zlatic (1973), who calculated the temperature dependence of R_{imp} for a virtual bound state undergoing spin fluctuations. Defining a spin fluctuation temperature $kT_{sf} = \hbar/\tau_{sf}$ where τ_{sf} is the lifetime of the fluctuations, the resistivity is a universal function of T/T_{sf}. It displays a quadratic

dependence at low temperatures, which becomes linear at $T_{sf}/6$, and flattens off around $T_{sf}/3$, just as observed experimentally if one choses $T_{sf} = 900^{o}K$. It seems therefore, that this approach, in spite of the theory is not renormalized, is successful in explaining the resistivity of AlMn, with an arbitrary chosen parameter T_{sf}. It has to be mentioned, that this approximation is not capable to give the correct relation between T_{sf} and the basic parameters of the Anderson model, and more ambitious attempts by Suhl, Hamman and Kuroda (for a Review see Fisher 1971) to improve the theory failed to arrive at the proper relation for large U/Δ values.

Due to the relative strong temperature dependence found in the case of AlMn and a somewhat smaller in case of AlCr the behaviour of the impurity resistivity versus the impurity atomic number becomes double peaked at high temperatures (Babic et al 1972, Kedves et al 1972), displays the similar behaviour to that found in the charge oscillation amplitude, and has a close similarity to the situation occurring in noble metal hosts, shown in Fig. 5. Due to the high characteristic temperatures for the 3d-transition metal impurities in aluminium only the onset of this process could be followed, although the similarity between the behaviour of the impurities in noble metal and in aluminium hosts seems to be convincingly demonstrated. There is a fairly similar behaviour of the Kondo temperatures of

3d transition metal impurities in different hosts as well. From the temperature dependence of the impurity resistivity Caplin and Rizzuto, 1968 and charge oscillation amplitude (Grüner 1972) the characteristic temperatures of Cr, Mn and Fe impurities were found to follow the same trend as in the case of noble metal hosts. A similar trend of the T_K values can be evaluated by inspecting the specific heat enhancements (Aoki and Ohtsuka 1969) and the impurity hyperfine properties (Narath and Weaver 1969). Recent careful analysis of the superconducting transition temperature using high concentration alloys (Babic et al 1972b) have demonstrated, that the behaviour of T_K versus N shows a similar V shaped curve in logarithmic representation to that in Cu and Au hosts shown in Figure 13. The temperature range spanned by the Kondo temperatures however, is much smaller than aluminium hosts as these alloys show weakly magnetic properties.

Nevertheless, these arguments strongly favour the picture, that above the characteristic temperature at least manganese becomes magnetic. Unfortunately, a direct test of this supposition does not exist. Susceptibility measurements in the liquid state (Flynn 1969) did not show a Curie-Weiss behaviour, which is probably masked by strong temperature dependent effects of toher origin. In a similar host Ga, however, while the low temperature susceptibilities have a

close resemblance to that found in aluminium alloys, a well observable Curie-Weiss behaviour was observable in case of Mn and Cr impurities in the liquid phase

Recent diffuse neutron scattering experiments, aiming to answer this question (Kroo and Szentirmai 1972, Bauer and Seitz 1972) seems not to be sufficient to arrive at a firm conclusion.

5.3. Common features of Kondo and spin fluctuation alloys

Although our goal in this chapter was to compare the experiments with the available theoretical formulas in both cases, and for historical reasons we compared CuFe with expressions derived from the s-d, and AlMn with those obtained from the spin fluctuation theories, we cannot escape from the conclusion, that it is hard to find any substantial difference between the two alloys on experimental grounds. Unlike four years ago (Heeger 1969), when the low temperature experiments on CuFe were heavily influenced by impurity-impurity interactions, now it is believed, and convincingly demonstrated, that both in AlMn and CuFe the temperature dependences are governed by simple power laws well below the characteristic temperature. This similarity calls for a unified theory with no fundamental distinction between Kondo and spin fluctuation system.

To demonstrate this point, we mention, that the characteristic temperature of AlMn, $T_K \sim 900^{\circ}K$ is reasonable looking at the expression of the Kondo temperature, Eq/56/. With Eq/45/, in the symmetrical case, where $E_d = U/2$ (and this is appropriate for AlMn where N = 5)

$$J_{eff}\,\rho_s(\varepsilon_F) = -\frac{4\Delta}{\pi^2 S \cdot u} \qquad /79/$$

and with $U/\pi\Delta = 1$, ($S=5/2$) $j_{eff}\,\rho_S(\varepsilon_F) = 0.16$. Inserting this into Eq/56/ $T_K \sim 100^{3o}$K is obtained in excellent agreement with the characteristic temperature observed. Although this agreement is certainly fortituous, as both Eq/56/ and /45/ break down for borderline cases, the drastic difference of T_K between CuFe and AlMn can, in principle be explained.

As regards the relevance of the experimental findings to the theory, one can reluctantly conclude, that a closer inspection shows vital disagreements. The s-d model seems to provide a reasonable description of the $T > T_K$ properties, the available approaches break down progressively going towards lower temperatures, with clear disagreements at $T < T_K$. The spin fluctuation theories seemingly reproduce the observed properties of AlMn even quantitatively, here however, objections against the existing approaches are raised from a theoretical point of view (see Zawadowski and Grüner 1974).

These difficulties are connected with the approximations used, but probably but not with the failure of the models themselves. It is essential, therefore, to compare the experimental information with the theory only at regions, where the particular approximations of the particular models are believed to be correct.

6. THE LOGARITHMIC AND SIMPLE POWER LOW REGIMES: THE HIGH AND LOW ENERGY FLUCTUATIONS

The two examples, discussed before have convincingly demonstrated the serious limitations of the available theories. These disagreements, however, are not fundamental ones regarding the models themselves, which are successful in explaining several anomalous properties. The s-d exchange model occounts well for Fermi surface phenomena at energies high compared with the Kondo temperature like magnetoresistance and logarithmic dependence of the resistivity on the temperature, as well as for interaction effects between the well defined impurity spins. The spin fluctuation concept, emphasising the interacting Fermi gas character of the electron system, on the other hand serves as a natural basis for the low energy fluctuations, leading to simple power laws, and explains interaction effects which have a character different from that in case of well defined moments in this temperature region.

There are some indications, for which situations the different models should work. For alloys, with well defined moments, and with weak interactions between the impurity and host (i.e. Mn impurities in noble metals) the transition temperatures are small, and so the characteristic impurity fluctuation time $\hbar/k_B T_K$ long, which may allow for a built-up the spin correlations in the surrounding electron gas. In alloys near to the

magnetic-nonmagnetic boundary, and having high Kondo temperatures CuCo or AlMn however, the fluctuations can be so fast, that no spin correlation can build up before the impurity spin is destroyed. The formal justification of this distinction is provided by the Schrieffer-Wolff transformation, according which the impurity can be pictureised as a well defined spin for large $(U + 4I)/\Delta$ values, but this visualization progressively breaks down with decreasing correlation energy. Experimental evidence presented in the previous Chapter calls for a unified description for CuFe and AlMn, with one key parameter T_k, depending however strongly on the correlation energy U + 4I, this requirement is supported by Fig. 13 too. The succes of the s-d model as regards the $T > T_k$ properties, and the spin fluctuation concept at $T < T_k$ suggest that the relevance of the model to the experimental situation does not depend only on the parameters of the Anderson model, but on the temperature too. The relevance of the s-d model to situations where magnetic behaviour is observed $T \gg T_k$ has been demonstrated repeatedly on the other hand spin fluctuation arguments require only that the impurity should be non-magnetic - and this is the case for $T \ll T_k$. Therefore in the following the $T > T_k$ properties will be examined in the light of s-d, the $T < T_k$ properties in the light of spin fluctuation models.

6.1. The logarithmic regime: experiments at $T \gg T_K$

The temperature region, where simple logarithmic temperature dependences are expected is restricted to well above the Kondo temperature, and serious deviations from the perturbation theories of the s-d model are expected here near to, although above T_K. In spite of this restriction, most experiments have been analysed based on the logarithmic scheme, and good agreement with the perturbation theory was claimed even for cases where the situation $T \gg T_K$ was far from being fulfilled. It is evident that this temperature range is accessible only in the case of alloys with very low Kondo temperatures, restricting the number of suitable systems considerably. In the following we will try to find a consistent picture of the various physical parameters, based on the s-d exchange model, and to obtain at least a semi-quantitive estimation of the parameters $\mathcal{J}_{eff}$ and S. The 'derivation' of $\mathcal{J}_{eff}$ from the Anderson-parameters, using available optical data, is followed by the discussion of experiments performed at $T \gg T_K$, i.e. at temperatures where the Kondo-effect is not operative, and the existence of the well defined impurity spin is not in question. Then we interpret the temperature dependences of the various physical parameters, approaching T_K from high temperatures, and finally we confine ourselves to the discussion of the Kondo temperatures.

The s-d exchange constant J_{eff} is related to the virtual bound state parameters by the Schrieffer-Wolff transformation, and is given by Eq/7/. This relation offers a determination of J_{eff} based on the optical experiments. For Mn impurities in silver, the parameters shown in Table 1 ($\rho_S(\varepsilon_F) = 0.11$ states eV atom spin) give

$$J_{eff} = 0.45 \text{ eV},$$

and, due to the similar Anderson parameters, similar J_{eff} values are expected for AuMn and CuMn alloys too. Although the Schrieffer-Wolff transformation can be applied only for the symmetrical case (E_d cannot be much larger than Δ for other cases due to the charge neutrality) an increase of J_{eff} is expected going towards the end and towards the beginning of the series.

Aldough it is chaimed (Schrieffer 1967) that Eq/7/ holds also for non-symmetrical cases, with S given by the Hund's rule, it seems to be more appropriate to describe J_{eff} by Eq/45/ in a phenomenological way, and than J_{eff} increases going towards the end and towards the beginning of the series because $\mathcal{J}$ decreases.

6.1.1. High temperature properties

Probably the most direct way of measuring J_{eff} is to measure the RKKY spin perturbation around the impurities. This perturbation has the amplitude proportional to J_{eff}, and can be evaluated by measuring the host NMR line broadening. Recently Mizuno (1971) has analyzed the line

boradening data of Sugavara (1960) on Cu-3d transition metal alloys, the j_{eff} values derived are shown in Table 5. j_{eff} shows a minimum for CuMn, as expected, and increases going to Cr and Fe impurities. Host and impurity line broadening data in other cases like AuV and AlMn (for a Review see Narath (1972)) indicate a large s-d coupling, in accordance with the expectation. The measurements, however have been performed in the nonmagnetic limit, below T_K, where the spin polarization might be modified compared with the high temperature region. Therefore, these values have limited significance in the present analysis.

Beside the single impurity properties, the s-d model provides an adequate basis for describing the intractions between the impurities too. The inelastic spin-flip scattering in presence of internal fields results in Kondo side-bands. It influences the Kondo slope and result in decreasing resistivity when the interaction energy is largen than kT_K. The temperature and concentration dependence of the measured resistivity is in excellent agreement with the computed ones for strongly magnetic cases (Beal-Monod 1969, Matho and Beal-Monod 1972), and the amplitudes of the RKKY perturbation which provides the coupling between the impurities derived in this way is in good agreement with those measured by NMR.

As the transport properties are influenced and in most cases in a dominating way by potential scattering effects, the evaluation of j_{eff} from those parameters

is not reliable. Magnetic field dependent effects, however, reflect mainly the spin-flip scattering, leaving the potential scattering backgorund unaffected and so, permit the evaluation of the parameters of the s-d model itself. The magnetic field dependence of the resistivity has been calculated recently both in second and third Born approximation (Beal-Monod and Weiner 1971) and comparing the calculated field dependence with measurements on CuMn and CuFe alloys taking into account potential scattering effects as well resulted in $\mathcal{J}_{eff} = -0.24$ eV for manganese, and -0.9 eV for iron impurities, although the latter value can be regarded only as a rough estimate, as experiments were performed in the $T > T_K$ range. Similar analysis resulted in similar value for AuFe (Rohrer 1969).

The $\mathcal{J}_{eff}$ values derived from the high temperature properties are collected in Table 5. They show the same trend as suggested by the Schrieffer-Wolff transformation, and by Eq/56/.

3.4.1.2. Logarithmic temperature dependences at $T > T_K$

Perturbation theory of the s-d exchange model predicts logarithmic dependences of the various physical parameters on the temperature. Kondo's third order calculation gives one logarithmic term $\mathcal{J}_{eff}^3 \ln \frac{kT}{D}$ and more sophisticated calculations reduce to Kondo's expression + correction terms at $T > T_K$. The ratio of the leading logarithmic terms is given by

$$\chi = \frac{\ln\left(\frac{kT}{D}\right)}{\ln\left(\frac{kT_K}{D}\right)} \qquad /75/$$

and X is not small, even at temperatures much higher than the Kondo temperature. Therefore, for numerical comparison with the experiments with the theory, expressions derived by the summation of all the leading logarithmic terms must be used. Moreover, only experiments performed on alloys with very low Kondo temperatures have a real significance although logarithmic behaviour has been observed over limited temperature range in certain other cases . see for example the universal resistivity curve of Figure 13 . In the following we analyse two experimental quantities: the impurity susceptibility and resistivity which are the most extensively measured quantities, although logarithmic dependences in other physical parameters appear at $T > T_K$ as well.

The susceptibility in leading logarithmic approximation is given by Eq/65/, and this expression is compatible with a Curie-Weiss law over a limited temperature range, with parameters $\Theta = 4{,}5\ T_K$ and $\mu_{eff}^2 = g^2 \mu_B^2\ S(S+1)$/1.22. Therefore, the s-d model in principle accounts for the strongly temperature dependent impurity susceptibility and finite Curie constant. Recent very high temperature susceptibility data on CuMn, CuCr and CuFe alloys (van Hoeve and van Ostenburg 1971) have been analyzed using Eq/65/. The authors claim, that $\chi(T)$ cannot be fitted with the above expression in the whole temperature range (up to about

1000°K). However, one can attribute this disagreement to factors, neglected in the analysis. The orbital susceptibility, which is temperature independent, and probably given by Eq/17/ plays a major role at high temperatures, causing a deviation found in all cases. Near room temperatures, where χ_{spin} is large, χ_{orb} can be neglected, and indeed a good fit to Eq/65/ was obtained by Smith and Smith (1970) who analyzed Hund's (1969) susceptibility data. While no similar analysis was performed for impurities other than Mn, the observed high temperature Curie-behaviours, with increasing values going towards the end or towards the beginning of 3d-series, suggest that, in principle, Eq/65/ accounts for the temperature dependence of the susceptibility also for these cases, and the increasing Curie-constants result in increasing j_{eff} values.

The impurity resistivity has the temperature dependence due to the s-d exchange scattering

$$R_{imp}(T) = cR_{sd}\left[1 + \rho_s(\varepsilon_F) j_{eff} \frac{kT}{D}\right] \qquad /176/$$

in the leading logarithmic approximation, serving as a firm basis of the logarithmic temperature dependences observed experimentally in many cases. The evaluation of from the experimental behaviours, however, is influenced by several factors. Aside from the problems, related to the derivations from Matthiessen's rule, which make the evaluation of the temperature dependence of R_{imp} due to the magnetic scattering ambiguous, the potential

scattering (though it gives a temperature independent background) has to be taken into account, and, moreover, the Kondo-slope is a sensitive function of the concentration (Matho and Beal-Monod 1972). Therefore, measurements on alloys with very low impurity concentrations must be chosen to compare with Eq/76/.

Among the borad area of experiments, the resistivity results of Gainon and Heeger (1969) on CuMn, Malm and Woods (1969) on AgMn and Loram et al (1968) on AuMn are the most valuable in this respect. In these cases R_{imp} is a linear function of lnT in broad temperature intervals. Comparing the measured temperature dependences with Eq/76/, the j_{eff} values can be determined, and these are shown in Table 5 together with those determined from $\chi(T)$.

Although the resulting j_{eff} values, derived from $R_{imp}(T)$ are smaller by a factor of 2 than those obtained from the analysis of the susceptibility, they show the similar trend in both cases. The requirement $T \gg T_k$ does not hold for impurities, other than Mn, logarithmic dependences were also found in case of chromium and iron impurities although in limited temperature regions. The situation is clearly visible in the universal resistivity curve of Loram et al (1971), shown in Fig. 4. The temperature dependence can be fitted with logarithmic law over about one decade, however, different slopes are obtained for different temperature intervals, the slope changes markedly even at temperatures above 100 T_k. Therefore, the j_{eff} values derived from the analysis of experiments based on Eq/76/ are questionable, and can be

regarded as an order of magnitude estimates. However, they indicate increasing j_{eff} in the Mn, Cr, Fe series; a similar trend that found from the high temperature properties.

6.3. Kondo temperatures

The Kondo temperature is given in terms of $j_{eff}\rho_s(\varepsilon_F)$ by Eq/56/, where j_{eff} couples to the Anderson parameters. The exact relation between T_k defined by Eq/56/ and the temperature T_k exp defined on experimental grounds is not exactly known in the case of resistivity for example it is usually defined as the temperature, where R_{imp} reaches half ot it's T = 0°K value and depends on the expression chosen to describe the temperature dependences, the exponential dependence of T_k on $j_{eff}\rho_s(\varepsilon_F)$ makes j_{eff} rather insensitive to small changes in T_k^{exp}. From the transition temperatures, found experimentally, therefore the s-d coupling can be evaluated rather precisely, these values are shown in Table 5, and in Fig. 21. While there are quantitative differences between the values determined from the different physical parameters, measured in different temperature regions, these differences can be attributed to the uncertainties of the experiments, and to the different average of $J(k,k')$ appearing in different experiments. The two main systematics, however; the dependence of j_{eff} on the impurity in the same host,

showing a minimum in the middle of the series, as well as the dependence of j_{eff} on the host for Mn impurities are the same when determined in a different way*.

Note: The j_{eff} values presented in Fig.21 and Table 5 have been derived on the assumption that formulas derived for S = 1/2 can be simply extended to the degenerate case, by simply replacing 3/4 with S(S + 1) in the relevant expressions. We think however, that this procedure is not entirely justified. A spin flip process in the case of degenerate impurity level changes the z-component of the spin from, say 5/2 to 3/2, with S being unchanged, this process corresponds to a spin flip scattering wit S = 1/2 and successive spin flip processes are needed to reverse the direction of the spin completly. Replacing simply S = 1/2 with S = 5/2 however leads to a complete spin reversal for one spin flip. It seems therefore, that the above replacement is not justified for the resistivity, where the S = 1/2 result should be used even for degenerate cases, for magnetic properties like the RKKY perturbation, however the total spin in the relevant quantity. This disparity might explain the differences between the j_{eff} values derived from differed physical parameters.

The above analysis, leading to a support of the s-d exchange model from the experimental side, is based mainly on experiments, performed alloys with very low Kondo temperatures. Thus, the conclusion, that the Kondo-model accounts for the main features of the various physical parameters, holds strictly only for these cases. As the s-d model is most appropriate for these situations (a low Kondo-temperature requires large$(U + 4\mathcal{D}/\Delta$ ratio) the succes of the model when related to these cases, is not surprising.

Furthermore, it should be emphasised, that the close corresponedence of the s-d exchange model and the HF approximation of the Anderson model in the magnetic limit which was emphasised in Chapter 3, holds for logarithmic region as well. Perturbation expnasions of the Anderson model in the large U limit result in the same temperature dependences as given by the s-d model (Scalapino 1966, Hamman 1966), the parameters of the two models, are linked together again by the Schrieffer-Wolff trans-formation.

---

* Note: As for U = 0 the characteristic temperature should be determined by Δ and not by T_F, we have replaced Eq/56/ with

$$T_k = \Delta \exp\left(-\frac{1}{j_{eff}\rho_s(\varepsilon_F)}\right) \qquad /77/$$

in evaluating j_{eff} from the measured Kondo temperatures.

The similar behaviour of the different alloys, and the general schemes, emerging from the inspection of the different properties and shown in Fig. 21, however, strongly indicate that the s-d model can be applied also for border line situations like CuCo or even for AlMn. This point of view has been demonstrated by Caplin (1968) who analysed the susceptibility data of $Cu_{1-x}Zn_{-x}Fe$ alloys. While the effective moment is a sensitive function of the zinc concentration, an experimental relationship

$$\frac{\partial R_{imp}(T)}{\partial \ln T} \sim j_{eff}^3 \mu_{eff}^2$$

predicted by the s-d model, holds for a broad range of μ_{eff} values, showing clearly the origin of the logarithmic dependence of the resistivity.

Looking at Fig. 21, which shows the correlation between j_{eff} determined from the $T > T_k$ properties and from the Kondo temperatures, one may conclude that the s-d model can be applied to describe the transition to the low temperature state, whenever there is a well defined experimentally observable moment at high temperatures. The model accounts well for both the high energy fluctuations, and for the transition temperatures. Therefore we cannot accept of having different processes, which determined separately the $T > T_k$ properties/like the logarithmic behavious , and the transition to the $T < T_k$ nonmagnetic state, as a crude distinction between Kondo effect and spin fluctuations would suggest; the

transition and the low temperature state should have the main features predicted by the s-d model. The continuous breakdown of the available solutions of the model going towards $T < T_k$ and their serious disagreement with the experiments well below the Kondo temperature, seems therefore due to the incompletemess of the approximations and not due to the irrelevance of the model itself.

6.2. The Simple Power Low Regime: Experiments at $T < T_K$

Probably the most important progress in the last two or three years is the clearing up of the role played by interactions between the impurities on the low temperature macroscopic properties. Recent experiments, using very dilute alloys, demonstrated that many "anomalous" logarithmic-type behaviours near T = 0 arise in fact from impurity interactions. In the light of th ese experiments, the general pattern of the low temperature single-impurity effects is completely different from the situation reviewed by Heeger in 1969, and there is growing belief among the experimentalists, that well below the characteristic temperatures, the temperature dependence of the various macroscopic parameters are determined by simple power laws of the temperature in the infinite dilution limit. Moreover, the low energy fluctuations of the system, reflected by the macroscopic properties, are similar to that of an interacting fermi gas.

This similarity is natural in the light of the localised spin fluctuation concept, which is based on the recognition, that even for a non-interacting Fermi gas, Curie-type susceptibility, so "magnetic" behaviour is expected for $T > T_f$, as the moment exists for a time $\hbar/\varepsilon_F$ even in a pure metal. The lifetime of the spin-fluctuations can be much larger, than the single-electron lifetime in dilute alloys $\hbar/\Delta$, and can be related to an effective density of states. It is assumed to have a Lorentzian form, characteristic to a lifetime broadening

$$\rho_d^{eff}(\omega) = \frac{2l+1}{\pi} \frac{\Gamma}{\Gamma^2+\omega^2} \qquad /78/$$

where $\Gamma = \hbar/\tau_{sf}$. The thermal fluctuations break up this resonance, leading to enhanced Fermi gas characteristics, at $kT \ll \Gamma$. As the localised spin fluctuation theory was the first physical idea, capable to account for the simple power laws observed experimentally, the low temperature experiments are usually interpreted within the framework of this tehory, and alloys displaying such behaviour are regarded as spin-fluctuation systems.

Any lifetime effect, irrespectible of whether it arises purely from d-d correlations in the spin fluctuation sense, or from s-d correlations which result in a finite spin memory time, should however give Fermi gas characteristics at low energies, and therefore would be in agreement with Eq/78/. In this sense, the following analysis is model independent, the main point of the

analysis is the assumption, that the many-body effects can be incorporated into an effective width Γ, appearing in the scattering amplitude, which then behaves as a simple single particle resonance, this is called a narrow resonance level /NRL/.

6.2.1. Resistivity at T = 0

The impurity resistivity extrapolated to T = 0 has a particular importance as it is related to the amplitude of the resonance at ε_F. The single peaked behaviour of R versus the impurity atomic number N was described by the phase shift $\eta_2(\varepsilon_F)$ as

$$R_{imp}(T=0) = R_0 5 \sin^2 \eta_2(\varepsilon_F) \qquad /79/$$

with $\eta_2(\varepsilon_F) = \frac{N\pi}{10}$ according to the charge neutrality in the non-magnetic limit, where $\eta_{2\sigma}(\varepsilon_F) = \eta_{2-\sigma}(\varepsilon_F)$. Fig. 22 shows the available T = 0 resistivity data for copper, gold and aluminium based alloys. Although no experiments are available in CuMn, AuMn, and AuCr alloys, due to their low Kondo temperatures, $R_{imp}(T=0)$ is remarkably similar for the different hosts, and shows,

---

* Note: Incorporating a finite spin memory time (τ_{sm}) into the s-d model in a phenomenological way (Larsen 1972 and references cited therein) result in simple power ldws, and temperature dependences determined by τ_{sm}.

that even for impurities with pronounced magnetic properties at high temperatures, the T = 0 resistivity is determined by the charge neutrality. The full line of Fig. 22 is computed from Eq/66/ with impurity atomic numbers shown in the figure; the deviations, most pronounced for Ti and V impurities can be ascribed to the non-resonant phase shifts η_0 and η_1.

6.2.2. Temperature dependences of the macroscopic properties

Using the standard Sommerfeld expansion, Eqs/13/-/15/ the NRL gives the following temperature dependence of the resistivity,

$$R_{imp}(T) = R_{imp}(T=0)\left[1 - \frac{\pi^2 k_B^2 T^2}{6\Gamma^2}\right] \qquad /80/$$

and similarly

$$C_v(T) = \frac{2(2l+1)\pi k_B^2 T}{3}\left[1 - \frac{4\pi^2 k_B^2 T^2}{\Gamma^2}\right] \qquad /81/$$

$$\chi(T) = \frac{2(2l+1)\mu_B^2}{\pi\Gamma}\left[1 - \frac{\pi^2 k_B^2 T^2}{3\Gamma^2}\right] \qquad /82/$$

at $kT \ll \Gamma$, neglecting the temperature dependence of the narrow resonance itself. While all of the parameters are related to the behaviour of $\rho_d(\omega)$ in the immediate vicinity of the Fermi energy, the transport properties and specific heat are determined by the effect of thermal fluctuations, $\chi(T = 0)$ measures the response of the system against an external magnetic field.

We confine ourselves to three typical alloys, two of them were already discussed at length in previous chapters: CuFe, AuV and AlMn. While manganese in aluminium is near to the magnetic-non-magnetic boundary in HF sense, and can be thought of as a nearly magnetic impurity, CuFe is a typical Kondo-alloy, and $(U + 4I)\,\rho_d(\varepsilon_F)$ is certainly larger than one. AuV represents an intermediate situation, $T_k \sim 300^\circ K$. We list (in fact for CuFe and AlMn repeat) those transport, specific heat ans susceptibility measurements, which are free from impurity-impurity interactions, and represent single impurity properties at $T < T_k$, and evaluate the effective width of the resonance from experimental data.

The impurity resistivity has a quadratic temperature dependence at low temperatures and

$$R_{imp}(T) = R_{imp}(T=0)\left[1 - \left(\frac{T}{\Theta_R}\right)^2\right] \qquad /83/$$

in all three alloys, but with rather different parameters. The quadratic dependence extends to about $\Theta_R/6$ in all three systems, where it flattens off and can be represented as a linear function of temperature. Comparing Eqs/80/ and /83/ $\Theta_R = \frac{\pi k_B}{\Gamma 6^{1/2}}$ and Γ derived from the measured Θ_R values are shown in Table 6. The thermo-electric power is a linear function of T where the resistivity diplays a T^2 dependence, and therefore shows the Fermi-gas character. Though various schemes are worked out to include the effect of normal potential scattering, all of them suffer from the shortcoming,

that the relation between the phase shift δ, introduced into the expression of the scattering amplitude, and the phase shift obtained from the Anderson-model is not known. The same holds for the Lorentz number, which can be related to $R_{imp}(T)$ and $S(T)$ by Eq/19/.

The impurity contribution to the electronic specific heat is proportional to T in the zero concentration limit, and shows a strong enhancement in all three cases.

$C_v = 800\,mJT/mole\,K^2$, $60\,mJT/mole\,K^2$

and 44 mJ/mole K^2 for CuFe, AuV and AlMn respectively. Using Eq/81/, the resulting Γ values are displayed in Table 6. The flattening off of C_v at higher temperatures in also in accordance with Eq/81/.

The impurity susceptibility, extrapolated to $T=0^oK$ follows the same trend as the specific heat. While in CuFe the spin component of the susceptibility dominates, due to the large enhancement, in the other two cases the orbital susceptibility has to be taken into account. From the impurity Knight-shift and relaxation times $X_{orb} = 5.10^{-4}$ emu/mole for AuV (Narath and Gossard 1968), and so $X_{spin} = 43.10^{-5}$ emu/mole. In AlMn besides the orbital term, the diamagnetic contribution to the impurity susceptibility is also important, of about -10.10^{-5} emu/mole. Together with $X_{orb} = 2.10^{-4}$ emu/mole gives $X_{spin} = 23.10^{-4}$ emu/mole. The Γ values, evaluated from Eq/83/ are given in Table 6. The temperature dependence of X_{imp} shows a fairly similar behaviour for

the three alloys, though different temperature intervals, compared to T_k were investigated in detail. In AuV the susceptibility is given by a T^2 dependence at low temperatures, and

$$\chi_{imp}(T) = \chi_{imp}(T=0)\left[1-\left(\frac{T}{\theta_\chi}\right)^2\right] \qquad /84/$$

with $\theta_\chi = 250^\circ K$ (van Dam et al 1972), and changes gradually to a Curie-Weiss dependence at about $70^\circ K$ (van Dam et al 1972, Kume 1967). In CuFe the susceptibility shows a Curie-Weiss dependence down to about $1^\circ K$ (Tholence and Tournier 1970), and specific heat measurements at various external magnetic fields (Triplett and Phillips 1971) indicate a T^2 dependence below $1^\circ K$ with $\theta_\chi = 7^\circ K$. In AlMn only the $T \ll T_k$ region is accessible due to the high Kondo temperature, and here $\chi_{imp} \tilde{} 1-\left(\frac{T}{\theta_\chi}\right)^2$ with $\theta_\chi = 1300^\circ K$. This dependence however is influenced heavily by the temperature dependence of the susceptibility of the pure Al, which results in a temperature dependent diamagnetic contribution. Due to these problems the derivation of the effective width from $\chi_{imp}(T)$ is not meaningful and only the temperature dependence, given by a simple power law in accordance with Eq/82/ should be emphasised.

The temperature dependences of the macroscopic parameters reveal the interacting Fermi-gas character of the low wnergy fluctuations, and the internal consistency of the effective width's derived from the various physical parameters demonstrates, that both the magnetic,

thermal and transport properties are controlled by the same type of fluctuations.

However, from Eq/81/ and /82/ immediately follows, that

$$\xi = \frac{\gamma_{imp}}{\chi_{imp}} \quad \frac{\chi_{host}}{\gamma_{host}} = 3/2 \qquad /85/$$

for a simple ordinary resonance, while from the experiments $\xi < 1$ is obtained. This discrepancy is due to the internal structure of the resonance, which result in a different enhancement against a static polarization driven by the extemal magnetic field, and against thermal excitations. In the s-d model, the susceptibility for $S \neq 1/2$ is enhanced by the factor $\frac{4}{3} S(S + 1)$ compared with the $S = 1/2$ case (the difference between $\mu_{eff}^2 = g^2 \mu_B^2 S(S + 1)$ for $S \neq 1/2$ and $S = 1/2$), therefore

$$\xi = \frac{9}{8S(S+1)}$$

is expected. In the spin fluctuation picture, if the $2\ell + 1$ states are fluctuating independently, Eq/85/ is recovered, but for the strong coupling limit and for the symmetrical case

$$\xi = \frac{3}{2(2\ell + 1)}$$

(Caroli et al 1969). Table 6 shows, that the ξ values are close to that predicted by both the Kondo and by the spin fluctuation scheme including orbital degeneracy, the experimental limitations however do not allow a distinction between the two predictions.

Furthermore, the effective width's, derived from the resistivity are always smaller, than those obtained from the specific heat enhancement. As both parameters are determined by the effect of thermal fluctuations, they should be the same, in case of a temperature independent resonance. If, however, $\rho_d(\varepsilon_F)$ is temperature dependent, and the energy and temperature dependence enters symmetrically into the resistivity see Eq/13 , and than $\Gamma_R = 2^{1/2}\Gamma_\gamma$, this is in much better in agreement with the experimental values. Therefore, it appears, that $\rho_d(\varepsilon_F)$ itself is temperature dependent too, its temperature dependence in the case of AlMn has been measured by NMR, and is shown in Fig. 19.

6.2.3. Local Properties

While the zero frequency susceptibility can be in all cases described by an effective width near T = 0, the frequency dependence of X_{imp} characterizes the dynamical response of the impurity + conduction electron system. The simple form of the dynamical susceptibility, suggested by the spin fluctuation theories (Rivier and Zuckermann 1968, Rivier 1968)

$$\chi(\omega) = \frac{2(2l+1)\mu_B^2}{\pi}\,\frac{1}{\Gamma + i\omega} \qquad /86/$$

immediately leads to the Koninga product Eq/40/ for the spin susceptibility. While Eq/43/ has been shown to be valid for $U/\pi\Delta < 1$,

and is based on a random phase approximation, as the effective width drops out from the Korringa product, it should have a more general validity. Alternatively, a theory for the magnetic limit of the Anderson model (Dworin 1971) gives at low temperatures

$$K_d^2 T_1 T = \pi S_{imp} S'$$

where S' is defined in Eq/40/.

While in the latter case the impurity spin appears in the Korringa equation in contrast to that obtained on the basis of the spin fluctuation concept (the situation is analogous that the relation between X_{imp} and γ_{imp} discussed in Chapter 6.2.2) the numerical factors are close to each other for all the cases considered, and for both AuV and AlMn, the experimental values consistent with both expressions allowing no distinction between the predictions based on s-d and spin fluctuation concept.

The local spin perturbation around the impurities, appearing in the host and impurity NMR line broadening gives a measure of the coupling strength between the impurity and conduction electrons. This perturbation has the familiar RKKY form in the nonmagnetic limit, as it has been demonstrated on CuCo recently (Ho et al 1972), and no anomalous term seems to appear below the Kondo temperature even for distances close to the impurity (Narath 1972). The amplitude of the perturbation, however, is expected to be different from that in the

high temperature limit. As $m = g\mu_B \langle S^z_{imp} \rangle$ goes to zero as $T \to 0$, Eq/45/ immediately leads to

$$J_{eff}\, \rho_s(\varepsilon_F) = 1 \qquad /87/$$

in this case (strong coupling limit). In this limit therefore J_{eff} defined in a phenomenological way as in Eq/45/, is independent on the impurity structure. The experimentally measured J_{eff} values, derived from the impurity (H^i_{nf}) and host (H^h_{nf}) studies are shown for different alloys in Table 7. In all cases the value of the coupling constant is in excellent agreement with the value of Eq/87/; therefore the strong coupling situation for $T < T_k$ seems to be well established.

6.2.4. Transition temperatures, given by the concept of NRL

The NRL concept, which provides a natural basis for the simple power law behaviours at low temperatures as well as of the impurity and host hyperfine properties also seems to be capable of accounting for the temperatures of the transition to the high temperature magnetic state. In this concept the impurity appears to be magnetic, when $k_B T < \Gamma$ and so smooth transition is expected between the non-magnetic and magnetic regimes around Γ/k_B This situation is analogous to a free electron gas where the degeneracy temperature is T_F

With the effective width's derived from the $T \ll T_k$ properties, this transition is expected to be around 30°, 400° and 900°K for CuFe, AuV and AlMn, in good agreement in the first two cases with temperatures, where the transitions were found experimentally.

The NRL scheme, while predicting correct $T \ll T_k$ properties and transition temperatures, does not lead, however, to logartihmic dependences at $T > T_k$, which are presetn for CuFe and probably also for AuV.* It seems, therefore, that this scheme oversimplifies the actual state of affairs, and the separation of the problem into many-body effects determining the width of the resonance and one electron effects thermal smearing of the resonance is unsuccessful as regards large fluctuation energies; the magnetic-nonmagnetic transition is more than a simple straightforward degeneracy.

The similar behaviour of the $T < T_k$ properties of the broad range of alloys, with rather different Anderson parameters, implies again, that the distinction between "magnetic" and "non-magnetic" impurities is artificial, the only difference appears in the effective width's of the narrow resonances formed at E_F.

---

* Note: the thermal smearing of a narrow resonance of the form of Eq/78/ results, for example, $R_{imp}(T) \sim T^{-1}$ at $K_B T > \Gamma$ (See Star 1971).

7. PHENOMENOLOGICAL DESCRIPTION OF THE RESONANCE FORMATION IN DILUTE ALLOYS

In the previous chapters we summarised the main experimental information on the local moment formation in dilute magnetic alloys, as well as the relation of the experiments to the theoretical situation in this field- excluding however the comparison with the more sophisticated theoretical methods .

First of all, the fairly similar behaviour of the different alloys - spanning nonetheless a broad range of Kondo temperatures, ranging from the mK region to well above room temperature - should be emphasised. Beside the similar overall behaviour of the transport, thermal and magnetic properties when going through T_k (see Chapter 4), this similarity has been demonstrated to exist both at $T > T_k$ and $T < T_k$, as discussed in Chapter 6. Here we refer to Fig. of Rizzuto's Review Paper (1974) as well, on which $\mathcal{R}_{imp}(T)$ is displayed for a broad range of alloys having essentially the same temperature dependence in reduced scale T/T_k. A clear-cut evidence of this universality has been presented recently by Schilling et al (1973) who measured $\mathcal{R}_{imp}(T)$ at various pressures in CuFe alloys. While T_k depends drastically on the pressure, again in reduced temperature scale $\mathcal{R}_{imp}(T)$ is the same. These universal behaviours give a strong experimental support to the conjecture, that all these alloys should be treated by

a common theoretical basis. Objections, raised against the s-d or LSF scheme by arguing that the former works only for $(U + 4I)/\Delta \gg 1$ the latter for $(U + 4I)/\Delta \ll 1$ are well grounded as far as a strict comparison with experiments is concerned, the main features of the models however probably survive to account for borderline situations as well. Second generation approaches of the s-d model (for references see the Review Paper of Heeger (1969)), however, have been disproved by the experiments, as it has been demonstrated in Chapter 5. As regards the spin-fluctuation concept, although it seems to work well in restricted temperatures (with a freely chosen parameter, the spin fluctuation lifetime), no renormalised theory exists at present. We therefore attempt to collect the main experimental evidences into a phemomenological model (Grüner and Zawadowski 1972), which contains the features to be explained by a complete theoretical treatment.

The high temperature $T \gg T_k$ state of the impurity seems to be relatively simple: it can be described adequately by the HF approximation of the Anderson model, including spin flip processes, the correlation effects are smeared out by the thermal fluctuations. The electronic structure is represented by atomic levels essential broadened due to interactions with the conduction electrons, and have the width Δ, these are the single particle resonances. When $(U + 4I)\rho_d(\varepsilon_F) < 1$ these levels are spin degenerate and have a Lorentzian

form. By increasing the correlation $(U + 4I)\rho_d(E_F)$ the impurity states become more and more polarised, and in the strongly magnetic limit the density of states becomes double peaked, and can be represented by two Lorentzian resonances, charge neutrality fixes the positions of the resonances with respect to E_F in all cases. The former situation applies to CuNi, the latter for CuMn for example, as confirmed by optical experiments. In the strongly magnetic limit the magnetic properties can also be described by assuming, that the impurity has a well defined spin, and, when using the s-d exchange model, the coupling between the impurity spin and the conduction electrons is weak, and depends strongly on the features of the impurity (Schrieffer-Wolff limit). There should be a smooth transition between the essentially non-magnetic and strongly magnetic limits as a function of the Anderson parameters; AuV is an appropriate example for a borderline case. The s-d exchange model might be extended even for these intermediate cases, where $(U + 4I)\rho_d(\varepsilon_F) \sim 1$ with J_{eff} defined in a phenomenological way, and then J_{eff} increases as $(U + 4I)\rho_d(\varepsilon_F)$ decreases. Correlation effects arise even at high temperatures, when the splitting of the virtual bound state is not large compared to U + 4I, this effect is evidenced by the preasymptotic behaviour of the spin perturbations, this preasymptotic effect is determined mainly by Δ and E_d and might be incorporated into the s-d model by assuming a k and k' dependent s-d coupling.

The low temperature state of the impurity is more complex, and the real nature of the nonmagnetic state at T=0 is still an unresolved question. For situations where $(U + 4I)\,\rho_d(\varepsilon_F) \ll 1$ (CuNi for example) the zero temperature state is well reproduced by the HF approximation as correlation effects are small, but for cases where well defined spin exists at high temperatures, i.e. where $(U + 4I)\,\rho_d(\varepsilon_F) > 1$ the finite susceptibility at T=0 is the result of many-body correlations, and should be distinctly different from the HF result. In fact, while a singlet state at T=0 is the essential feature of the various approximations of the s-d model (appropriate for the latter situation), it is often thought to be the result of a compensating spin polarized cloud around the impurity (Heeger 1969).

Instead of thinking, however, that this disappearance is due to a build up of a negative definite spin polarization in the surrounding matrix (which is disproved by the NMR experiments performed in CuFe and discussed in Chapter 4) it is more appropriate to visualize this disappearance as arising from the fact the impurity spin cannot be aligned by the external magnetic field due to the strong interaction with the conduction electrons. The finite susceptibility - and impurity hyperfine field - however means, that $\langle S_z \rangle = 0$ at T = 0 but not the impurity spin itself - in fact in the s-d model it is constant. On the other hand, the total spin - impurity + conduction electrons -

is removed from the system as evidenced by the measured total entropy change when going through the transition.

As regards the electronic structure of the Kondo-state, first of all charge neutrality is essential, and the density of states at E_F is determined by the Friedel sum rule, see Fig. 22 and Fig. 18. The energy dependence of the density of states, however, depends sensitively on the correlations. The $T \ll T_K$ properties have been discussed in Chapter 6 on the basis of a narrow resonance, which appears at the Fermi level and has the width of the order of kT_k. In the macroscopic properties, like resistivity and specific heat therefore the impurity looks like an ordinary resonance (there is no spin flip scattering at $T \ll T_k$), but NMR evidences presented for AlMn in Chapter 5 rule out the possibility of having a single narrow resonance i.e. parts of the density of states are distributed in large energy intervals. It is conceivable therefore, that the many-body resonance is sitting on a broad single particle background, which is hardly effected by thermal fluctuations. The energy dependence of the density of states is schematically plotted in Fig. 23a and 23b for two cases, for AlMn and CuFe. In both cases, the double peaked background shows up in the high temperature resistivities, for the CuFe situation it has been discussed in Chapter 3 and is essentially the same as displayed in Fig. 3. The low temperature many-body peak is sensed by the macroscopic properties, near to

$\mathcal{E}_F$ it has a Lorentzian form as shown by the simple power laws observed at $T \ll T_k$, but at high energies it must be logarithmic, this is correctly described by the s-d model. These main features of the resonance formation are well reproduced by the Kondo and LSF theories. In the Kondo model the HF background which serves as a microscopic basis of the s-d model is double peaked as $(U + 4I)/\Delta \gg 1$, in this limit, the appearance of the many-body peak (the Abrikosov-Suhl resonance) is the common feature of the various approximations, which disagree only in the detailed shape of the many-body resonance.

Alternatively, this picture is characteristic to that obtained from the spin fluctuation point of view. Using the dominant pole approximation of the Anderson model, a simple model calculation of the density of states reproduces all of the essential features discussed above, the energy dependence of the density of states, appropriate to the situation AlMn and CuFe is shown in Fig. 24. Both the double-peaked broad background and the many-body peak at E_F is recovered by this calculation, which also describes correctly the smooth transition from the strongly magnetic to the nonmagnetic limit. Therefore this calculation demonstrates, that the localised spin fluctuation concept aldough the approximation used is not entirely verified - can in principle produce a genuine magnetic impurity. No logarithmic behaviour is however obtained at $T > T_k$ from this model. The above description

of the density of states, together with the effect of temperature on the many-body resonance is entirely different from that anticipated by several authors (Souletie 1971, Stewart 1971) who suggested that the magnetic-nonmagnetic transition is in fact connected with a shift of the single particle resonances, and that below T_k the virtual bound state has form of unsplit Lorentzian and above T_k the structure is double peaked*. This behaviour has been described by $\eta_{k\sigma}(T)$ and $\eta_{2-\sigma}(T)$ the temperature dependence of the various physical parameters than has been related to these temperature dependent phase shifts (Souletie 1971, Loram et al 1971). This description however essentially neglects the correlation effects, which modify the character of the density of states, the difference between this description and that we described is similar to that between a metal-nonmetal transition of Wilson and Mott-type. The picture should also be distinguished from a simple motional narrowing effect, where either a narrow resonance or two broad resonances appear, depending on the frequency of interaction compared with the measuring frequency, in our case both features exist at low temperatures.

---

* Note: This point of view probably originates from the hypothesis often used for discussing transition metals, that correaltion effects can be incorporated into an effective interaction U_{eff}, and then the problem can be treated in HF approximation. In the presen case U_{eff} at T=0, and therefore a single Lorentzian resonance is obtained for all cases below T_k from this argument.

The energy dependence of the density of states is in strong correlation with the spatial extension of the localised state. Although it does not appear in the spin polarization, a coherence length $\xi = \frac{V_F}{2k_B T_K}$ characterises the extension of this state in space. This feature is well confirmed in the charge perturbation, discussed in Chapter 5, and probably appears in correlation functions of the form like $\langle S_{imp}\, S(r)\rangle$ too, but has not yet been observed experimentally. Although it has been claimed, that at that point Kondo and LSF approaches should give fundamentally different answers, the similarilty of $\rho_d(\omega)$ obtained from both approaches, and the strong relation of this feature to the spatial extension implies, that this is not the case. Outside the correlation range, however, the effect of the impurity is similar to that of an ordinary resonant scatter; that is why the resistivity is insensitive to these correlations as it describes the scattering of a conduction electron initially outside this range to a final state which is outside this region too. These "asymptotic" effects might be treated separately from the correlations, for example in this limit the spin perturbation can be described as having an ordinary RKKY form, but with a large s-d coupling constant $J_{eff}\,\rho_S(\varepsilon_F) = 1$ independent on the nature of the impurity strong coupling limit .

The width of the many-body resonance, which is strongly connected to T_k, is a sensitive function of the Anderson-parameters. Looking at Fig. 23a and 23b one can claim, that a larger "background" density of states leads to larger T_k as then it is easier to build up the narrow resonance, which has to reach the T = 0 charge neutrality limit; both U + 4I and Δ influence this background. The expression

$$k_B T_K = \Delta \exp\left(-\frac{1}{j_{eff}\rho_s(\varepsilon_F)}\right)$$

essentially reflects the effect of both factors. Although this expression should work only for the strongly magnetic cases, it might be approximately correct for the whole range of parameters, and describes properly the shift of the transition temperature from 10^3 ^oK to the milli-degree region by changing j_{eff} by a factor of two or three. The detailed temperature dependence of the various physical parameters depends on the detailed form and temperature dependence of the many-body peak. The Fermi gas character at $T \ll T_K$ and the logarithmic behaviours at $T > T_K$ are well confirmed experimentally and can be accounted by the present approaches of the spin fluctuation and s-d models it must be mentioned, however, that a logarithmic behaviour of any physical parameter is for more significant than a nonsingular (simple power law) character. Neither approach can, however, in it's present versions to describe the temperature dependences in the whole temperature regions,

in particular the change of regime from logarithmic to simple power laws. This is probably the main unresolved question to be answered; this question has initiated new theoretical ways and approaches to solve the problem. These attempts (reviewed by Anderson 1973), while rather promising, provide us with guidelines, and at the present stage merely with warnings on the complexity of the problem, than formulas to compare experimental results with. A full solution of the question, although being nearer than a few years ago, still needs considerable efforts from theoretical side.

8. CONCLUSIONS

The experimental results on classical dilute alloys were interpreted on the light of the available theoretical models, and were absorbed into a phenomenological model. The main features of this model can be visualised as a sum of single particle resonances accounted by the HF approximation of the Anderson model (these are the virtual bound states in Firedel's notation) and a many-body resonance (called as Suhl-Abrikosov resonance) pinned at the Fermi level, due to the fermi character of conduction electrons and due to the internal structure of the impurity which acts as a coupling between the conduction electrons; there is a well defined realtion between the two types of resonances. It appears that the nondegenerate Anderson model, and the s-d exchange model - together with the Schrieffer-Wolff transformation - can, in principle, account for all the main features of the experimental results, although the available approximations of the models are insufficient to explain fine, but nevertheless rather important details. Additional effects, like crystalline field splitting, spin-orbit coupling, anisotropy etc. seem not to influence heavily the general picture, and are not so important than in, for example, alloys of rare earths. During the discussion we have avoided the crucial question, namely why does the nondegenerate model work well, although orbital degeneracy is expected to play an important roel, similarly to the case of 3d

metals. The answer probably lies in the fact, that the impurity states are strongly coupled by the Hund's coupling, and the impurity spin from the dynamical point of view behaves as one entity, or in other words spin states not corresponding to the Hund's rule have a high energy compared to the energy of Hund's rule states. No separate evaluation of U and I is possible from the previous analysis, where we have assumed that the correlation energy is given by U + 4I, but the absence of orbital magnetism suggests, that $(U-I)/\pi\Delta < 1$, and then with our estimates of $(U + 4I) \sim 5$ eV and $\Delta \sim 0.5$ for noble metals values of $U \sim 3$ eV and $I \sim 0.5$ eV are reasonable. It has to be mentioned, that experimental evidences seem to emerge, which suggest, that the above representation is violated sometimes (Narath 1973), these observations can be related to speculations about anti-Hund's rule states (Caplin and Coles 1973), (Flynn et al 1972), which while rather interesting are far from being quantitative.

In spite of considerable progress, relatively little can be said about the relevance of the question of "bulk" magnetism to the dilute alloy case, although to understand some of the basic features of 3d metals on the basis of the Anderson model have been attempted (Wang et al 1969). Rather well defined efforts, with the aim to bridge the gap between the two fields of interest are becoming evident, in particular interaction effects in disordered systems (spin glasses) are more or less understood on the basis of the properties of single im-

purities, this seems to be the case for dilute compounds of 3d transition elements with simple metals, where the 3d atoms are far from each other and there is no direct d-d wave function overlap (Caplin and Dunlop 1973). One cannot however, escape from the conclusion, that in these cases strong local effects - not considered by the Anderson model - are operating too, and beside the two parameters correlation energy U and bandwidth D the question of Hund's rule has to be raised again; the strength of magnetism not being determined only by the ratio U/D. As a particular example for this situation the Au-V system should be mentioned. Single V impurities in gold are on the verge of magnetism, and have well defined Kondo anomalies. Vanadium pairs, however are nonmagnetic (Narath and Gossard 1968), while the compound AuV - where no vanadium nearest neighbour pairs are present - is ferromagnetic at low temperatures (Creveling and Luo 1967). One possible explanation is, that the effect of a vanadioum atom broadens the virtual bound state at the place of first nearest neighbours, and leads to the depression of magnetism; in this picture V pairs have a high Kondo temperature. Another, and more likcly reason for having nonmagnetic pairs is, that strongly bound V apirs give rise to a strong crystalline field splitting, which destroys the Hund's coupling; the latter explanation has been suggested by Cohen et al (1964). This situation however cannot be described by the Anderson

model, such type of effects lead probably to a broad variety of phenomena where a purely itinerant model breaks down, and where beside the correlation energy and bandwidth strong local configurational effects play on important role too.

9. ACKNOWLEDGEMENTS

The author should like to thank Prof. L. Pál and Dr. B. Vasvári for supporting this work, to Prof. K. Tompa and Dr. C. Hargitai for their continuous interest.

It is a pleasure to thank Dr. A. Zawadowski the numerous converstion and discussions during the course this paper. I would also like to thank Prof. B. R. Coles for various advices and permanent encouragement, he and Dr. P. Ford have critically red the manuscript.

I have especially benefited by the stimulating converstions with Dr. A. D. Caplin, Prof. N. F. Mott Dr. N. Rivier and Professor C. Rizzuto. Thanks are also du to Dr. H. Alloul, Dr. E. Babic, Dr. C. Berthier and Dr. M. Minier for discussing various parts of the paper.

This work was supported by the Scientific Research Council.

REFERENCES

ALLOUL H. and BERNIER P. 1972 J.Phys.F. 2, 21

ALLOUL H. and BERNIER P. 1974 Conference on Low Temperature Physics, Bouldar /to be published/

ALLOUL H., BERNIER P., LAUNOIS H. and POUGET J.P. 1971 J.Phys.Soc.Jap. 30, 101

ANDERSON P.W. 1961 Phys. Rev. 124, 41

ANDERSON P.W. and CLOGSTON A.M. 1961 Bull.Am.Phys. Soc. 6, 124- "Theory of Magnetism in Transition Metals", Varenna 1966 Ed: W. Marshal /New York and London, Acedemic Press/

ANDERSON P.W. 1968, Les Houches Ecole d'été 1967 The Many-body problem Eds: R. Balian and C De Witt, New York Gordon and Breach 1968

ANDERSON P.W. and McMILLAN W.L. 1967 in "Theory of Magnetism in Transition Metals" Varenna 1966 Ed: W. Marshal /New York and London, Academic Press/

AOKI R., OHTSUKA T. 1967 J.Phys.Soc.Jap. 23, 955

AOKI R., OHTSUKA T. 1969 J.Phys.Soc.Jap. 26, 651

APPELBAUM J.A., KONOD J. 1968 Phys.Rev. 170, 542

ASIK J.R., BALL M.A., SLICHTER C.R. 1966 Phys.Rev.Lett. 16, 740

BABIC E., KRSNIK R., LEONTIC B., OCKO M., VUCIC Z., ZORIC I., GIRT E. 1972 Solid State Comm. 10, 691

BABIC E., FORD P.C., RIZZUTO C., SALAMONI E. 1972a J.Low Temp. Phys. 8, 217

BABIC E., FORD P.C., RIZZUTO C., SALAMONI E. 1972b Solid State Comm. 11, 519

BAUER G., SEITZ E. 1972 Solid State Comm. 11, 179

BEAGLEHOLE D., HENDRICKSON T.J. 1969 Phys.Rev.Lett 22, 133

BEAGLEHOLE D., WILL H. 1972 J.Phys.F. 2, 43

BEAL-MONOD M.T. 1969 Phys.Rev. 178, 874

BEAL-MONOD M.T., WEINER R.A. 1968 Phys.Rev. 170, 552

BELL A.E. 1973 Thesis, Imperial College of Science and Technology

BENOIT H., DE GENNES P.G., SILHOVETTE D. 1963, C.R.Acad. Sci. 256, 3841

BERTHIER C., MINIER M. 1973a J.Phys.F. 3, 1169

BERTHIER C., MINIER M. 1973b J.Phys.F. 3, 1268

BLANDIN A. 1968 J.Appl.Phys. 39, 1285

BLOEMBERGEN N., ROWLAND T.J. 1953 Acta Met. 1, 731

BLOOMFIELD P.E., HAMMAN D.R. 1967 Phys.Rev. 164, 856

BOATO G., VIG J. 1967 Solid State Comm. 5, 649

BRETTEL J.M., HEEGER A.J. 1967 Phys.Rev. 153, 319

BREWIG E., KIERSPE W., SHOTTE V., WAGNER D. 1969 J.Phys. Chem.Sol. 30, 483

BROCK J.C.F., HO J.C., SCHWARTZ G.P., PHILLIPS N.E. 1970 Solid State Comm. 8, 139

CAMPBELL J.A. 1971 Solid State Comm. 9, 301

CAMPBELL J.A., COMPTON J.P., WILLIAMS F.R., WILSON G.V.H. 1967 Phys.Rev.Lett. 19, 1319

CAPLIN A.D. 1967 Phys.Lett. 26A, 46

CAPLIN A.D., DUNLOP J.B. 1973 J.Phys.F. 3, 1621

CAPLIN A.D., FOILES C.L., PENDORD J. 1968 J.Appl.Phys. 39, 842

CAPLIN A.D., RIZZUTO C. 1968 Phys.Rev.Lett. 21, 746

CAPLIN A.D., COLES B.R. 1973 Annual Solid State Physics Conference, Manchester

CAROLI B., LEDERER P., SAINT-JAMES D. 1969. Phys.Rev. Lett. 23, 700

CHAIKIN P.M., JENSEN M.A. 1975 Solid State Comm. 8, 977

CHAPMAN A.C., SEYMOUR E.F.W. 1958 Proc.Phys.Soc. 72, 797

CHRISTIENSON E.L. 1963 J.Appl.Phys. 34, 1485

COHEN M.H., REIF F. 1957 in: Solid State Phys. Ed: SEITZ F., TURNBULL D., Academic Press N.Y.

COHEN R.L., WERNICK J.H., WEST K.W., SHERWOOD R.C., CHIN G.Y. 1964 Phys.Rev. 188, 684

COLERIDGE P.T., TEMPLETON T.M. 1970 Phys.Rev.Lett 24, 108

COOPER J., BABIC E., VUCIC J. 1974 /to be published/

CREVELING L., LUO H.L. 1968 Phys.Rev. 176, 614

DU CHATELIER F.J., NOBEL J. 1962 Physica 28, 281

K-CSETÉNYI E., KEDVES F.J., GERGELY L., GRÜNER G. 1972 J.Phys.F. 2, 199

DANIEL E. 1962 J.Phys.Chem.Sol. 23, 975

DAS T.P., HAHN E.L. 1958 Solid State Physics Suppl. 1. Ed: SETZ F., TURNBULL D. Academic Press inc. New York London

DAYBELL H.D., STEYERT W.A. 1967 Phys.Rev.Lett. 21, 359

DAYBELL H.D., STEYERT W.A. 1968a Rev.Mod.Phys. 40, 380

DAYBELL H.D., STEYERT W.A. 1968b Phys.Rev. 167, 536

DREW H.D., DOEZEMA R.E. 1972 Phys.Rev.Lett. 28, 1581

DREW H.D., DOEZEMA R.E. 1973 Bull.Am.Phys.Soc. ser II. p.94

DWORIN L. 1971 Phys.Rev.Lett. 26, 1372

DWORIN L., NARATH A. 1970 Phys.Rev.Lett. 25, 1287

FISHER K. 1970 Springer Tracts in Modern Physics Ed:
G.HÖHLER, Vol 54 p:1

FISHER K. 1971 Phys.Stat.Sol. 46, 11

FLOQUET J. 1971 J.Phys.F. 2, 87

FLYNN C.P., RIGNEY D.A., GARDNER J.A. GARDNER 1967
Phil.Mag. 15, 138

FLYNN C.P., RIGNEY D.A. 1972 Phys.Rev. B6, 3358

FERDEL R.A., PRANGLE R.E. 1966 Phys.Rev.Lett. 17, 663

FORD P.J., LORAM J.W. 1974 /to be published/

FORD P.J., WHALL T.E., LORAM J.W. 1970 Phys.Rev. 2B, 1541

FRANKEL R.B., BLUM N.A., SCHWARTZ B.B. KIM D.J. 1967
Phys.Rev.Lett. 18, 1050

FRANCK J.P., MANCHESTER F.D., MARTIN D.L. 1961 Proc.Roy.
Soc. A263, 404

FRIEDEL J. 1956 Can.J.Phys. 34, 1190

FRIEDEL J. 1958 Nuovo Cimento Suppl. 7, 287

GAINON D., HEEGER A.J. 1964 Phys.Rev.Lett. 22, 1420

GIOVANNINI B., HEEGER A.J. 1969 Solid Stat.Comm. 7, 287

GOLIBERSUCH D.G. 1970 Thesis, Univ of Pennsilvania

GOLIBERSUCH D.G., HEEGER A.J. 1969. Phys.Rev. 182, 584

GOSSARD A.C., HEEGER A.J., WERNICK J.H. 1967 J.Appl.
Phys. 38, 1251

GRÜNER G. 1972 Solid State Comm. 10, 1039

GRÜNER G., HARGITAI C. 1971 Phys.Rev.Lett. 26, 772

GRÜNER G., K-CSETÉNYI E., TOMPA K., WASSEL C.R. 1971
Phys.Stat.Sol. 45, 663

GRÜNER G., ZAWADOWSKI A. 1972 Solid State Comm. 10, 1039

GRÜNER G., ZAWADOWSKI A. 1974 Reports on Progress in Physics /to be published/

HAMMANN D.R. 1966 Phys.Rev.Lett. 17, 145

HAMMANN D.R. 1967 Phys.Rev. 158, 570

HEEGER J.A. 1969 Solid State Phys., Ed: F.Seitz, D.Turnbull, New York Academic Press p:

HEEGER A.J., WELSH L.B., JENSEN M.A., GLADSTONE G. 1968 Phys.Rev. 172, 302

HERRING L. 1966 Magnetism IV. Ed: G.T.Rado, H.Suhl Academic Press, New York

HIRSCHKOFF E.C., SHANABARGER M.R., SYMKO O.G., WHEATLEY J. 1971 Phys.Lett. 34A, 341

HIRST L.L. 1970 Phys.Kondens Mat. 11, 255

HUISJEN M.A., SIEBERT J.F., SILSBEE R.H. 1971 Conference on Magnetism and Magnetic Materials, Chicago

HURD C.M. 1967 J.Phys.Chem.Sol. 28, 1345

HURD C.M. 1969 J.Phys.Chem.Sol. 30, 539

KEDVES J.P., HORDÓS M., GERGELY L. 1972 Solid State Comm. 19, 1067

KITCHENS T.A., STEYERT W.A., TAYLOR R.D. 1965 Phys. Rev. 138, A465

KITTEL C. 1963 Quantum Theory of Solids Whiley, New York

KJÖLLERSTROM B. 1969 Phil.Mag. 19, 1207

KLEIN A.P. 1969 Phys.Rev. 181, 579

KLEIN A.P., HEEGER A.J. 1966 Phys.Rev. 144, 458

KONDO J. 1969 Solid State Phys. Ed: F.Seitz, D.Turnbull, New York: Academic Press Vol 23. p:

KOO N., SZENTIRMAI Zs. 1971, Phys. Lett.

KUME K. 1967 J.Phys.Soc.Jap. 23, 1226

LANG D.V., BOYCE J.B., LO D.C., SLICHTER C.P. 1972 Phys. Rev.Lett. 29, 776

LORAM J.W., GRASSIE A.D.G., SWALLOW G.A., 1970a Phys. Rev. 2B, 2760

LORAM J.W., WHALL T.E., FORD P.J. 1970b Phys.Rev. 2B, 857

LUMPKIN H. 1967 Phys.Rev. 164, 324

MALM H.L., WOODS S.B. Con.J.Phys. 44, 2293

MATHO K., BEAL-MONOD M.T. 1972 Phys.Rev. 5B, 1899

MEZEI F., GRÜNER G. 1972 Phys.Rev.Lett. 29, 1465

MINIER M. 1969 Phys.Rev. 182, 437

MIZUNO K. 1971 J.Phys.Soc.Japan 30, 742

MONOD P. 1967 Phys.Rev.Lett. 19, 1113

MONOD P. 1968 Thesis, Orsay

MONOD P. and SCHULTZ S. 1968 Phys.Rev. 173. 645

MOTT N.F., ZINAMON Z. 1970 Rep.Progr.Phys. 33, 881

MYERS H.P., WALLDEN L., KARLSSON A. 1968 Phil.Mag.18,725

NARATH A. 1972a Solid State Comm. 10, 521

NARATH A. 1972b Crit.Rev. of Solid State Sci 3, 1

NARATH A. 1974 in Magnetism V. Ed: Rado and Suhl

NARATH A., GOSSARD A.C. 1969 Phys.Rev. 183, 391

NARATH A., WEAWER H.T. 1969 Phys.Rev.Lett. 23, 233

NORRIS N., WALLDEN L. 1969 Solid State Comm. 7, 99

NORRIS C., NILSSON P.O. 1968 Solid State Comm. 6, 641

OWEN J., BROWN M., KNIGHT W.D., KITTEL C. 1956 Phys. Rev. 102, 1501

PATON B.E. 1971 Can.J.Phys. 49, 1813

POTTS J.E.,WELSH L.B. 1972 Phys.Rev. 5B, 3421

RIVIER N. 1968 Thesis, Univ of Cambridge

RIVIER N., ZITKOVA J. 1971 Adv. in Physics 20, 143

RIVIER N., ZLATIC V. 1973 J.Phys.F. 2, L87

RIVIER N., ZUCKERMANN M. 1968 Phys.Rev.Lett. 24, 225

RIZZUTO C. 1974 Reports on Progress in Physics /to be published/

ROHRER H. 1968 Phys.Rev. 174, 583

ROWLAND T.J. 1960 Phys.Rev. 119, 900

ROWLAND T.J., SHIOTANI N. 1968 AIME Conf. /unpublished/

SCALAPINO D.J. 1966 Phys.Rev.Lett. 16, 973

SCHILLING J.S., HOLZAPFEL W.B., LÜSCHER E. 1972 Phys. Lett. 28A, 129

SARACHIK M.P., CORENZWIT E., LONGINOTTI L.D. 1964 Phys.Rev. 135, A1041

SCHRIEFFER J.R. 1967 J.Appl.Phys. 38, 1143

SCHRIEFFER J.R., MATTIS D.C. 1965 Phys.Rev. 140, A1412

SCHRIEFFER J.R., WOLFF P.A. 1966 Phys.Rev. 149, 491

SEIB D.H., SPICER W.E. 1970 Phys.Rev. 2B, 1676

SCHILLING J.S., HOLZAPFEL W.B., LUSHER E. 1972 Phys. Lett. 38A, 129

SILVERSTEIN S.D. 1965 Phys.Rev.Lett. 16, 466

SMITH D.A., SMITH G.B. 1971 Phys.Rev. 4B, 191

SÓLYOM J. 1970 Z.Physik 238, 195

SOULETIE J. 1971 J.Low Temp.Phys. 7, 141

STAR W.M. 1971 Thesis, Univ. of Leiden

STAR W.M., DE VROEDE E., VAN BAARBE L. Physica 59, 128

STASSIS C., SHULL C.G. 1972 Phys.Rev. B5, 1040

STEINER P., ZDROJEWSKI W.V., GUMPRECHT D., HÜFNER S. 1973 Phys.Rev.Lett. 31, 355

STEEL M.R. 1972 J.Phys.F. 2, 605

STEEL M.R., THERENE D.M. 1972 J.Phys.F. 2, 199

STEWART A.M. 1971 Nuovo Cimento Lett. 2, 1236

SUGAWARA T. 1969 J.Phys.Soc.Jap. 14, 643

TRIPLETT B.B., PHILLIPS N.E. 1971 Phys.Rev.Lett. 27, 1001

THOLENCE J.L., TOURNIER R. 1970 Phys.Rev.Lett. 25,867

TOMPA K. 1972 J.Phys.Chem.Sol. 33, 163

TOMPA K. 1971 Tihany Conference on the magnetic and electric properties of dilute alloys /unpublished/

TOURNIER R., BLANDIN A. 1970 Phys.Rev.Lett. 24, 397

VAN DAM J.E., VAN DEN BERG G.J. 1970. Phys.Stat Sol. 3, 11

VAN DAM J.E., GUBBENS P.C.M., VAN DEN BERG G.J. 1972 Physica 62, 389

VAN DEN BERG G.J. 1964 Progress in Low Temp. Phys. Ed: G.J.Gorter Amsterdam, North Holland Publishing Co Vol 4, p:194

VAN HOEVE H.G., VAN OSTENBURG D.O. 1971 Phys.Rev.Lett. 26, 1020

WADA S., ASAYAMA K. 1971 J.Phys.Soc.Jap. 30, 1337

WANG S.Q., EVERSON W.E., SHRIEFFER J.R. 1969 Phys.Rev. Lett. 23, 92

WASZINK J.H., COLES B.R. 1967 Proc.Phys.Soc. 92, 731

WILLIAMS J.R., CAMPBELL J.A., SANCTUARY C.J., WILSON C.V.H. 1969 Solid State Comm. 8, 125

WOLLEBEN D., COLES B.R. 1973 in Magnetism V. Ed: H.Suhl,
Academic Press New York

WOLFF P.A. 1961 Phys.Rev. 124, 1080

YOSHIDA K. 1957 Phys.Rev. 106, 893

YOSHIDA K., OKIJI A. Progr.Theor.Phys. /Kyoto/ 34, 505

ZLATIC V., GRÜNER G., RIVIER N. 1974 Solid State
Comm. /to be published/

TABLE CAPTIONS

Table 1. Virtual bound state parameters derived from the optical experiments.

Table 2. Impurity hyperfine fields and relaxation times for "non-magnetic" impurities (Narath 1972).

Table 3. Classifications of the dilute alloys according to the HF approximation of the Anderson model. The symbols are explained in the text.

Table 4. Effective width's of the virtual bound state of AlMn, determined from the low temperature macroscopic properties.

Table 5. $\mathcal{J}_{eff}$ values determined from the high temperature properties of alloys, from the logarithmic T dependences of X and $\mathcal{R}$ and from the Kondo temperatures.

Table 6. Effective width's of the alloys CuFe, AuV and AlMn derived from the phenomehological analysis of the low temperature macroscopic properties.

Table 7. $\mathcal{J}_{eff}\,\rho_S(\varepsilon_F)$ values of various alloys in the $T \gg T_k$ temperature region, determined from the NMR line broadening (see Narath 1972).

FIGURE CAPTIONS

Fig. 1. Differential obsorptivity of CuNi alloys with different nickel concentrations (Drew and Doezema 1972).

Fig. 2. Intraband optical absorption in AlMn alloys (Myers et al. 1968).

Fig. 3. Positions of the virtual bound states with respect the fermi level derived from the optical absorption experiments.

Fig. 4. Low temperature impurity resistivites of Al-based alloys.

Fig. 5. Room temperature impurity resistivities of Cu and Au based alloys.

Fig. 6. Impurity resistivites in Cu and Au based alloys. The abscissa is normalised to the impurity d-occupation numbers, as explained in the text.

Fig. 7. Impurity hyperfine field values H/ T +29 in CuFe alloys (Golibersuch and Heeger 1968).

Fig. 8. Temperature dependence of the resistivity in CuMn alloys. The resistance maximum for the highest Mn concentrations arises from magnetic ordering.

Fig. 9. Temperature dependence of the magnetic momem in AuV alloys (Van Dam et al 1972).

Fig. 10. Temperature dependence of the impurity specific heat in CuCr alloys (Triplett and Phillips 1971).

Fig. 11. Temperature dependence of the thermoelectric power of various alloys. For reference see Rizzuto (1974).

Fig. 12. Temperature dependence of the impurity resistivity in CuFe alloys (Dybell and Steyert 1968).

Fig. 13. Kondo temperatures of 3d-transition metal impurities in Cu and Au host. The values are averages obtained from different experiments. For reference see Rizzuto (1974).

Fig. 14. Temperature dependence of the impurity resistivity in $Cu_xAu_{1-x}Fe$ alloys, normalised to a characteristic temperature T_c. The full line is the Hamman- curve with S = 0.77. (Loram et al 1970b).

Fig. 15. Impurity resistivity of CuFe at $T \ll T_k$. The full line is the Appelbaum-Kondo expression, which gives a good description for the high concentration alloys, but is in disagreement with the experiments on the Cu 50 ppm Fe sample (Star 1971).

Fig. 16. Impurity specific heat of CuFe at $T \ll T_k$. The dotted line is the zero concentration limit according to Triplett and Phillips (1971). The full line is the Appelbaum-Kondo expression (Star 1971).

Fig. 17. Impurity hyperfine field versus applied field in CuFe. The dotted line is calculated by assuming that the susceptibility is localised at the impurity site. The experimental data are taken from Golibersuch and Heeger (1968).

Fig. 18. Amplitude of the charge perturbation around the impurities in Al. The full line is calculated from the expression $\alpha = 5 \sin \frac{N\pi}{10}$ with N shown in the Figure (Grüner 1972).

Fig. 19. Temperature dependence of the oscillation amplitude and impurity resistivity in AlMn alloys (Grüner 1972).

Fig. 20. Radial dependence of the charge perturbation around impurities in Al. The full line is calculated using the asymptotic expression of the perturbation, the dotted line by assuming an averaga width of the resonance $\Gamma_{av} = 0.5$ eV. (Berthier and Minier 1972)

Fig. 21. j_{eff} values determined from host NMR line broadening and from the Kondo temperatures, using Eq/7/, from the magnetoresistance $\mathcal{R}(H)$ and from the Kondo-slope of the resistivity $\mathcal{R}(T)$

Fig. 22. Impurity resistivites of 3d transition metal impurities in Au, Cu and Al at T=0. The full line is calculated using the expression $R_{imp} = R_0\ 5 \sin^2 \frac{N\pi}{10}$ with N as shown in the figure (Grüner and Zawadowski 1972).

Fig. 23. Schematic plot of the density of states for Cu and Al alloys (Grüner and Zawadowski 1972).

Fig. 24. Spectral density, characteristic to AlMn and CuFe obtained from the dominant pole approximation of the Anderson model. The insert shows the narrow resonance in an extended scale (Zlatic et al 1974).

Table 1.

Alloy	$E_{d\sigma}$ (eV)	$E_{d-\sigma}$ (eV)	Δ (eV)	$U+4I \sim \partial E_d$ (eV)
AgMn	1,6 a/ 1,5 b/ 2,0 c/	-2,25 a/ -3,2 c/	0,5 a/	5 a/ 4,8 c/
AuMn	2,7 c/	-2,0 c/		4,6 c/
AuCr	1,2 d/			
AuV	~0 d/			
AuFe	3-5 e/			
AuNi	-0.7 f/		0.2 f/	
CuNi	-0,95±0,05 g/ -0,75±0,02 b/		0,42±0,05 g/ 0,17±0,02 h/	
AgPd	2,6 c/			

a/ Myers H.P., Wallden L., Karlsson A. /1968/
b/ Wallden L. /1970/
c/ Steel M.R., Therene D.M. /1972/
d/ Steel M.R. /1972/
e/ Beaglehole and Mendrickson /1969/
f/ Drew M.D, Doezema R.E /1973/
g/ Seib D.M. Spicer W.E. /1970/
h/ Drew M.D., Doezema R.E. /1972/

Table 2.

Alloy	$K[\%]$	T_1T [msec°K]	$K_d[\%]$	$K_{orb}[\%]$	H_{nf}^d [kOe/μ_B]
CuNi	+ 1,28	6,8	- 0,3	+ 1,6	100
CuCo	+ 5,2	20	-1,4...-2,8	+8,0...+6,4	70...100
AlV	+ 0,30	28	- 0,4	+ 0,7	
AlCr	+ 0,38	3,5	- 1,4	+ 1,0	130
AlMn	- 2,01	0,8	- 3,5	+ 1,5	140

Table 3.

HOST / IMPURITY	Au	Cu	Zn	Al
Ti	NM	NM	NM	NM
V	?		NM	NM
Cr	M	M	M	?
Mn	M	M	M	?
Fe	M	M	M	NM
Co	?	?	NM	NM
Ni	NM	NM	NM	NM

Table 4.

PARAMETER	T dependence	$(\gamma_\Delta)^{-1}$ eV	$\theta(^\circ K)$
X	$X(T) = X(0)\left(1-(T/\theta)^2\right)$	0,08	1300
$\mathcal{R}$	$\mathcal{R}(T) = \mathcal{R}(0)\left(1-(T/\theta)\right)^2$	0,083	530
S	$S(T) \sim T$	0,16	
C_v	$C_v = \gamma T$	0,17	
$\frac{dTc}{dc}$		0,16	
dHvA eff.		0,13	

Table 5.

Alloy	NMR	$\mathcal{R}(H)$	$\chi(T)$	$\mathcal{R}(T)$	T_K	INTERACTION EFFECTS
CuCr	4,5 a/				- 0,3	
CuMn	2,5 a/	- 0,33 b/	-0,55 d/	-0,29 d/ -0,55 e/	- 0,24	- 0,36 f/
CuFe	5,0 a/	- 0,9 b/		-0,9 e/	- 0,36	
CuCo	15,0 a/ 5,0				- 0,80	
AgMn	1,1		-0,48 d/	-0,24 d/	- 0,22	- 0,26 f/
AuV	5,6				- 0,6	
AuMn			-0,49 d/	-0,17 d/	- 0,6	- 0,31 f/

a/ Mizuno /1971/
b/ Monod P. /1967/
c/ Rohrer /1971/
d/ Smith and Smith /1970/
e/ Star /1971/
f/ Matho and Beal-Monod /1972/

Table 6.

Alloy	Γ_x [$\times 10^2$ eV]	Γ_R [$\times 10^2$ eV]	Γ_{c_v} [$\times 10^2$ eV]	ξ	T_K
CuFe	0,18	0,35	0,75	0,24	20
AuV	2,4	4,0	10,3	0,24	250
AlMn	4,1	8,3	17	0,23	500
AlCr	6,5	23	23	0,28	1400
AuCo	1,2		19	0,06	400

Table 7.

Alloy	AlMn	AuV	CuCo
$(2\ell + 1)\ j^{h}_{eff}$ (eV)	4,7	7,4	15
$(2\ell + 1)\ j^{i}_{eff}$ (eV)	6,0	5,6	5
$j_{eff}\ \rho_S\ (E_F)$	1,0	0,9	1,1

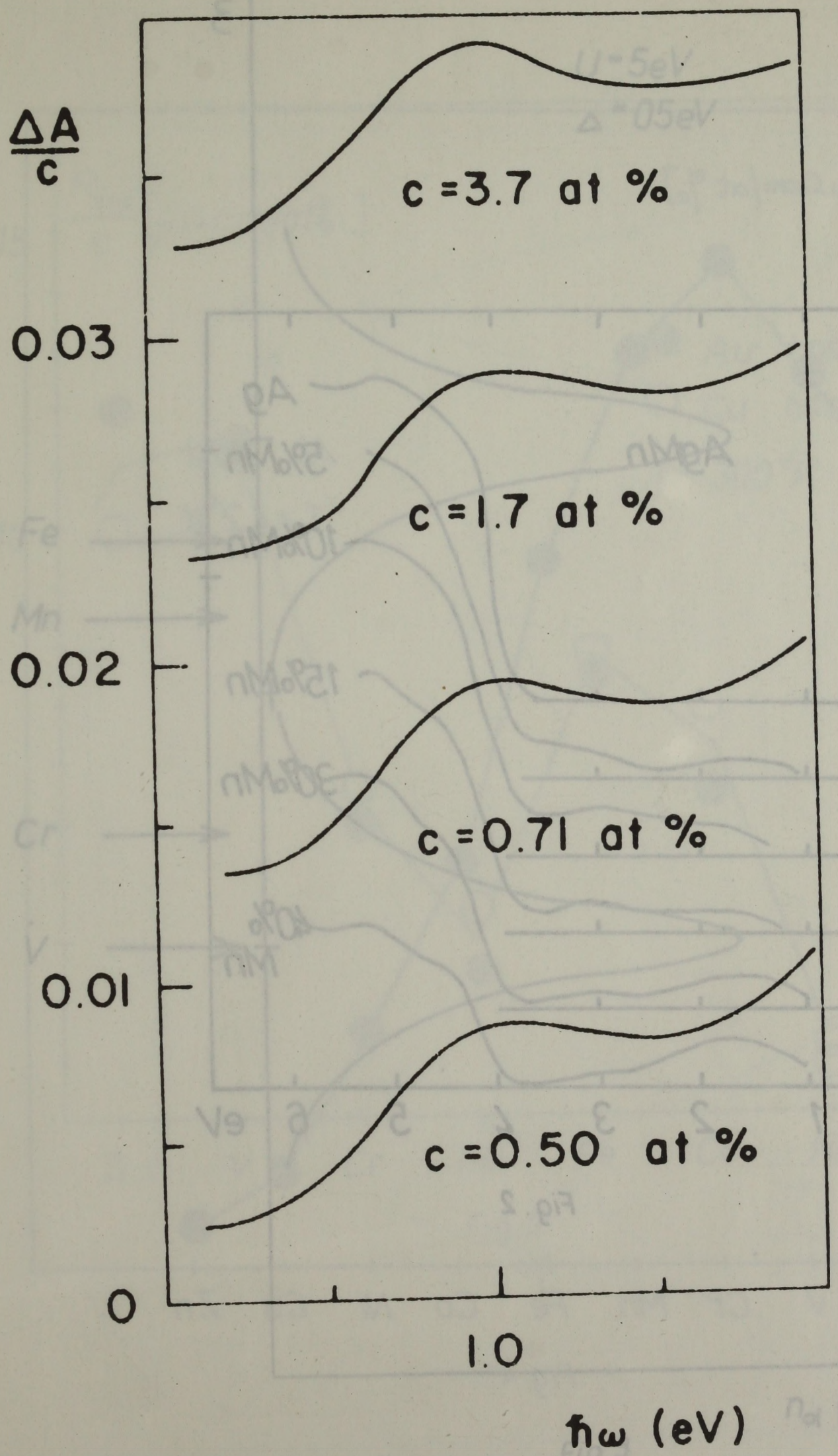

Fig. 1

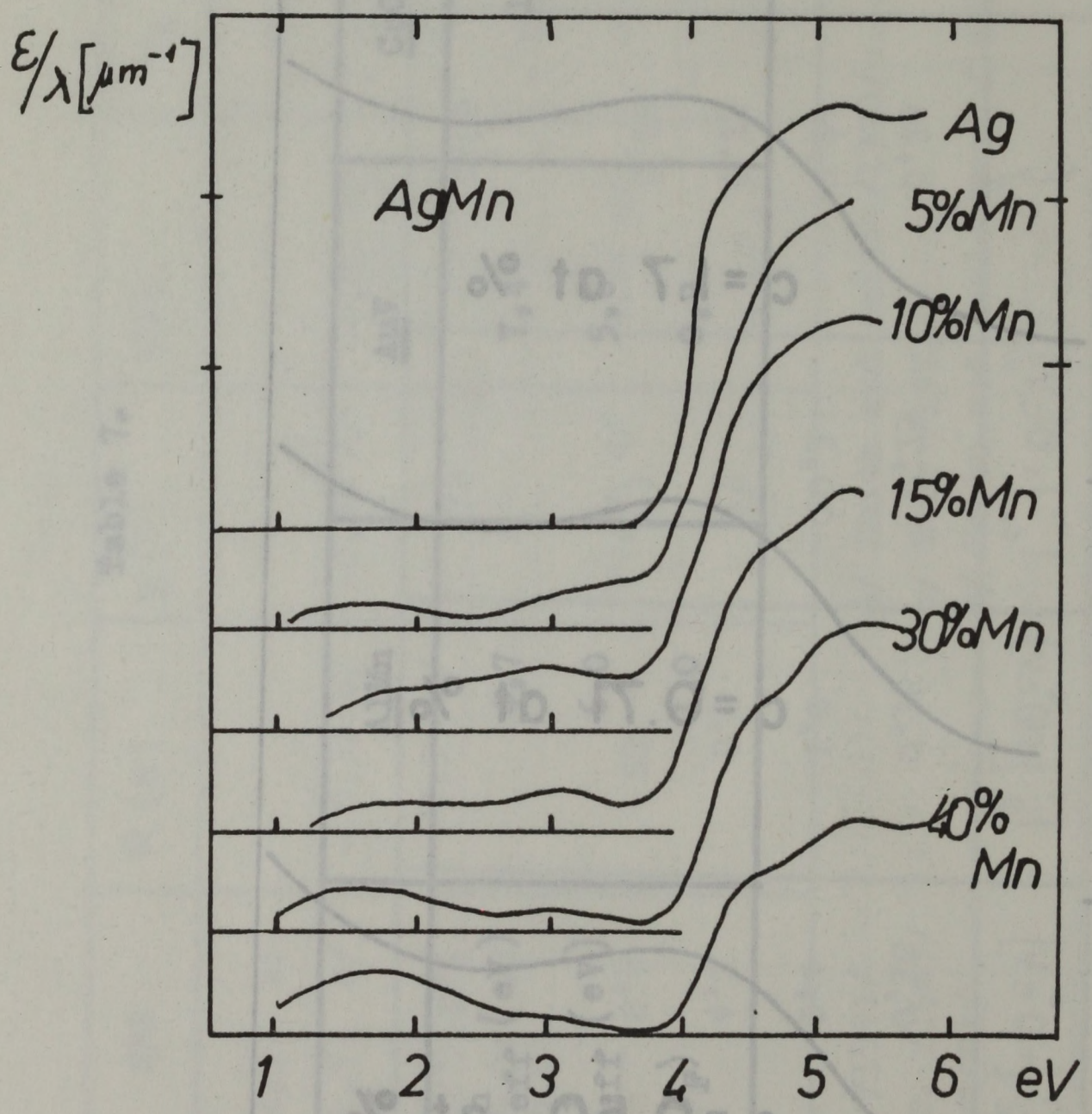

Fig. 2

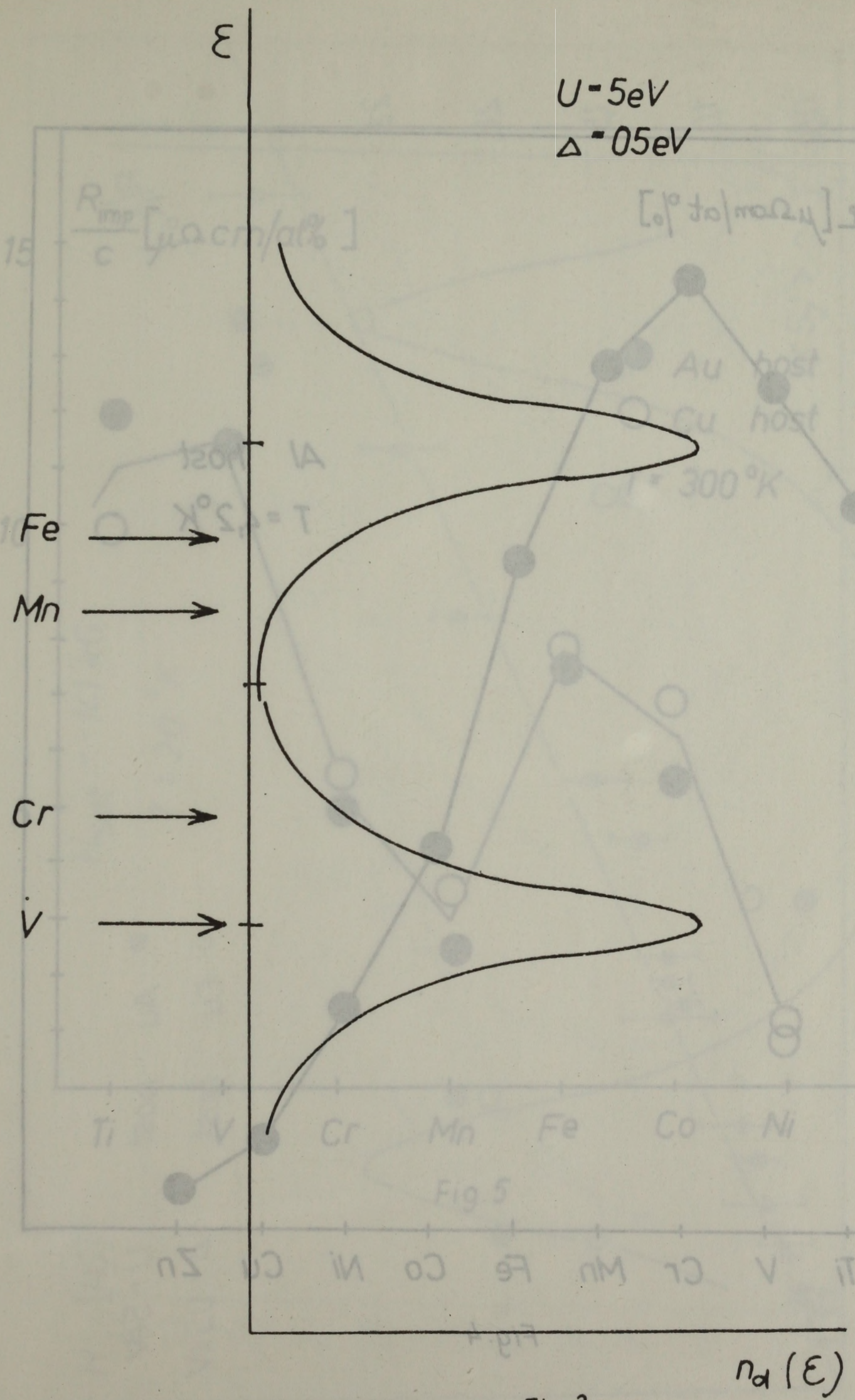

Fig. 3

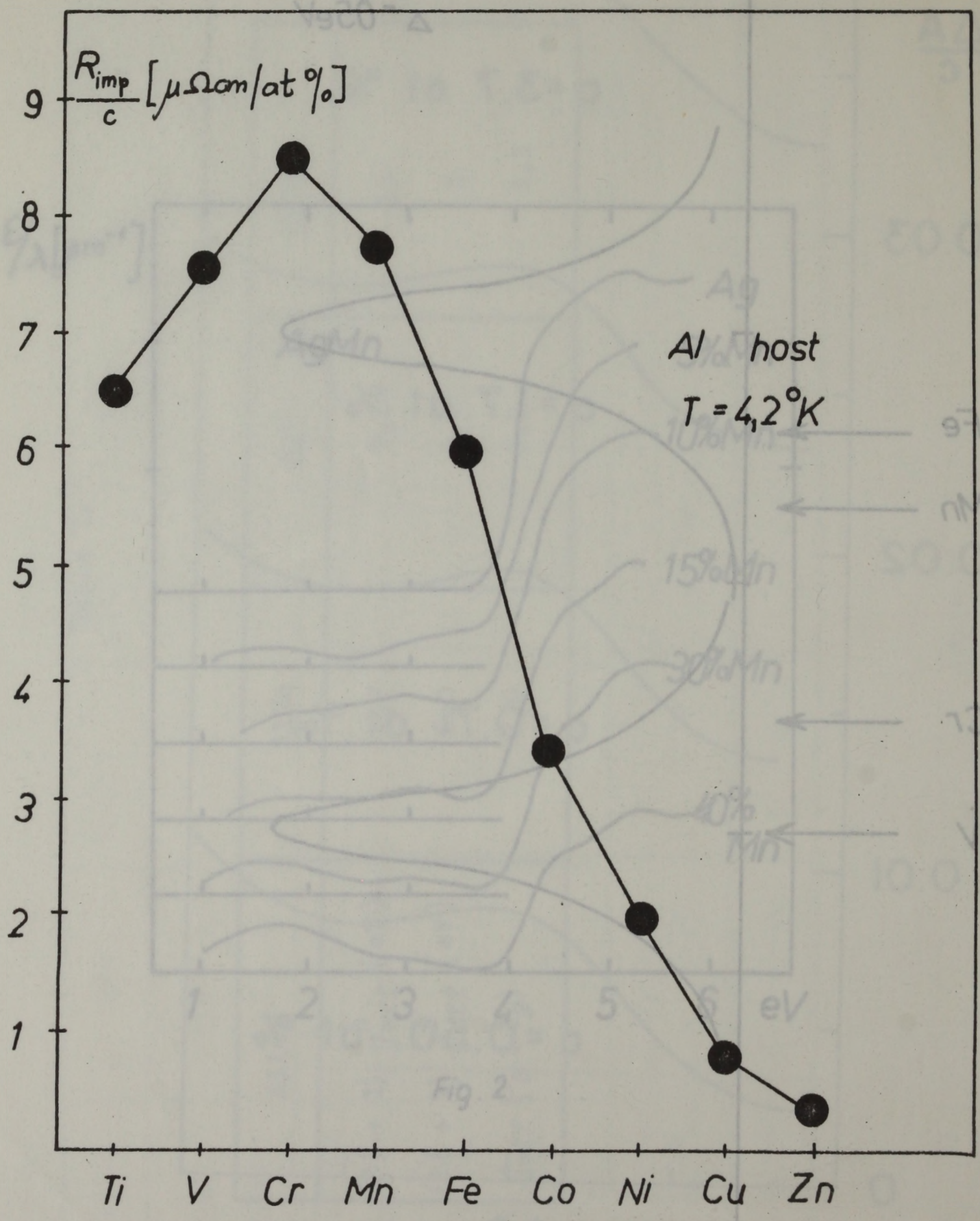
$\frac{R_{imp}}{c}$ [μΩcm/at %]
9
8
7
6
5
4
3
2
1
Al host
T = 4,2°K
Ti
V
Cr
Mn
Fe
Co
Ni
Cu
Zn

Fig. 4

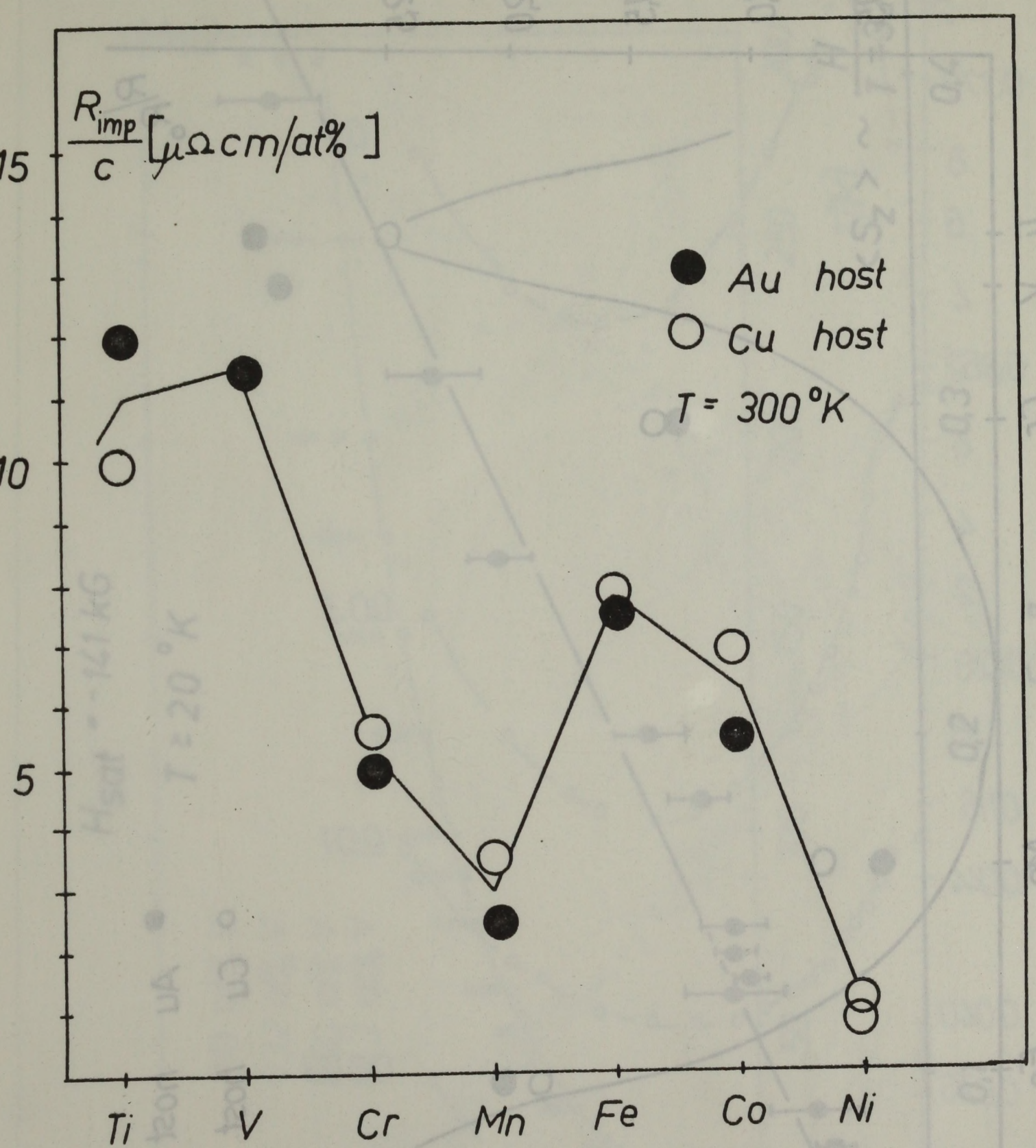
$\frac{R_{imp}}{c}$ [μΩcm/at%]
15
10
5
Au host
Cu host
T = 300 °K
Ti
V
Cr
Mn
Fe
Co
Ni

Fig. 5

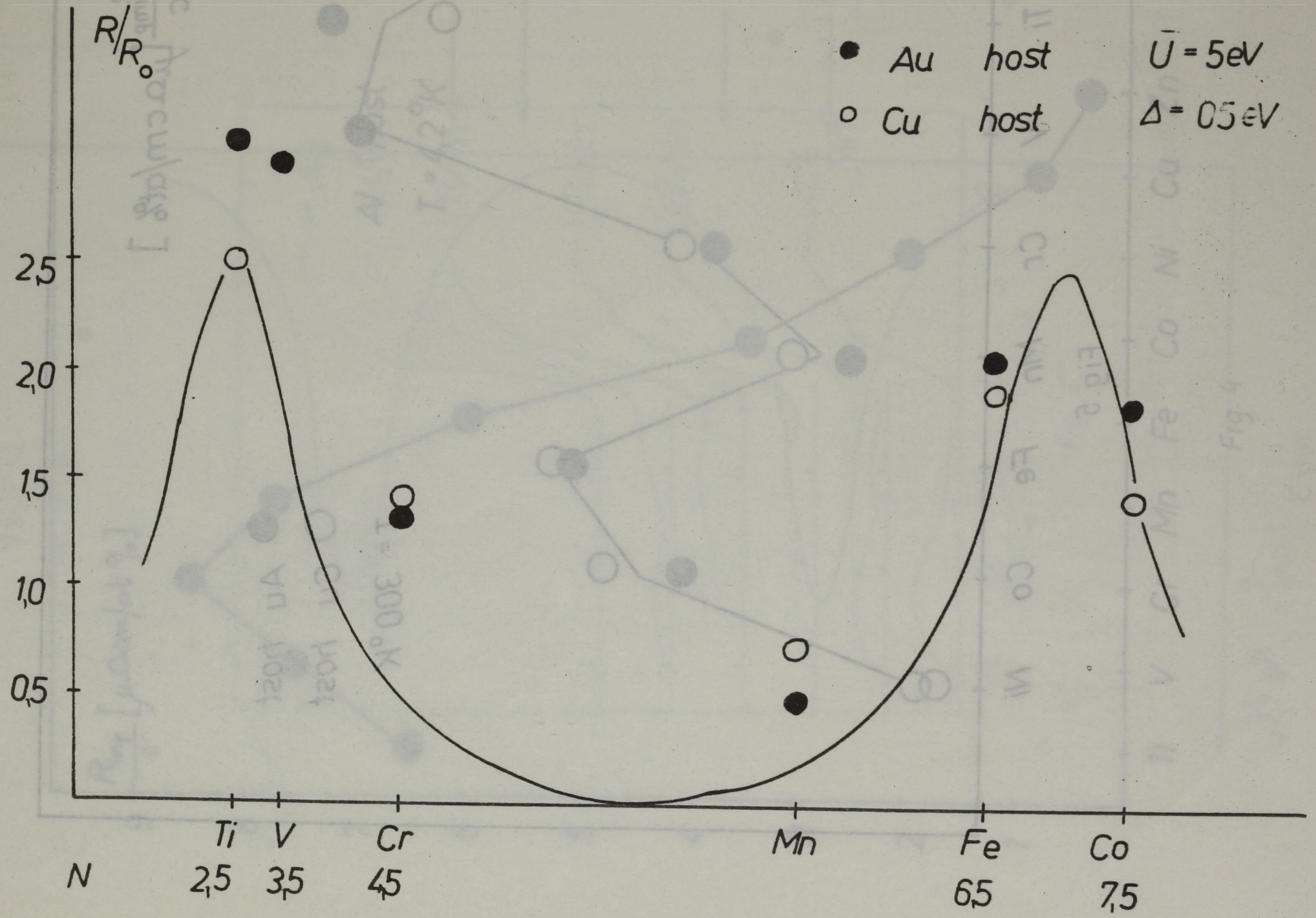
R/R₀
2,5
2,0
1,5
1,0
0,5
Au host
Cu host
Ū = 5eV
Δ = 0,5 eV
N
Ti
V
Cr
Mn
Fe
Co
2,5
3,5
4,5
6,5
7,5

Fig. 6

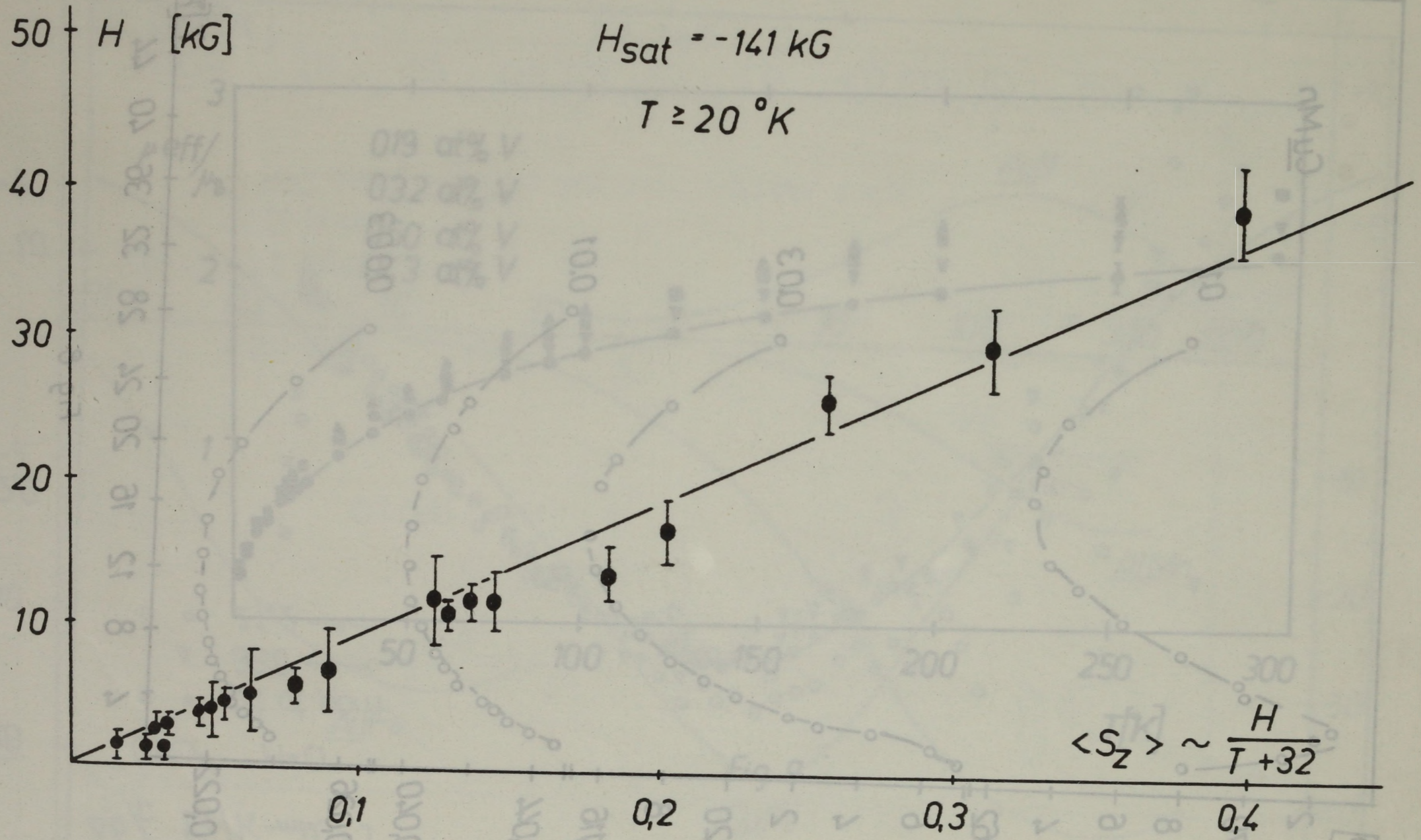
50
H [kG]
40
30
20
10
$H_{sat} = -141$ kG
$T \geq 20$ °K
0,1
0,2
0,3
0,4
$\langle S_z \rangle \sim \frac{H}{T+32}$

Fig. 7

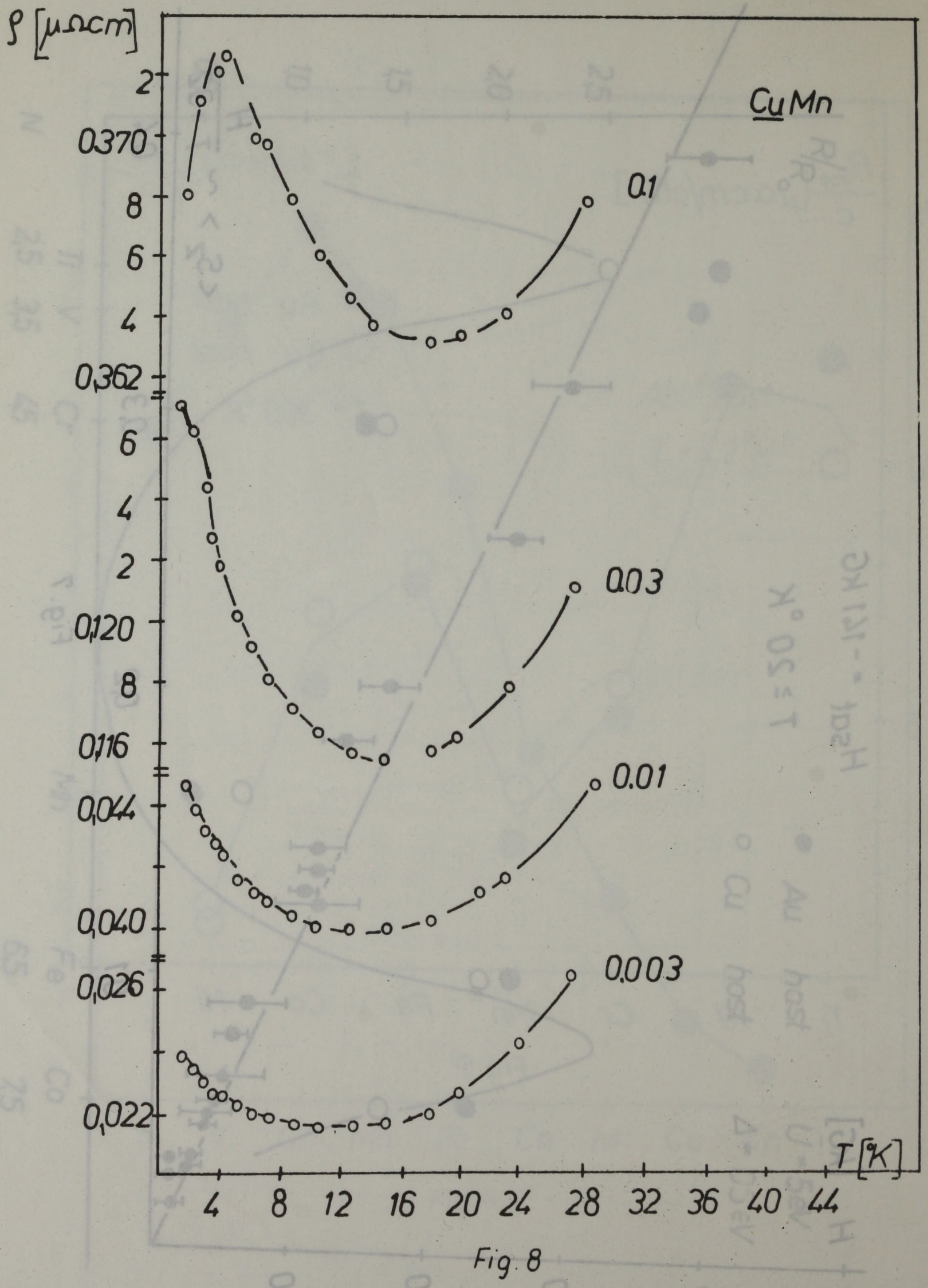
ρ [μΩcm]
2
0,370
8
6
4
0,362
6
4
2
0,120
8
0,116
0,044
0,040
0,026
0,022
CuMn
0.1
0.03
0.01
0.003
T [°K]
4
8
12
16
20
24
28
32
36
40
44

Fig. 8

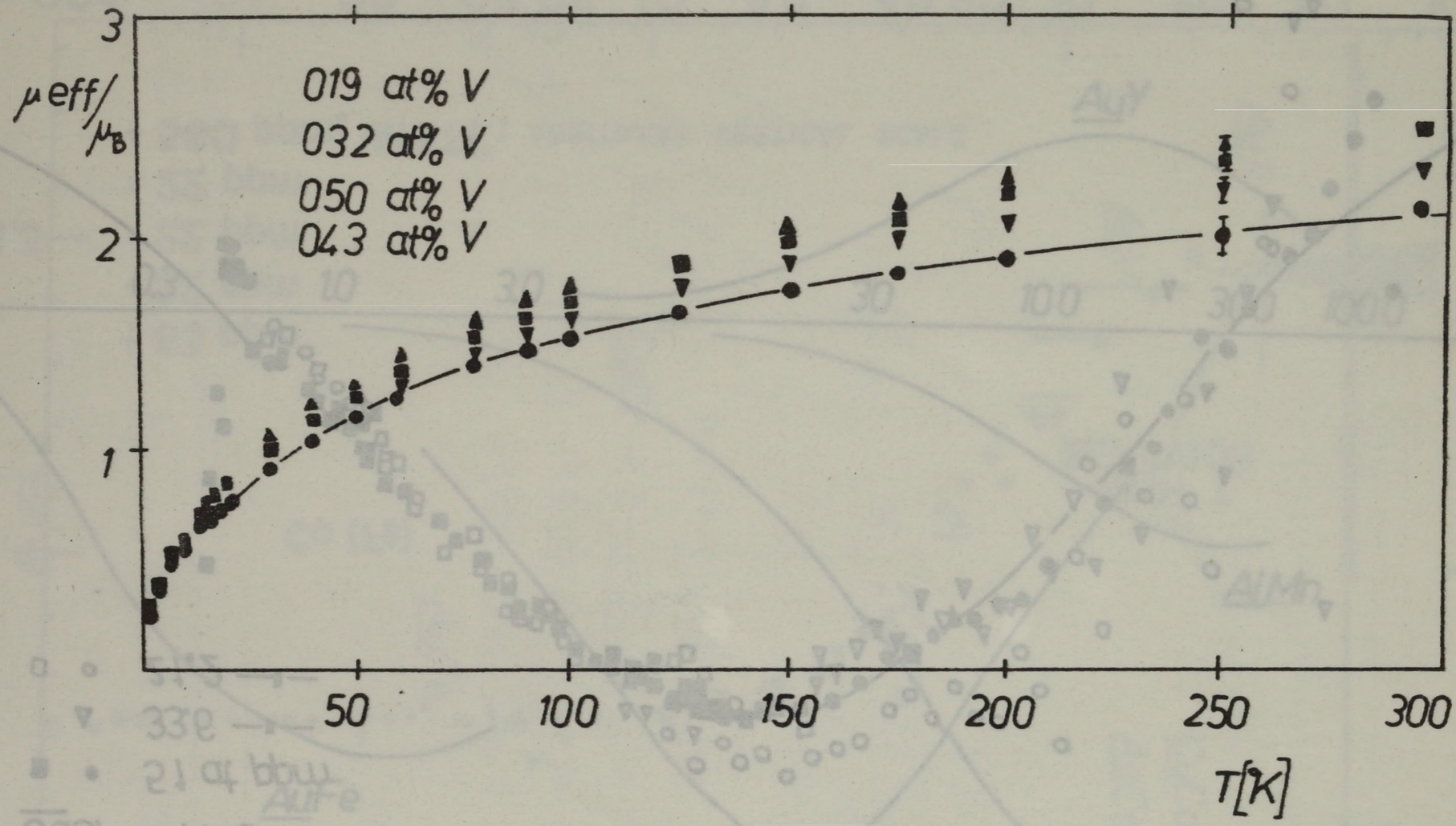
3
2
1
μeff/μB
019 at% V
032 at% V
050 at% V
043 at% V
50
100
150
200
250
300
T[K]

Fig. 9

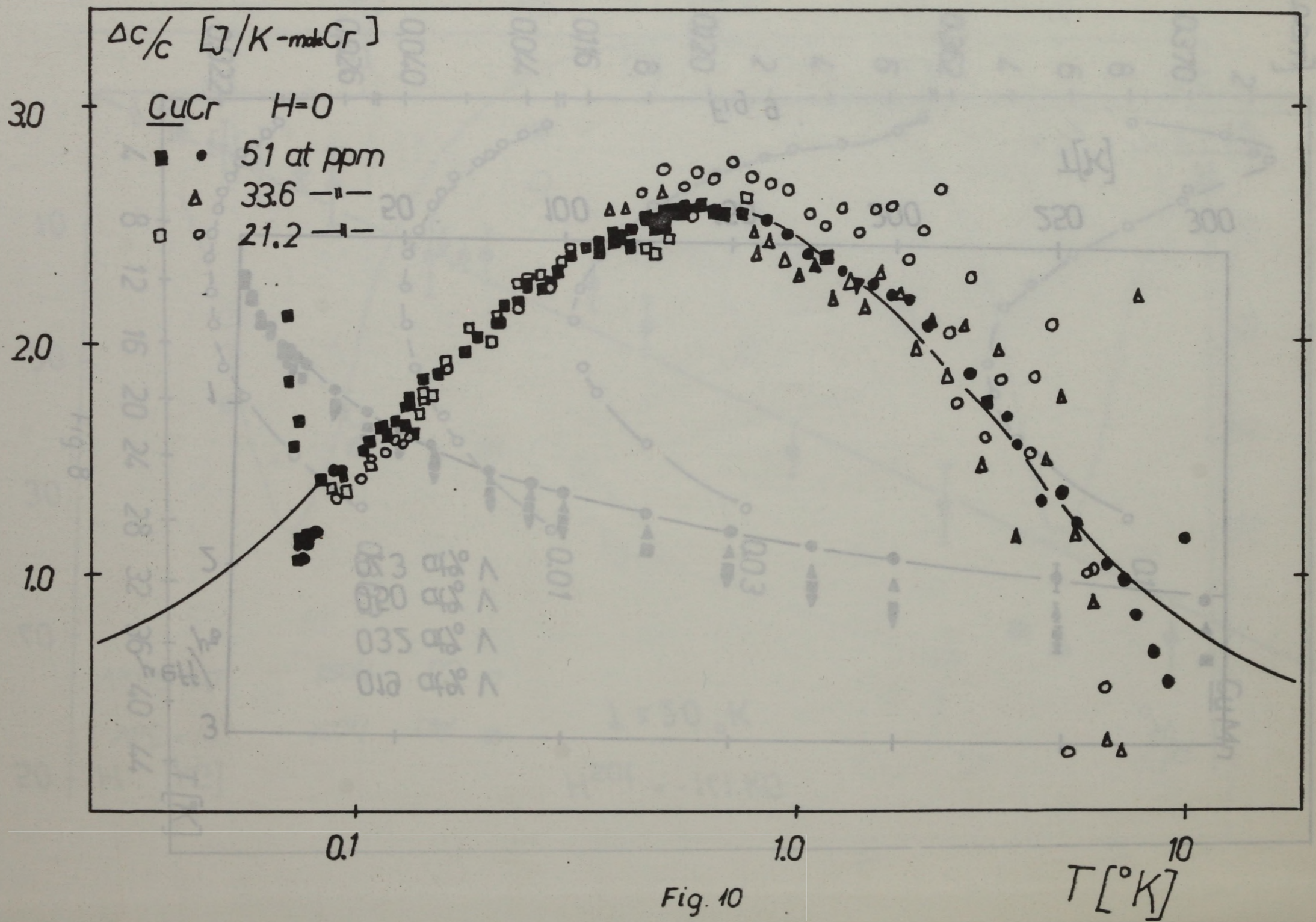

Fig. 10

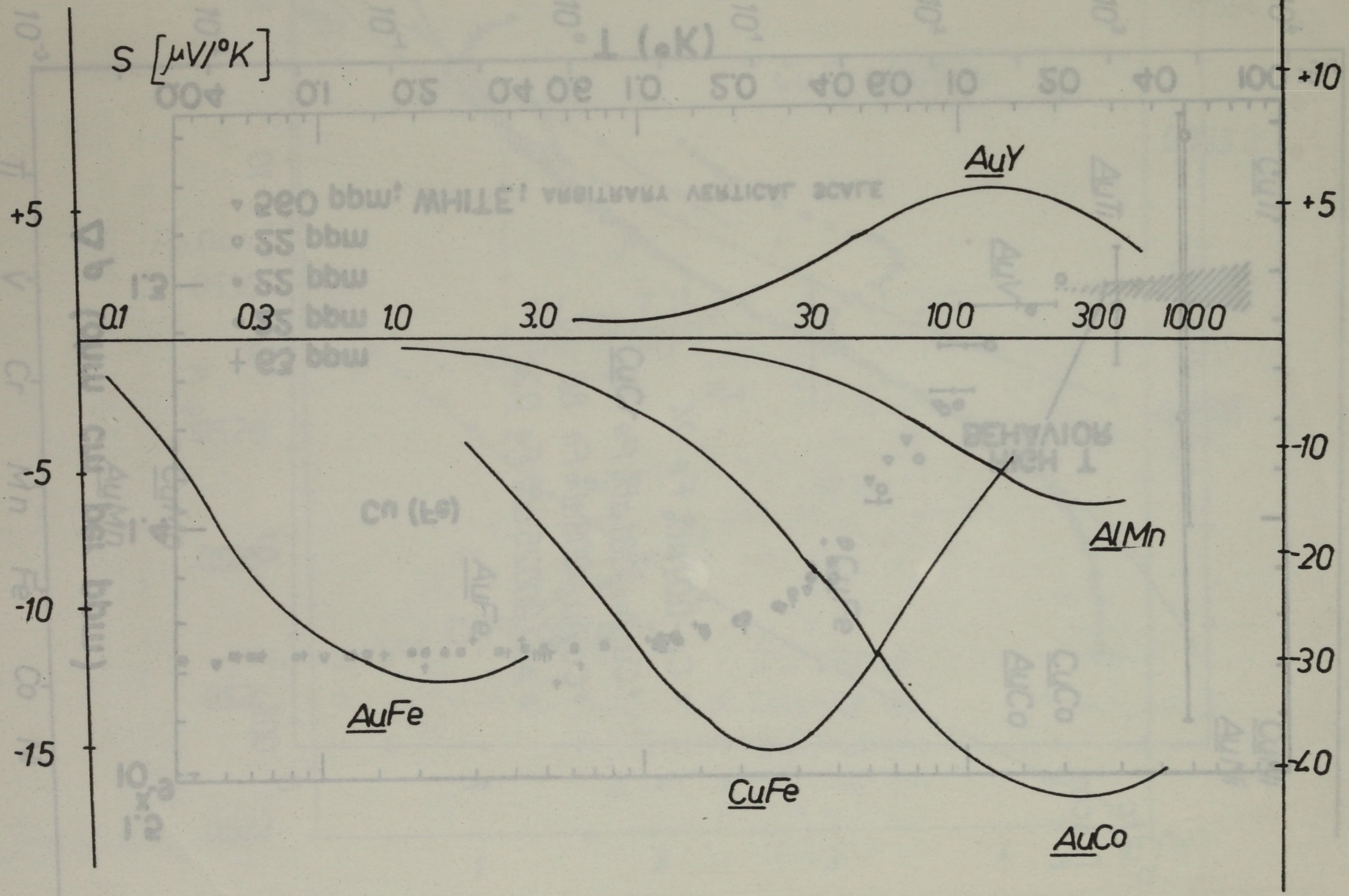
S [μV/°K]
+5
-5
-10
-15
0.1
0.3
1.0
3.0
30
100
300
1000
+10
+5
-10
-20
-30
-40
AuY
AlMn
AuFe
CuFe
AuCo

Fig. 11

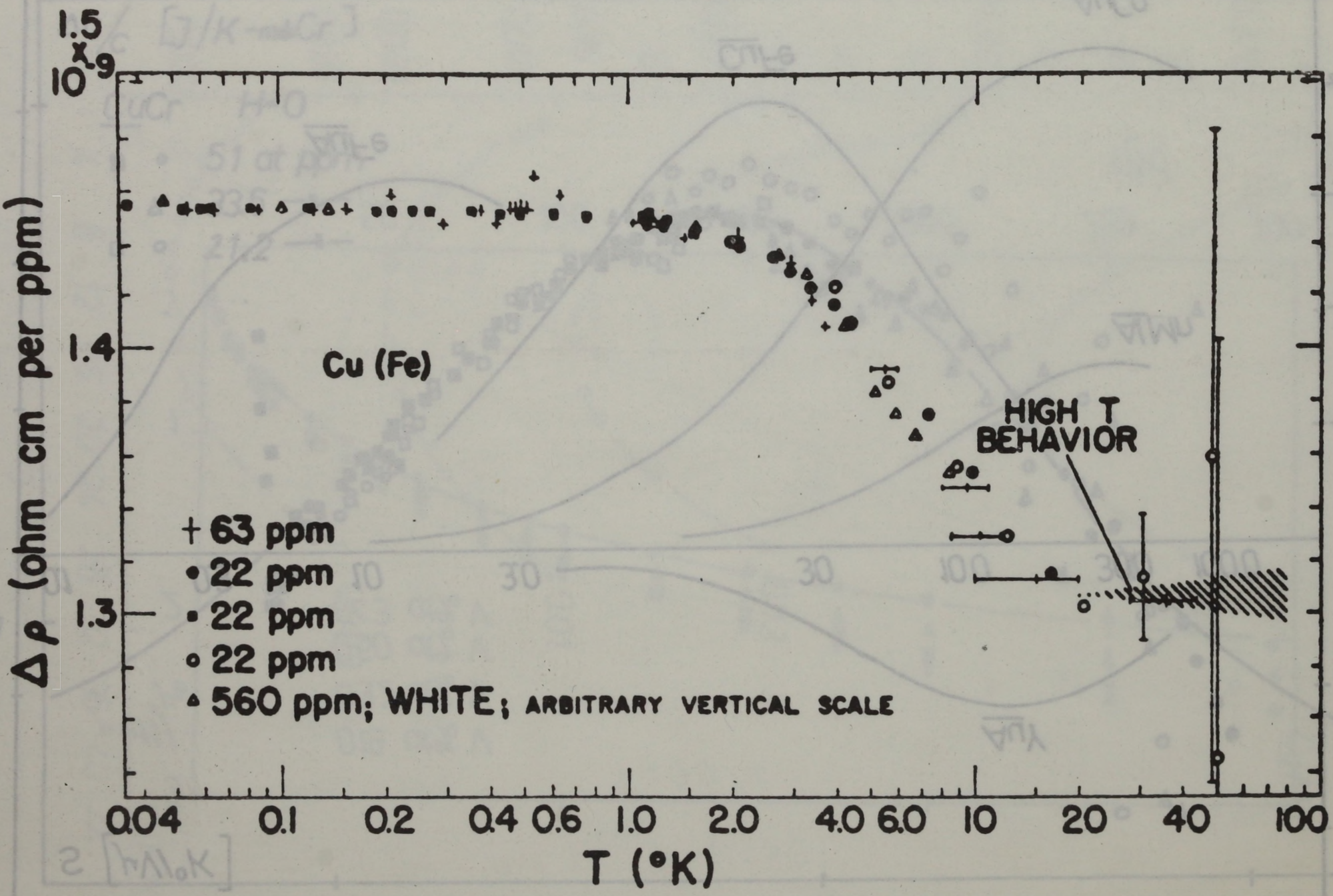
1.5
10^-9
Δρ (ohm cm per ppm)
1.4
1.3
Cu (Fe)
HIGH T
BEHAVIOR
+ 63 ppm
• 22 ppm
• 22 ppm
∘ 22 ppm
▲ 560 ppm; WHITE; ARBITRARY VERTICAL SCALE
0.04
0.1
0.2
0.4
0.6
1.0
2.0
4.0
6.0
10
20
40
100
T (°K)

Fig. 12

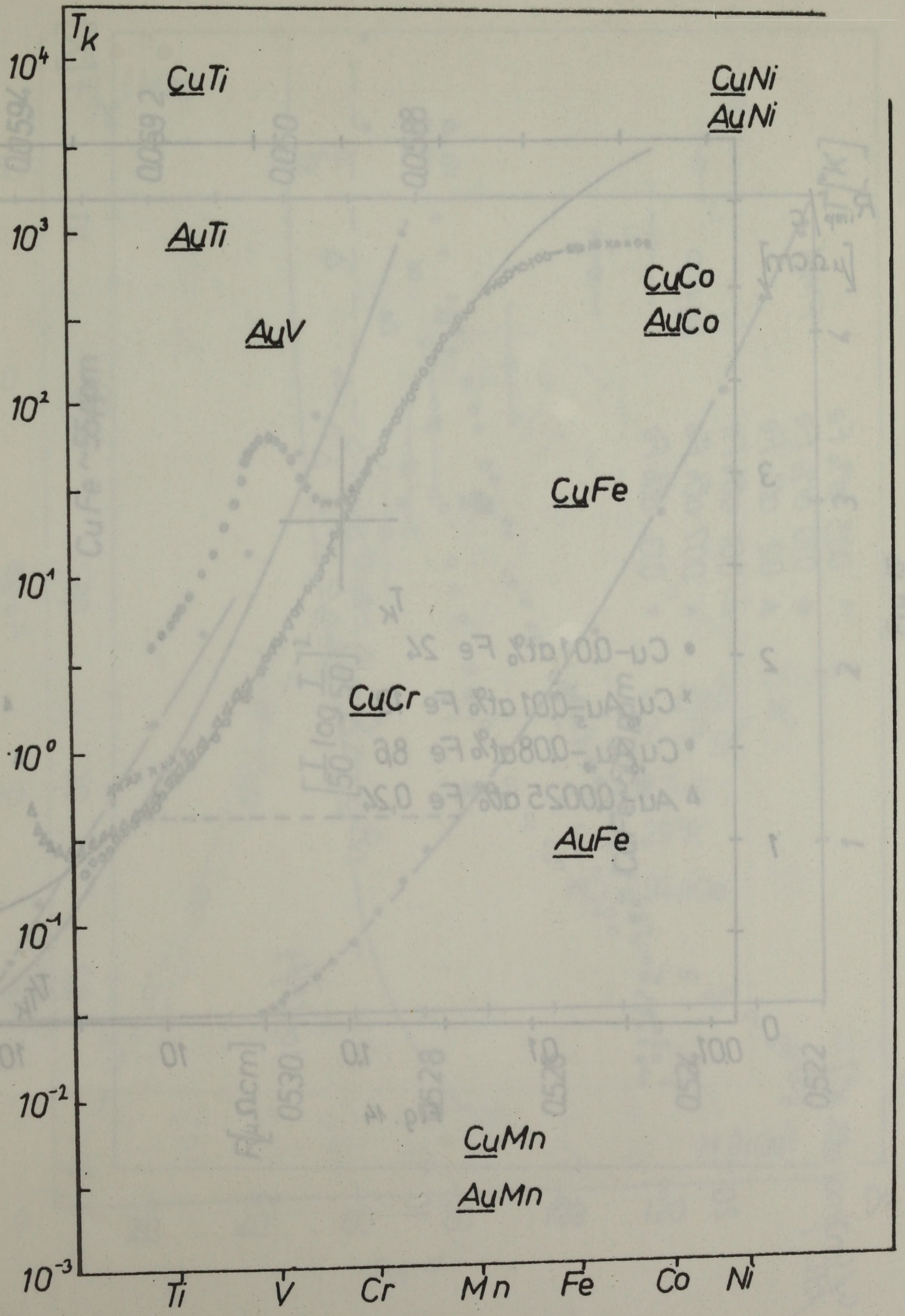
T_k
10^4
10^3
10^2
10^1
10^0
10^{-1}
10^{-2}
10^{-3}
CuTi
AuTi
AuV
CuCr
CuFe
AuFe
CuMn
AuMn
CuCo
AuCo
CuNi
AuNi
Ti
V
Cr
Mn
Fe
Co
Ni

Fig. 13

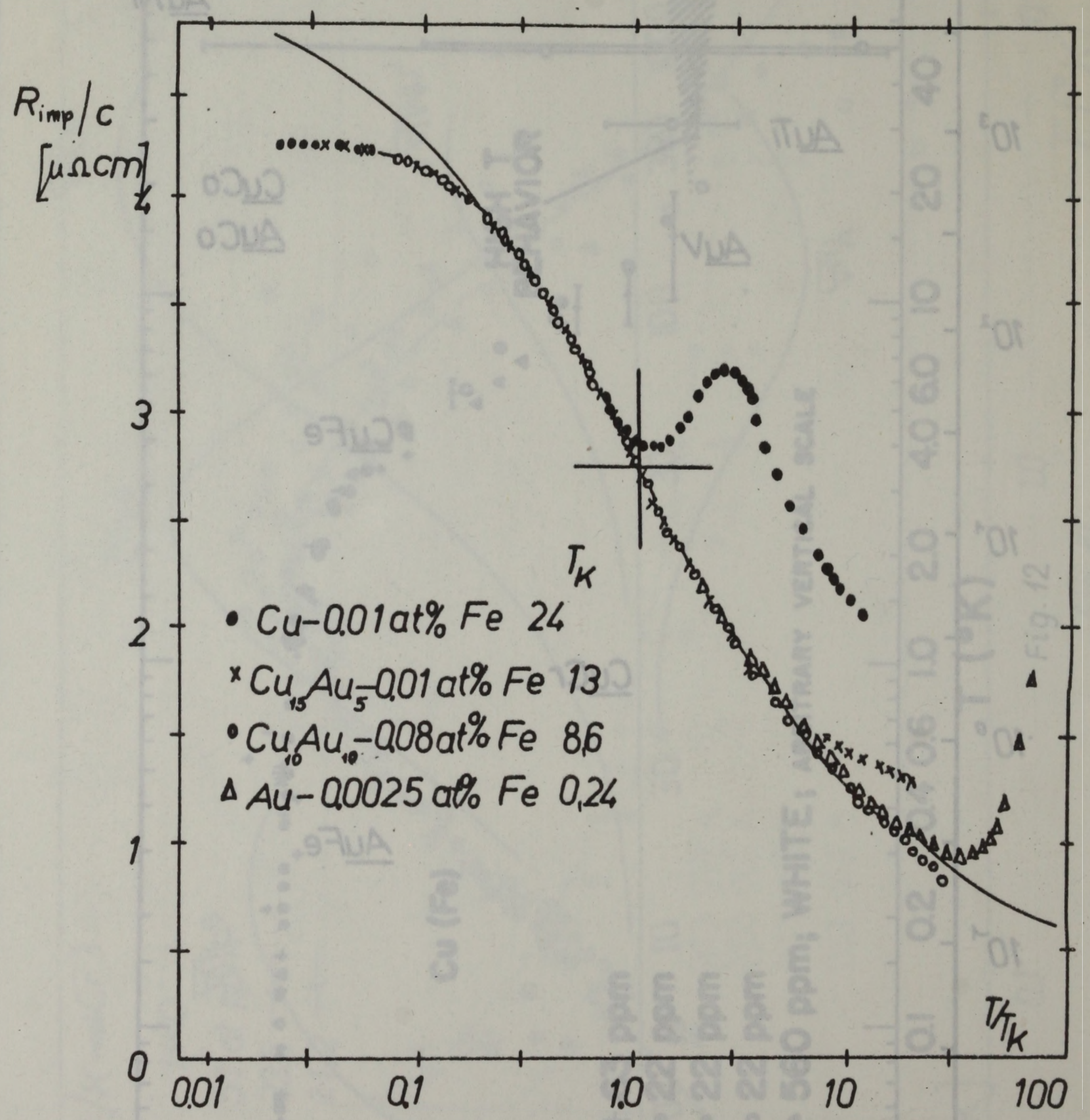
R_{imp}/c
$[\mu\Omega cm]$
4
3
2
1
0
0.01
0.1
1.0
10
100
T/T_K
T_K
• Cu-0.01at% Fe 24
× $Cu_{15}Au_5$-0.01at% Fe 13
• $Cu_{10}Au_{10}$-0.08at% Fe 8.6
Δ Au-0.0025at% Fe 0.24

Fig. 14

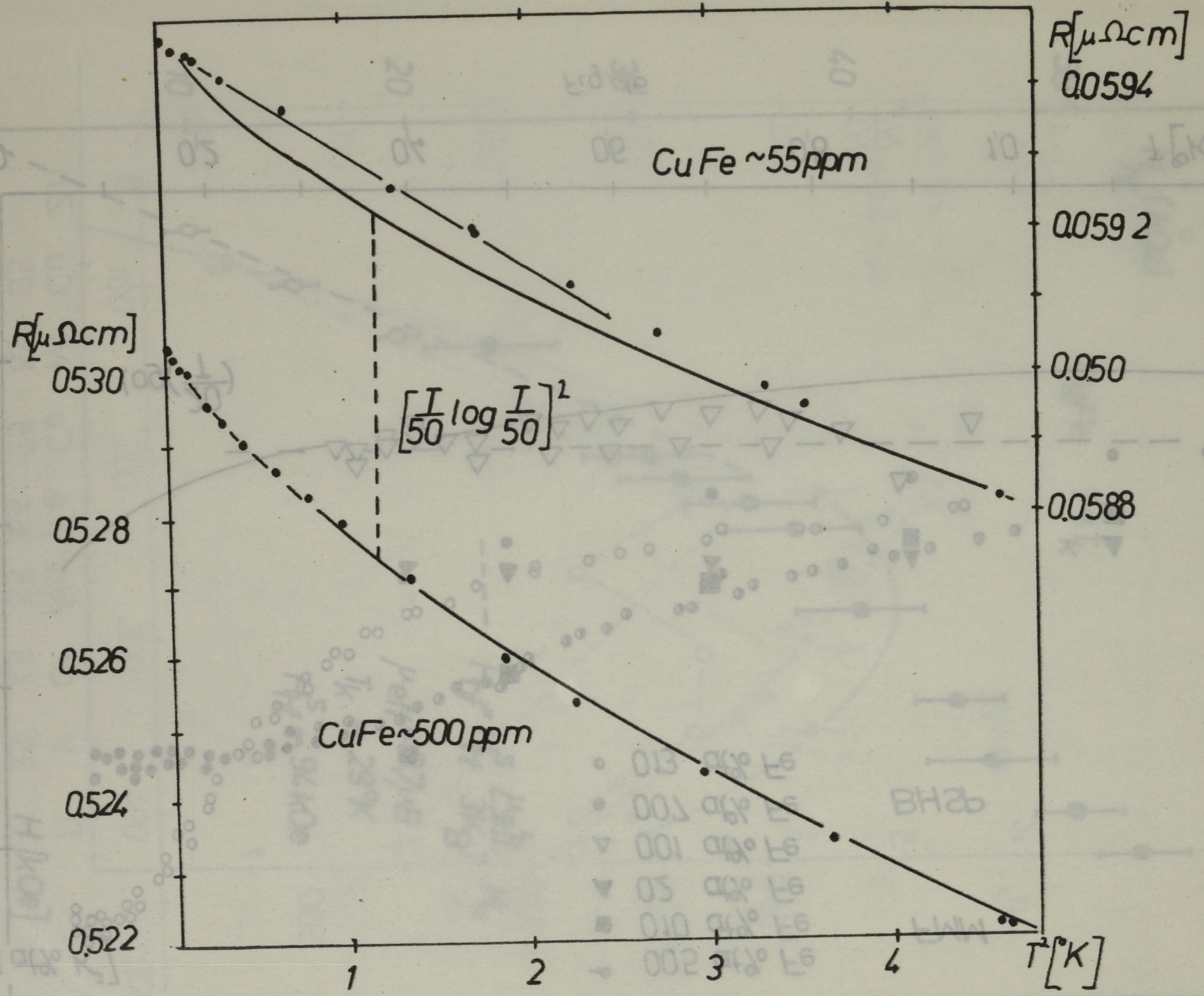
R[μΩcm]
0530
0528
0526
0524
0522
R[μΩcm]
0.0594
0.0592
0.050
0.0588
CuFe ~55ppm
$\left[\frac{I}{50}\log\frac{I}{50}\right]^2$
CuFe~500 ppm
1
2
3
4
T²[°K]

Fig. 15

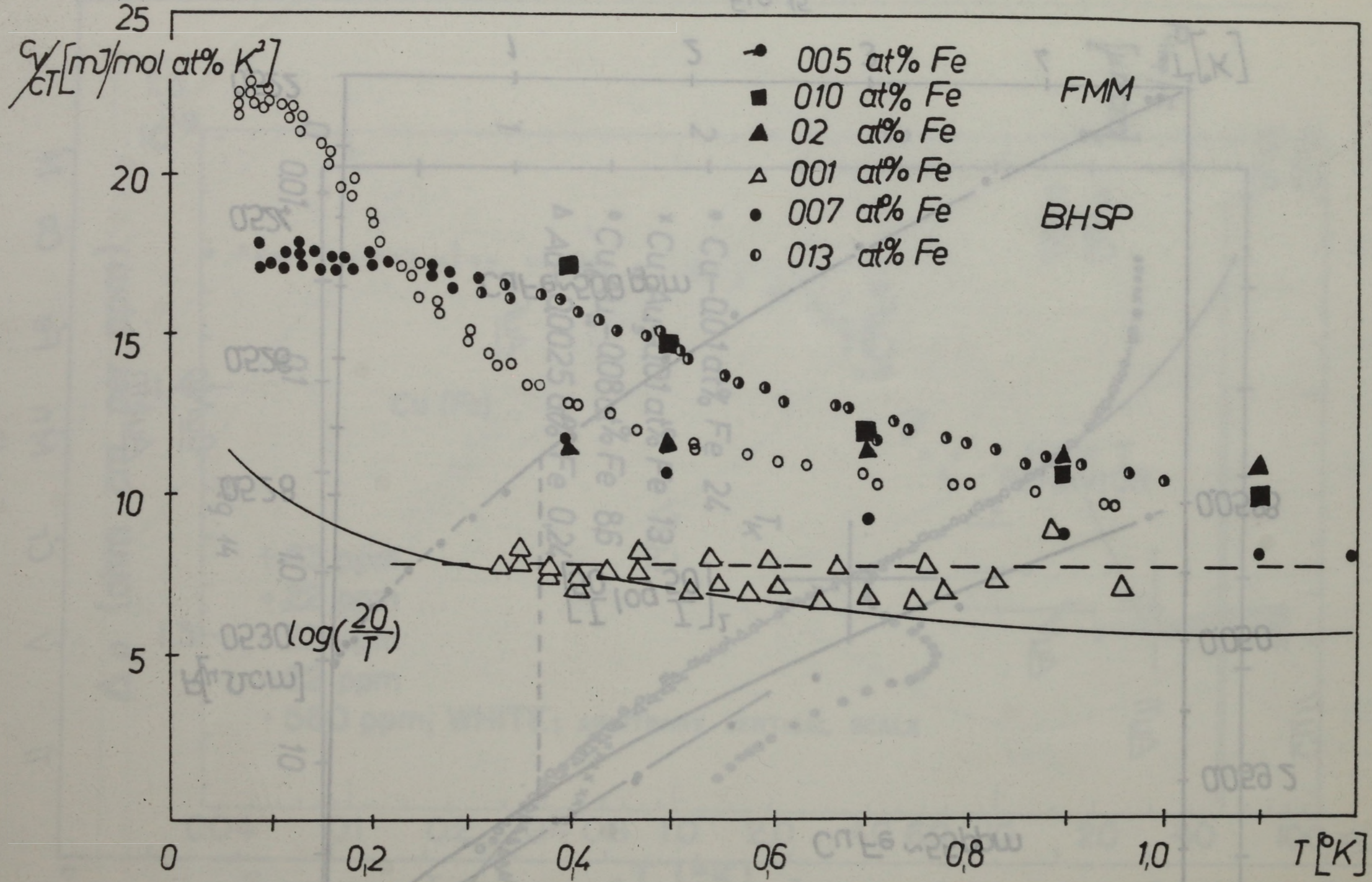
25
20
15
10
5
0
0,2
0,4
0,6
0,8
1,0
T [°K]
$C_V/\gamma T$ [mJ/mol at% K²]
005 at% Fe
010 at% Fe
02 at% Fe
001 at% Fe
007 at% Fe
013 at% Fe
FMM
BHSP
$\log(\frac{20}{T})$

Fig. 16

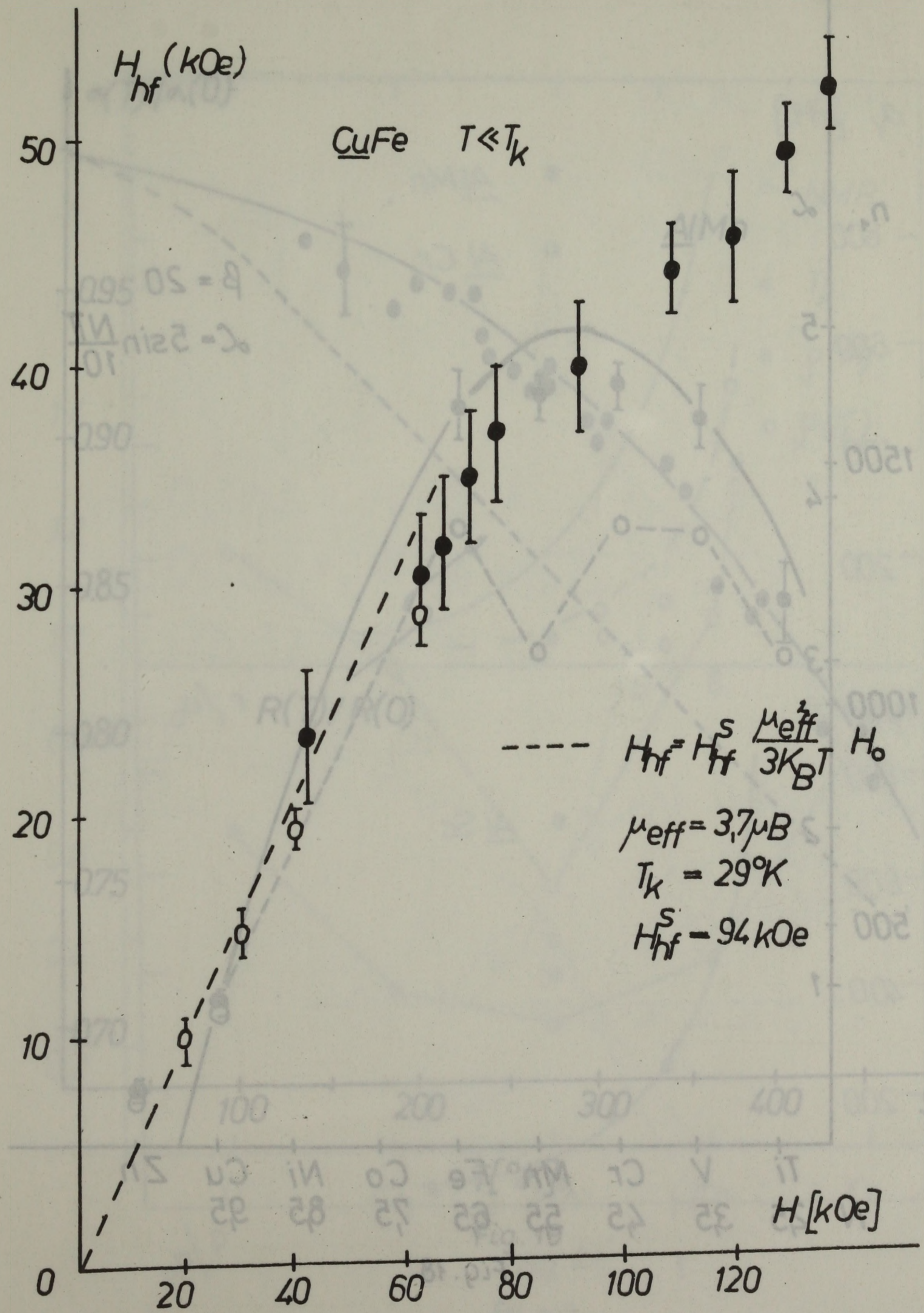
H_{hf} (kOe)
CuFe $T \ll T_k$
50
40
30
20
10
0
20
40
60
80
100
120
H [kOe]
---- $H_{hf} = H_{hf}^{s} \frac{\mu_{eff}^2}{3K_B T} H_o$
$\mu_{eff} = 3{,}7 \mu B$
$T_k = 29°K$
$H_{hf}^{s} = 94$ kOe

Fig. 17

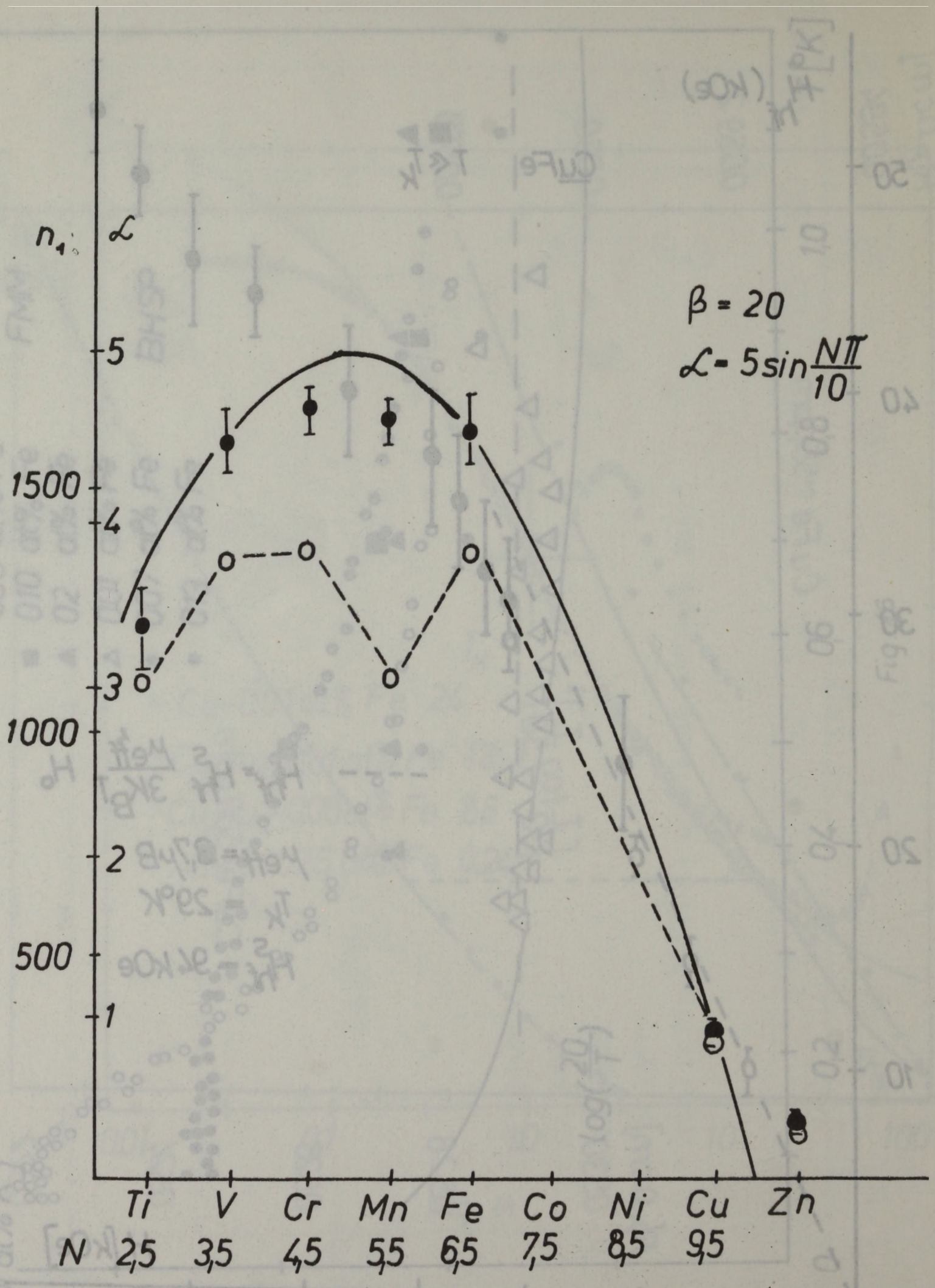
n_1
$\mathcal{L}$
5
1500
4
3
1000
2
500
1
$\beta = 20$
$\mathcal{L} = 5 \sin \frac{N\pi}{10}$
Ti V Cr Mn Fe Co Ni Cu Zn
N 2,5 3,5 4,5 5,5 6,5 7,5 8,5 9,5

Fig. 18

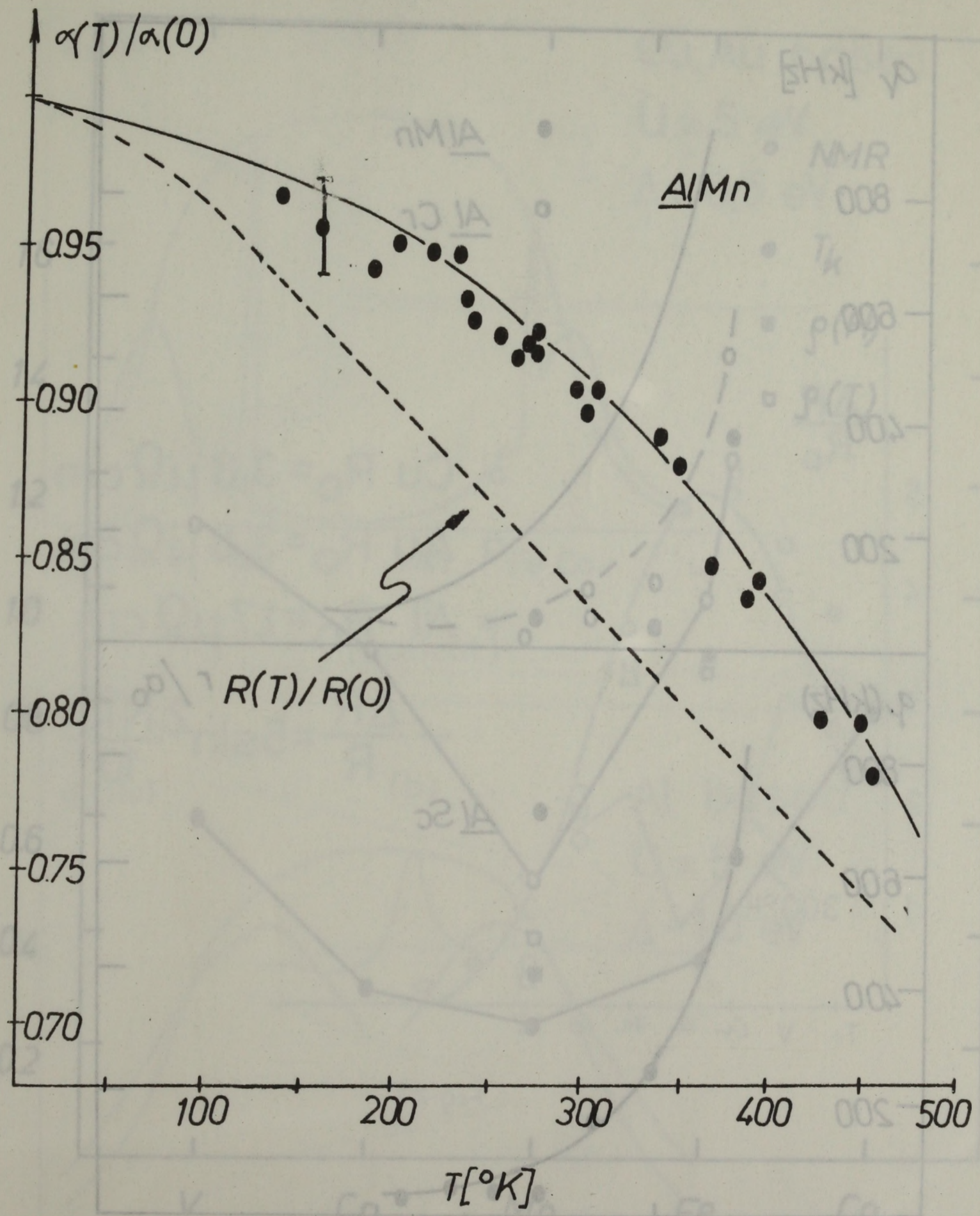

Fig. 19

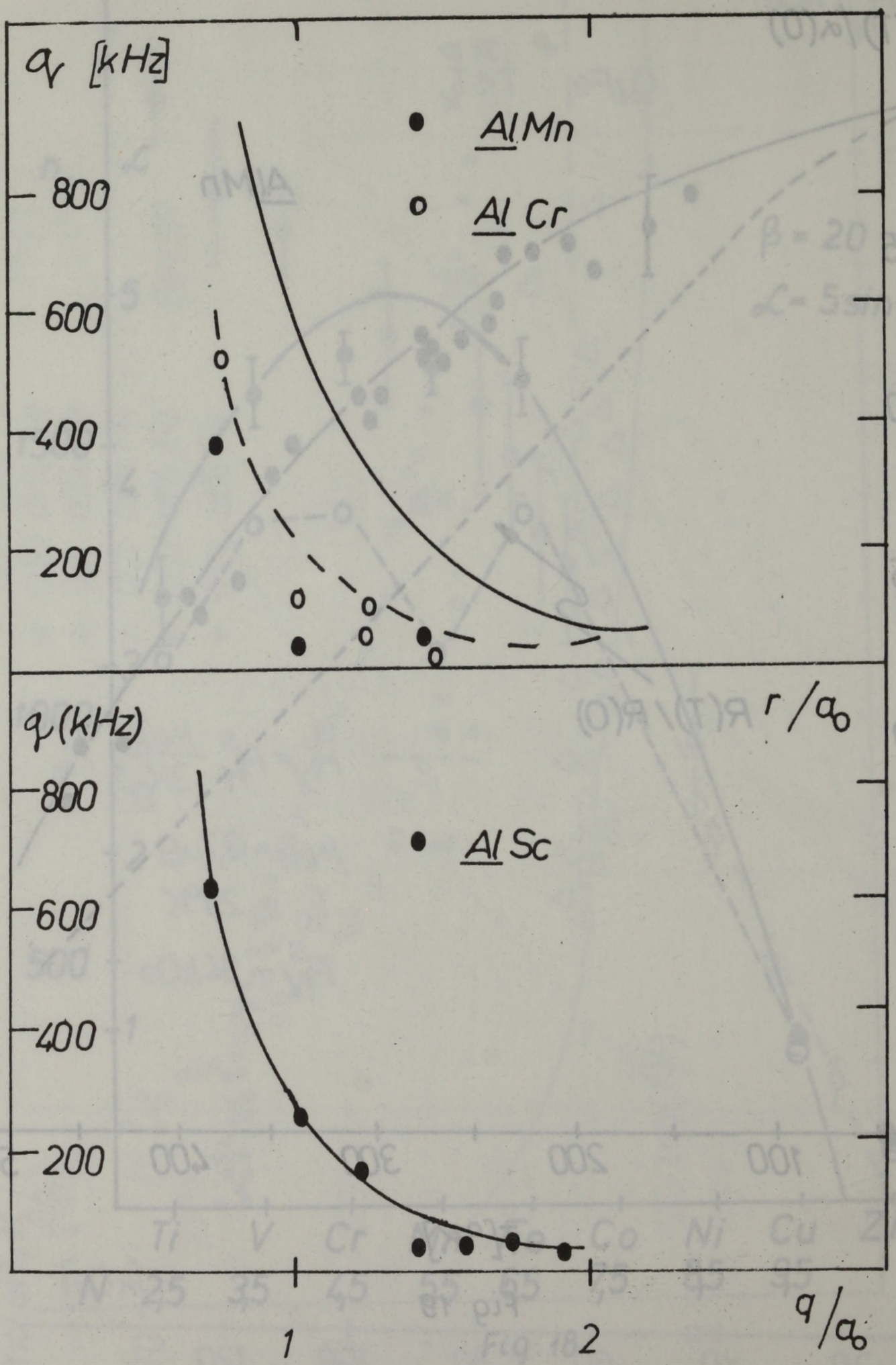
a_r [kHz]
800
600
400
200
Al Mn
Al Cr
q (kHz)
800
600
400
200
r/a₀
Al Sc
1
2
q/a₀

Fig. 20

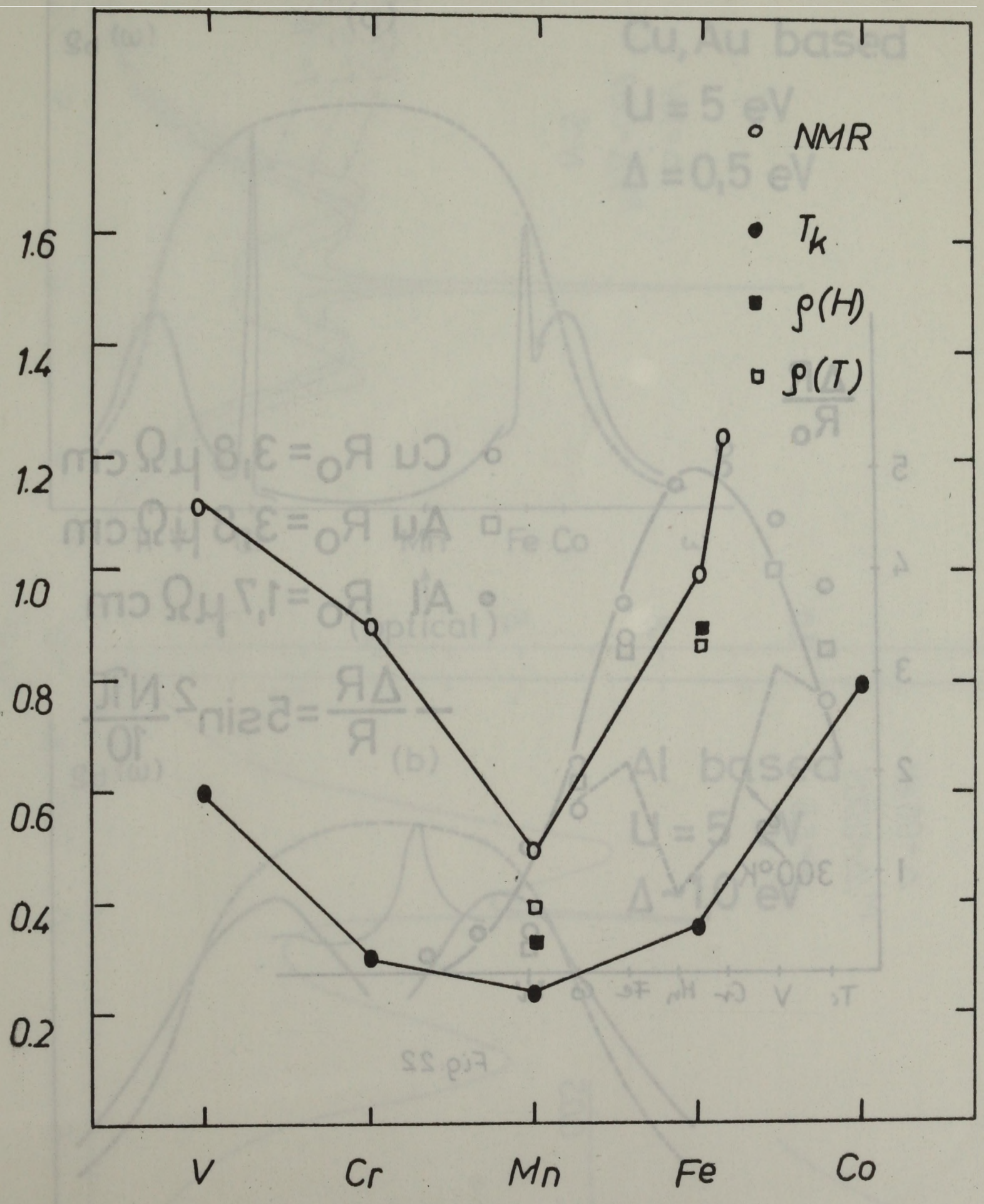

Fig. 21

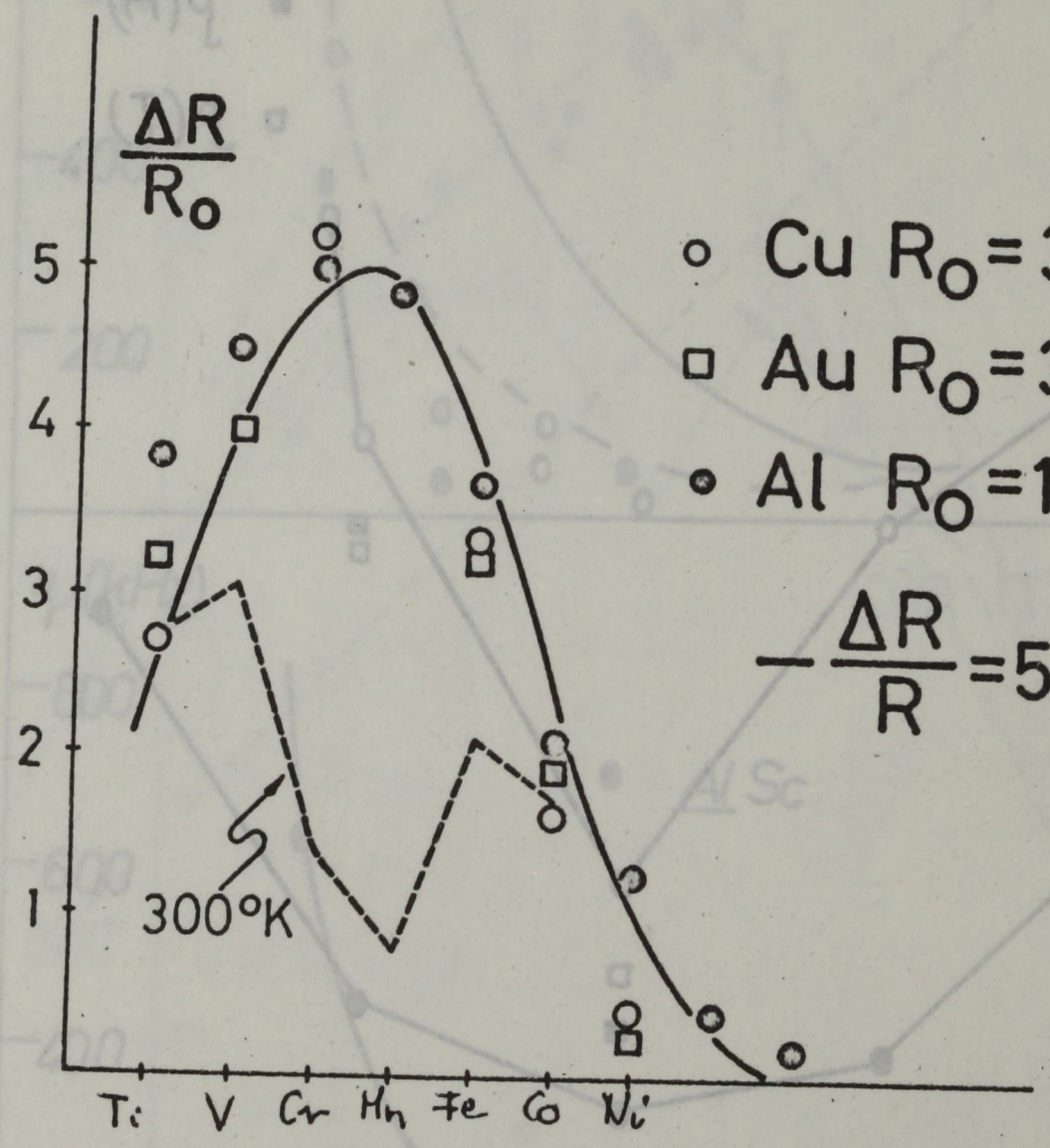

○ Cu $R_0 = 3{,}8\ \mu\Omega\,cm$

□ Au $R_0 = 3{,}8\ \mu\Omega\,cm$

⊙ Al $R_0 = 1{,}7\ \mu\Omega\,cm$

$$-\frac{\Delta R}{R} = 5\sin^2\frac{N\pi}{10}$$

Fig. 22

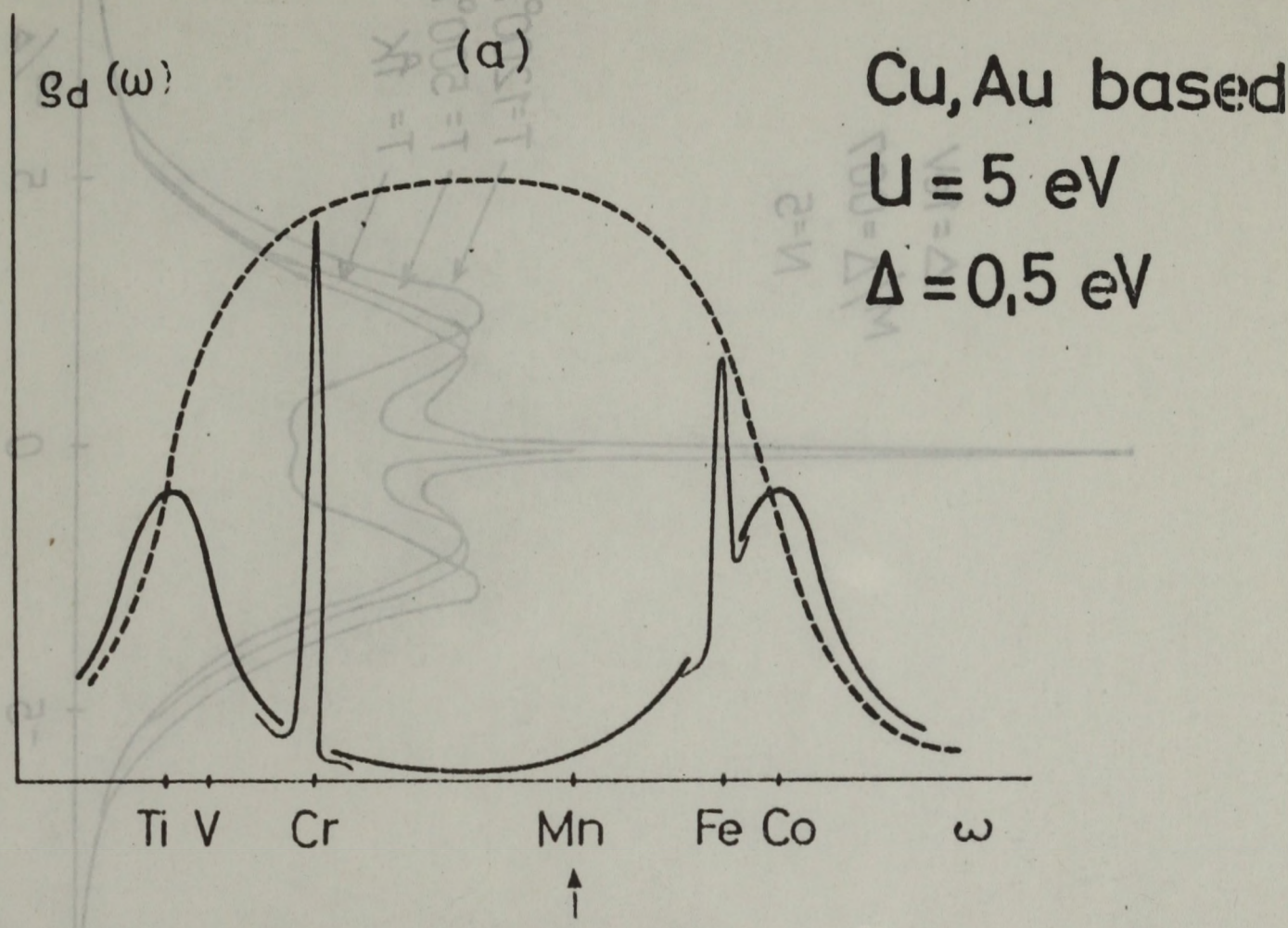
(a)
$g_d(\omega)$
Cu, Au based
U = 5 eV
Δ = 0,5 eV
Ti V Cr Mn Fe Co ω
(optical)

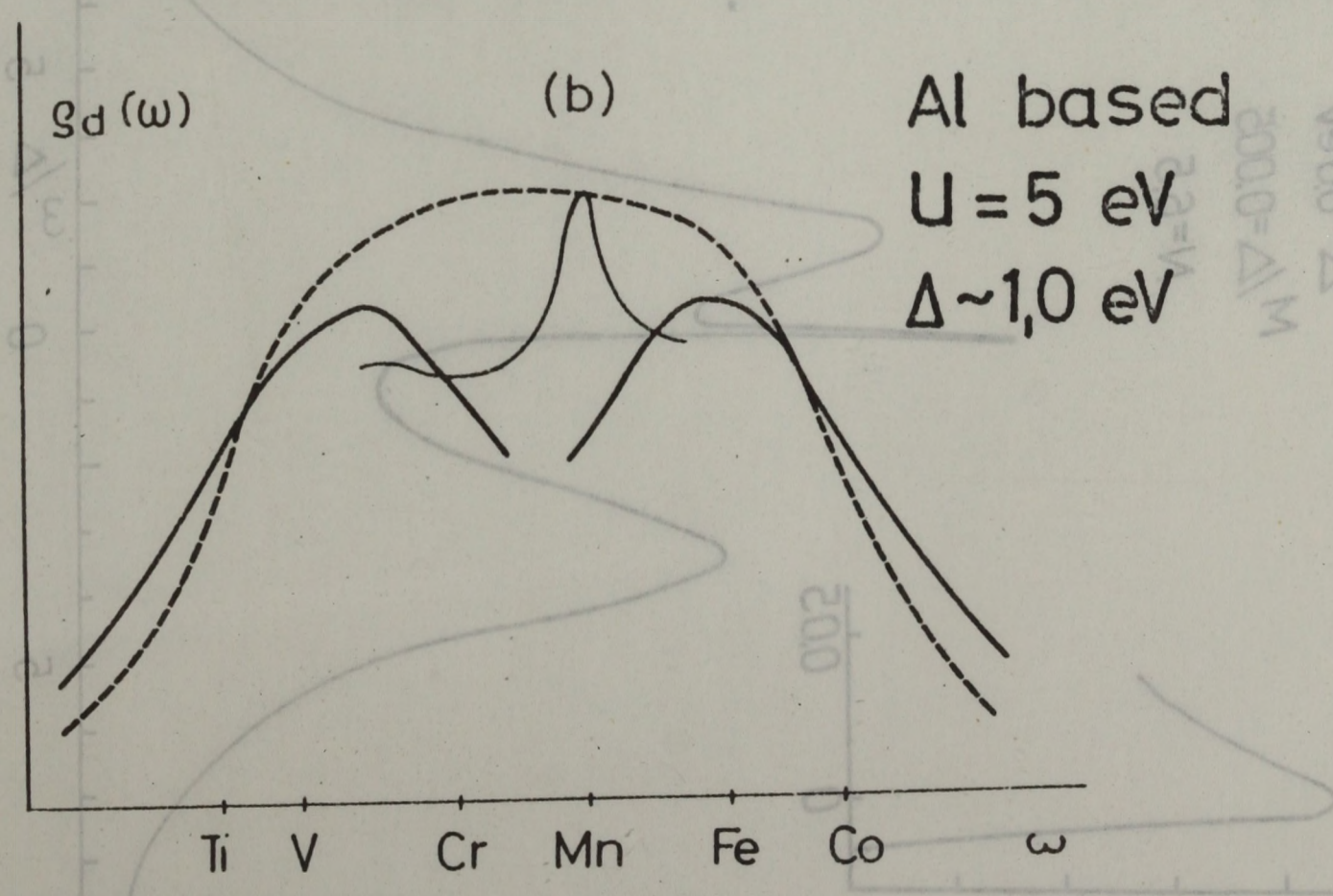
(b)
$g_d(\omega)$
Al based
U = 5 eV
Δ ~ 1,0 eV
Ti V Cr Mn Fe Co ω

Fig. 23

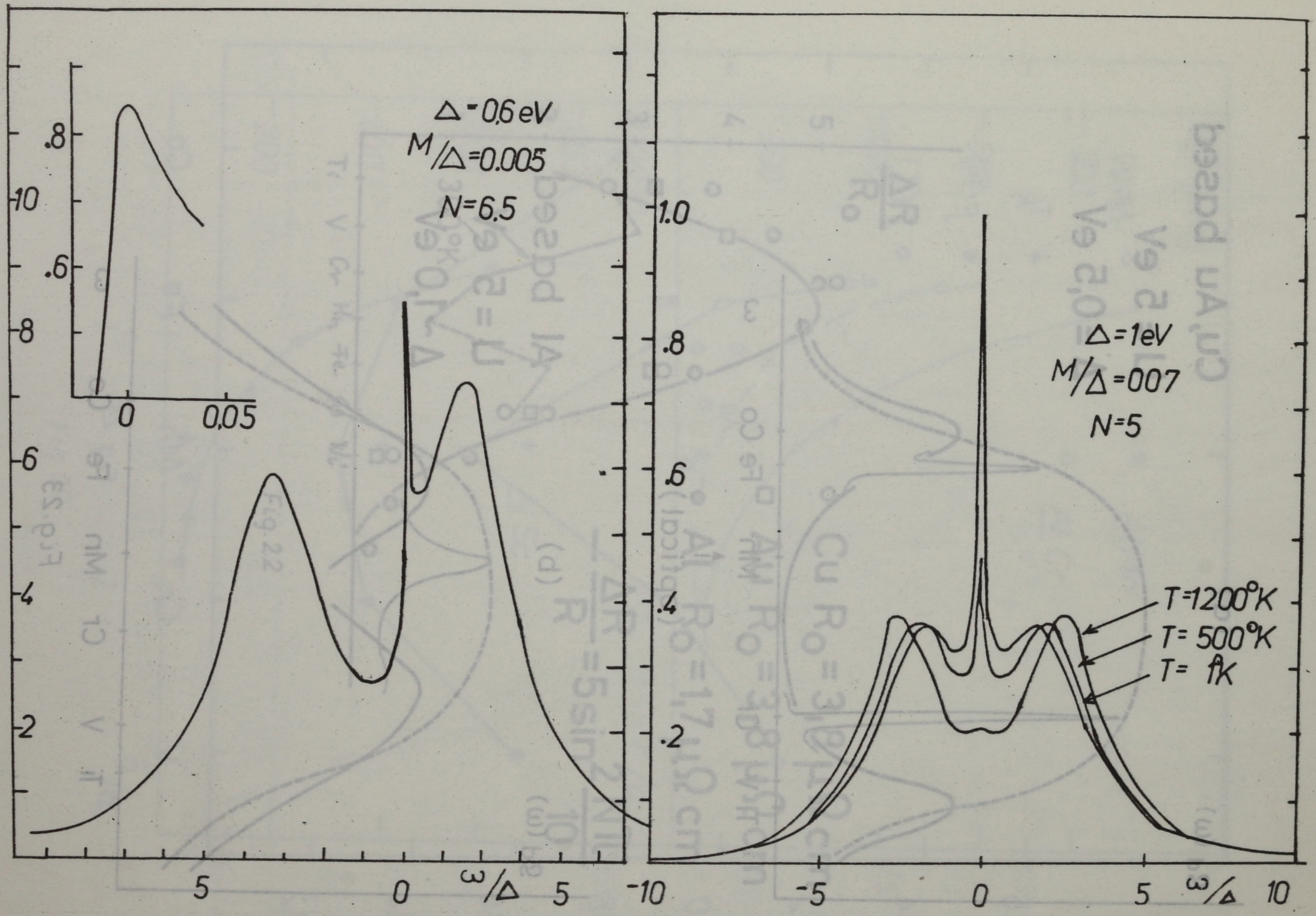
Δ = 0.6 eV
M/Δ = 0.005
N = 6.5
.8
.6
0
0.05
10
8
6
4
2
5
0
ω/Δ
5
Δ = 1eV
M/Δ = 007
N = 5
1.0
.8
.6
.4
.2
T = 1200°K
T = 500°K
T = 1K
-10
-5
0
5
ω/Δ
10

Fig. 24

Kiadja a Központi Fizikai Kutató Intézet
Felelős kiadó: Tompa Kálmán, a KFKI Szilárdtestkutatási Tudományos Tanácsának szekcióelnöke
Szakmai lektor: Zawadowski Alfréd
Nyelvi lektor: Zawadowski Alfréd
Példányszám: 290 Törzsszám: 74-9639
Készült a KFKI sokszorositó üzemében
Budapest, 1974. február hó